University of Washington
Department of Civil and Environmental Engineering

MODELING AND MONITORING TO PREDICT SPATIAL AND TEMPORAL HYDROLOGIC CHARACTERISTICS IN SMALL CATCHMENTS

Mark S. Wigmosta
Stephen J. Burges
Jack M. Meena

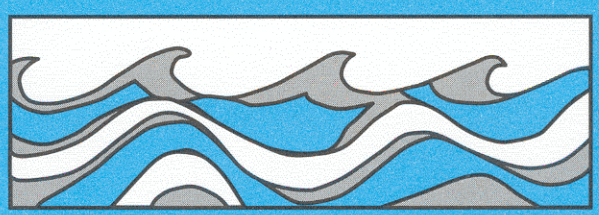

Water Resources Series
Technical Report No.137
June 1994

Seattle, Washington
98195

Department of Civil Engineering
University of Washington
Seattle, Washington 98195

MODELING AND MONITORING TO PREDICT SPATIAL AND TEMPORAL HYDROLOGIC CHARACTERISTICS IN SMALL CATCHMENTS

Mark S. Wigmosta
Stephen J. Burges
Jack M. Meena

Water Resources Series
Technical Report No. 137

June 1994

Department of Civil Engineering
University of Washington
Seattle, Washington, 98195

Modeling and Monitoring to Predict Spatial and Temporal Hydrologic Characteristics in Small Catchments

by

Mark S. Wigmosta
Stephen J. Burges
Jack M. Meena

Water Resources Series
Technical Report No. 137

June 1994

Project Completion Report:	Field Testing of a Small Catchment Model That Uses and Predicts Spatial and Temporal Information
Prepared for:	U.S. Geological Survey
USGS Award Number:	14-08-0001-G1887
Project Period:	July 2, 1990 - December 31, 1993
Principal Investigator:	Stephen J. Burges Professor of Civil Engineering

ABSTRACT

The purpose of this work was to develop a methodology for predicting in small catchments (tens to hundreds of hectares) the internal catchment states and fluxes, as well as integrated outflow. Catchments were selected for monitoring to permit the use of a limited field measurement program combined with appropriate modeling to estimate the hydrologic behavior in pre- and post- states where land-use change is anticipated. The work was planned in two parts. In the first part the objective was to develop a methodology that used short-term hydrologic monitoring and mapping of hydrologic process zones and an appropriate model to predict hydrologic states and fluxes. The second part involved continuation of the measuring program in two catchments for an additional two years and comparing predicted fluxes with the longer time series using the model as calibrated with the data series from the first part. The two catchments are located in the lowlands of King County, Washington State.

To facilitate development of the overall methodology, simple hydrologic monitoring and field mapping were conducted in a 37-hectare forested catchment and used in conjunction with hydrologic modeling to determine spatial and temporal variations in flow production. Precipitation, streamflow, and shallow water table elevations were recorded at 15-minute intervals for one year. Soil depths and the locations of flow production zones were mapped using simple field techniques. This information allowed an annual water balance to be determined, including the important separation between surface and subsurface flow volumes. Spatially-averaged estimates of saturated hydraulic conductivity and effective soil porosity were made using information measured at several piezometers. These soil properties were used to calibrate the continuous hydrologic model which was developed to simulate explicitly the flux rates and spatial distributions of evapotranspiration, Horton and saturation overland flow, return flow, and subsurface flow. Four physically-based model parameters were adjusted until simulated discharge, hillslope soil water levels, and locations of runoff production zones agreed with the field measurements and observations. The model predicted soil water level fluctuations at a downslope location that differed from the levels in the set of piezometers used for calibration so four additional piezometers were installed downslope to check the model's capability at predicting spatial hillslope soil water levels. The model was then tested using the next eight months of data and additional water table elevations from two piezometers installed after the calibration period. Model simulation of storm hydrograph peaks was good, but predicted storm volumes generally were greater than measured values. Simulation water levels at the piezometers were good.

The methodology was also used in a 17-hectare urbanized catchment. Detailed field mapping was used in conjunction with recorded rainfall and streamflow to separate volumes of Horton overland flow generated on impervious surfaces from discharge originating in pervious areas of the catchment. Discharge from

pervious areas -- lawns, gardens, and common areas -- (approximately 71% of the catchment) accounted for 60 percent of the runoff volume during large storms. The model was calibrated to field measurements by adjusting two soil input parameters. The total simulated runoff volume was within 2 percent of recorded. Model simulated storm peaks were excellent, although storm volumes were too large. These findings were based on time series for almost one water year.

The two years that followed the first phase were relatively dry and provided test conditions that differed substantially from the initial methodology development and test period. Vandalism precluded continuation of measurements at the piezometers at Novelty Hill so all comparisons had to be effected using measured precipitation, streamflow, and estimated potential evapotranspiration. For the Novelty Hill site, the model over simulated the response to the first storms that followed sustained dry periods suggesting that the representation of the soil moisture balance after sustained dry is inappropriate. In the third year of the four years of record at Novelty Hill, there was almost no runoff nor estimated leakage through the underlying dense till layer. A slightly smaller annual total rainfall in the fourth year yielded greater streamflow and till recharge than in year three emphasizing the importance of the wetting and drying time history of the soil to the overall catchment hydrology. The measurements and modeling demonstrate the importance of continuous hydrologic process representation relative to examination of only a few events. The methodology yields information for use in eco-hydrologic process representation that cannot be provided by considering only isolated events.

The additional time series for the Klahanie catchment demonstrate the lesser effect of the much thinner soil in the post-development state for smoothing the catchment response to precipitation relative to what would have occurred in the comparable natural state. This has significant implications for urban hydrologic design to mitigate hydrologic effects of urbanization. The stochastic sequencing of storms and the interaction of those storms reinforce the importance of measuring hydrologic fluxes for a variety of conditions. At the annual scale, water years 1991, 1992, and 1993, the pervious areas produced 60, 41, and 39% of the annual flow volume for precipitation depths of 1360, 1066, and 959 mm, respectively. A comparison of the peak flow rate produced per unit area of pervious land for Klahanie and Novelty Hill for a major storm in November 1990 shows the importance of the soil column depth in buffering runoff response. The Klahanie response was an order of magnitude larger than for Novelty Hill.

ACKNOWLEDGEMENT

This report reflects the influences of many people. Part A is based on the Doctoral Dissertation of the first author who accords deep appreciation to his wife, Kathy, and two young children, Eric and Tara, for all their support during his studies. We appreciate thoughtful discussions with colleagues Dennis Lettenmaier, Tom Dunne, and Terry Cundy. At various stages we received important help in the form of field work, discussions, and overall contributions to our understanding from Andy Tuthill, Brian Williams, and Bryson Bates; Gretchen Carlson provided critical editorial assistance. We are indebted particularly to Jim Kramer, Manager, King County Surface Water Management Division for his total backing of the project and the support he provided to his professional staff colleagues, Derek Booth, Joanna Richey, Bruce Barker, Rhett Jackson, instrumentation experts Dave Funke, John Koon, and Tim Egan, and graphics expert Fred Bentler. We appreciate the collegiality of all who were involved; we could not have undertaken the project without the essential help of the King County Surface Water Management Division.

This research was supported by the U.S. Geological Survey, Department of the Interior, under USGS award number 14-08-0001-G1887. The views and conclusions contained in this document are those of the authors and should not be interpreted as necessarily representing the official policies, either expressed or implied, of the U.S. Government.

TABLE OF CONTENTS

Modeling and Monitoring to Predict Spatial and Temporal Hydrologic Characteristics in Small Catchments -- Part A: Model Development, Experimental Catchment Selection and Instrumentation, and Short Record Model Calibration and Testing

by

Mark S. Wigmosta

and

Stephen J. Burges

TABLE OF CONTENTS

LIST OF FIGURES

LIST OF TABLES

Chapter 1. Introduction

1.1 Research Objectives

Runoff from land surfaces entrains and transports into channels sediment, chemicals, organic debris, and other materials which affect the characteristics of streamwater. Human activity frequently alters the intensity of runoff mechanisms or introduces mechanisms that did not occur in that area before disturbance. Thus, changes in land use may be accompanied by increases in the size of floods on small streams, water logging of soils, reduction of inter-storm and dry weather base flow, and changes in stream water quality (Dunne, 1982). The need to develop suitable quantitative hydrologic tools for describing flow paths and fluxes within a basin is the primary focus of this work. Because land-use change takes place incrementally, small (zero to third order -- from tens to thousands of hectares) catchments are the hydrologic units considered here.

Conventional lumped-parameter conceptual rainfall-runoff models are often inappropriate for evaluating the effects of land-use change, particularly in small catchments. These models treat a whole basin, or significant portions of it, as if it were hydrologically homogeneous. They are moisture-accounting models that conceptualize the catchment response, rather than represent physical runoff mechanisms. The most widely used models such as STORM (U.S. Army Corps of Engineers, 1976), SWMM (Huber et al., 1981) and HSPF (Johanson et al., 1984) require extensive precipitation and streamflow records for calibration and verification. These models tend to emphasize the hydraulics

of stormwater routing more than the physical hydrologic processes by which storm precipitation is transformed to channel runoff.

Lumped-parameter conceptual models have clearly been successful when applied to the types of problems for which they were developed, such as real-time flow forecasting and the extension of short streamflow records using longer rainfall records. However, problems arise when these models are applied to small (zero to third order) catchments, the scale at which incremental land use change takes place. Their general structure makes it difficult to capture the effects of topography and the spatial distribution of hydrologic properties at this small scale. There is generally a lack of physical interpretation of the fitted parameter values and the models are constrained to replicating integrated discharge hydrographs at the basin outlet. They can not simulate the spatial distributions of critical internal catchment states and fluxes. As a result, prediction of the effects of land use change, particularly where only part of the catchment is affected, is questionable.

Physically-based distributed models were developed to overcome many of the deficiencies of conceptual lumped-parameter models. In theory, physically-based models are "firmly based in our understanding of the physics of the hydrological processes which control catchment response" (Beven, 1985). The descriptive equations for these models are generally solved using numerical integration schemes, such as finite element or finite difference methods. One of the most complex models, the Systeme Hydrologique Europeen (SHE) model (Abbott et al., 1986), solves these equations using a grid of solution nodes. In principle, the parameters of a physically-based model have a direct physical

interpretation allowing them to be estimated from model-independent laboratory and field measurements. The physical basis of input parameters and the distributed nature of these models should make them well suited for evaluating the integrated and spatial hydrologic affects of land-use change, including the movements of pollutants and sediments.

Although physically-based models purport to simulate the internal responses of a catchment, the models are normally tested by their ability to simulate independent storm hydrographs at the basin outlet. Model application still requires calibration, which in many cases includes adjustments to initial state variables. When applied at the catchment scale, with grid nodes 10's or 100's of meters apart, many model parameters lose their physical representation and can not be measured or estimated from field or laboratory data. The model structure may also make it difficult to use internal state variables in calibration or verification. As Beven (1989a) notes, in the case of the SHE model, it is difficult to compare an average grid-square water table level predicted by the model with a piezometer measurement.

Beven (1989a) argues that current physically-based models "are founded in small-scale laboratory physics and are best suited to the essentially research task of exploring the implications of making specific sets of assumptions about the operations of hydrologic systems. They are not well suited to applications in real catchments. They do not overcome the various disadvantages of the "previous generation" of lumped conceptual models in this respect. They are themselves lumped conceptual models, in the sense of relying heavily on "effective" grid scale values of parameters and variables, and are subject to the

same disadvantages."

Wigmosta and Burges (1990) arrived independently at Beven's (1989a) observation that "any application in which physically correct predictions are considered important must involve a close cooperation between field observation and modeling". Direct matching of internal, spatially distributed flow production zones with their model predicted locations as well as measurements of rainfall and streamflow and other fluxes or states is necessary if physically plausible model predictions are to be made.

There remains a need for suitable quantitative hydrologic tools for describing flow paths and fluxes that are important when considering alternative land-use measures. The central objective of this study is to develop a methodology for describing and modeling internal catchment states and fluxes, as well as integrated basin outflow. To meet this objective I have used a combination of field mapping, simple hydrologic monitoring, and hydrologic modeling. This combination approach was tested by it's ability to characterize and predict (model) internal catchment states and flow production, along with basin outflow, in two diverse watersheds; one forested, the other urbanized.

1.2 Research Methodology

Most hydrologic monitoring and modeling is done in a fixed framework: the data have been collected or data are collected with a fixed spatial and temporal sampling scheme. Data are most usually collected without specific consideration of the types and locations of runoff mechanisms within the basin or the complexity and structure of the hydrologic models that may be used. As

a result, most existing methods simplify the hydrologic processes to the extent that they cannot predict catchment runoff response correctly, or the predictive methods require more data than available and hence can not be calibrated and verified properly. Most existing methods use catchment properties averaged over inappropriately large areas and therefore suffer from the inability to describe the spatial variations in the landscape that determine the storm runoff response.

In the combination approach a catchment is first field mapped using techniques described by Dunne et al. (1975) and Burges et al. (1989) to delineate the average areal or wet-season extent of hydrologic process zones based on topography, vegetation, soil depths, and soil type. Field mapping does not provide information on flow rates from production zones, how these zones change with time, or in many cases the locations where water enters the channel. This information guides the initial placement of monitoring stations and preliminary basin dissagregation for hydrologic modeling. The hydrologic process zones identified during field mapping indicate appropriate spatial scales for further hydrologic analysis.

I have used relatively simple hydrologic monitoring which includes streamflow, precipitation, and limited piezometer information. Recorded precipitation and catchment outflow can be used to determine a gross mass balance. When this information is used in conjunction with field mapping it is possible to separate total outflow into flow components (subsurface, surface, etc.). Water level measurements from piezometers at a limited number of locations provides information on hydrologic soil properties and on the nature

and timing of the subsurface response to rainfall.

To estimate the hydrologic response at smaller temporal and spatial scales, and how these responses may be affected by land use change requires the use of a hydrologic simulation model. The complexity of the model (and data collection) should reflect the spatial and temporal scale of the problem. The level of model detail must be consistent with the dominant physical processes present and the level of field measurements that will be used for model input and testing. This allows a feedback between model development and the field program. Field measurements determine what level of model detail is necessary and model simulations dictate where different, or more detailed data collection is required. This combination approach yields information on physical processes which may not be apparent using hydrologic modeling or field monitoring alone.

I have developed a relatively simple model to represent the broad spatial and temporal features of field observable flow processes. The model was designed specifically to simulate all relevant hydrologic processes when the effects of land-use change are to be evaluated. The model simulates flux rates and spatial distributions of evapotranspiration, Horton overland flow, saturation overland flow, return flow, subsurface stormflow, and dry weather base flow. The model is operated continuously in time and has parameters that are readily measured or estimated. The model structure allows simulation results to be verified at any location within the catchment.

Any model of any process incorporates the accumulated understanding of the model builders, their biases, and their prejudices. A model is constructed based on what is known, how what is known can be represented in algorithmic

form, and what observations are available or can be made available to test the fidelity of representation. I have been influenced by my observations in small catchments and predictions from an earlier model which caused me to examine more closely parts of a catchment where few observations had been made.

Catchment water flow production will vary by climatic and geologic region and by the specific basin characteristics. The approach discussed here has been developed using small basins in the Pacific Northwest. In this humid maritime climate the dominant hydrologic process zones are associated with open channels; wetlands; water storage from vegetation, forest litter, and soils; areas of Horton overland flow; saturation overland flow; return flow; and subsurface flow. The relative importance of these process zones changes with differing storm distributions and is strongly influenced by antecedent basin conditions.

Improvements in both modeling and computing capabilities, particularly the availability of catchment simulation models that can be run on microcomputers, suggests that the future use of simulation models for hydrologic analysis should be much more common. Use of accurate solid state recording equipment for collection and recording of meteorologic and hydrologic data for use with catchment models, promises improvements in model prediction accuracy for catchments for which lengthy historical data bases do not exist. While such improvements will make it possible to model flow at more stream locations within catchments than before, present models will still be constrained to providing average responses from subcatchments and will be unable to reflect the actual variations in space (and time) throughout each

subcatchment. It is these variations that are crucial to understanding and managing hydrologic impacts resulting from land-use change. Hydrologic models in general use do not capture enough of the landform aspects of hydrologic interactions at the scale of change (on the order of acres in many cases). Further model development of the form described here is necessary to accommodate changes in data collection, storage, and management protocols, and incorporation of field mappable hydrologic process zones.

To evaluate the effects of land-use change requires accurate quantitative representation of the mechanisms by which precipitation is transformed to runoff. Chapter 2 summarizes the relevant literature on flow production. Pertinent aspects of past research in runoff models is also presented. The primary focus of the present work is to develop a combination of field mapping, simple hydrologic monitoring, and hydrologic modeling to describe catchment hydrologic states and fluxes. Chapter 3 gives the research design utilized for this work, including specific research tasks and methodologies. The continuous hydrologic simulation model is described in chapter 4. The systematic modeling and monitoring approach is applied to a forested catchment in chapter 5 and to an urbanized basin in chapter 6. Chapter 7 provides a summary and conclusions.

Chapter 2. Literature Review

The review given herein focuses on the primary elements related to observed runoff processes, and past work that attempts to quantify or model the physics of such water movement. The respective merits, demerits, successes and limitations of theses works are discussed.

2.1 Runoff Mechanisms

To evaluate the effects of land-use change within a natural catchment, and ultimately what can be done to mitigate these effects, requires accurate quantitative representation of the mechanisms by which precipitation contributes to runoff in the natural (before) and changed (after) states. Large variations in subcatchment runoff production can occur even within relatively small catchments. Four basic mechanisms have been identified by which the rainfall-stormflow transformation takes place: Horton overland flow, saturation overland flow, subsurface storm flow, and return flow. The climatic and environmental factors governing these processes are summarized qualitatively in Figure 2-1.

2.1.1 Horton Overland Flow (HOF)

During a storm infiltration is reduced as soil pores fill with water and clays swell. In addition, if the soil is unprotected, rainsplash may pack the soil surface and disperse fine soil particles causing them to plug soil pores. Any time the infiltration rate falls below the rainfall intensity water will pond at the soil surface and fill small depressions. When the depression storage is filled,

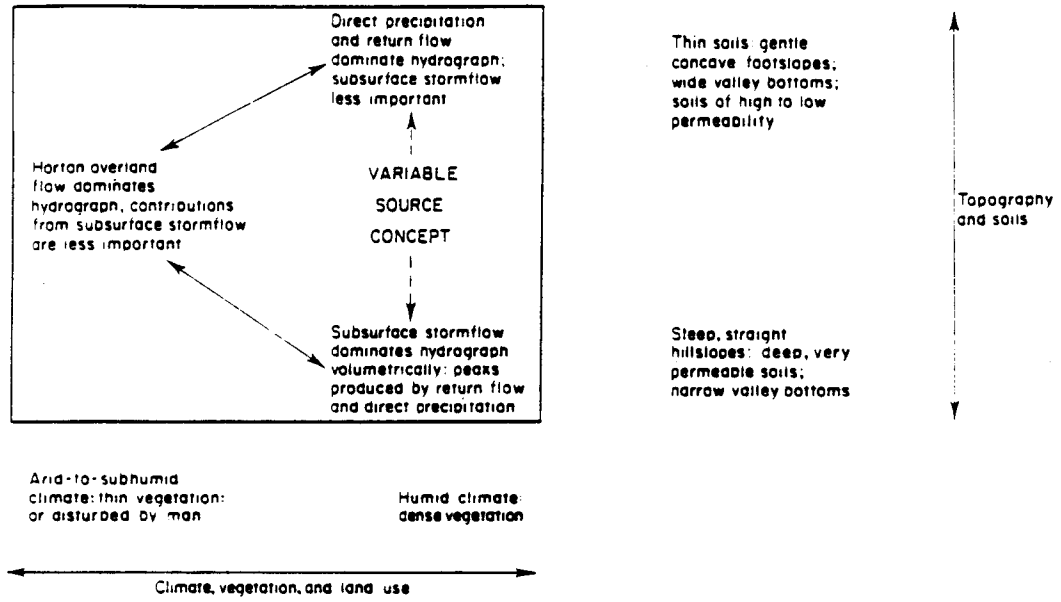

Fig. 2-1. Climatic and environmental factors governing runoff production (adapted from Dunne, 1982).

water spills over to run downslope as an irregular sheet or as ribbons of overland flow. This mechanism of runoff generation was first identified quantitatively by Robert Horton (1933 and 1940) and is termed Horton overland flow.

Horton overland flow occurs most frequently in arid and semi-arid landscapes where vegetation densities and infiltration rates are low. This mechanism also occurs in disturbed areas of humid landscapes, such as cultivated fields, pastures, lawns, paved areas, construction sites, and rural roads (Dunne, 1983). Horton overland flow typically moves at velocities of 0.003 to 0.15 m/s (Dunne, 1982).

2.1.2 Subsurface Storm Flow (SSF)

In densely vegetated humid regions the infiltration capacity is usually high enough to absorb all but the rarest, most-intense storms (Dunne, 1982). The existence of a litter zone protects the mineral soil from rain impact and maintains high surface permeabilities that promote high percolation rates to the A and B horizons. In many soils, infiltrating water may encounter a relatively impermeable layer and be diverted laterally toward the stream channel (Mosley, 1979; Pilgrim et al., 1978; Weyman, 1970, 1973; Whipkey, 1965).

Subsurface water may move slowly through the interganular and interpedal voids of the soil matrix, with velocities of the order 10^{-2} - 10^{-8} m/s (Dunne, 1982). Such flows are typically classified as Darcian and can be described by the continuity equation in conjunction with Darcy's law for porous media. Analytical and computer simulations indicate that rapid subsurface

responses by Darcian mechanisms may only occur under a limited set of conditions. Beven (1982a and 1982b) found rapid Darcian responses required a combination of very high hydraulic conductivities, wet initial conditions, shallow soil depths, relatively steep slopes, or short effective slope lengths. In an earlier examination of this mechanism using computer simulations of a Richard's equation (Richards, 1931) formulation, Freeze (1972a) concluded that rapid Darcian runoff was only feasible where convex hillslopes feed deeply incised channels.

Three mechanisms have been suggested to account for rapid subsurface flow response. Hewlett and Hibbert (1967) coined the term "translatory flow" to describe the process by which pre-storm soil water stored in the middle and lower portions of a hillslope is displaced by water infiltrating upslope. Other workers have suggested that rapid, perhaps turbulent flow through larger non-capillary "macropores" (approximately 1 mm and larger) such as root holes, shrinkage cracks, and the burrows of soil fauna may produce accelerated subsurface responses. Published macropore velocities (Beven and Germann, 1982) range from 2.4 x 10^{-4} m/s up to 2 x 10^{-2} m/s (1 - 70 m/hr). It is likely that the relative importance of macropore flow increases with rainfall intensity, antecedent soil moisture, the linearity of the moisture content-tension relationship, and decreases with increasing soil depth (Dunne, 1990). A third concept that has been used to account for rapid subsurface responses is "groundwater ridging", a term used by Sklash and Farvolden (1979), but originally described by Ragan (1968). Under this mechanism, a small addition of infiltrated water converts the capillary fringe near the stream channel into a

zone of positive pressure. The resulting rapid increase in near-stream hydraulic head causes a substantial increase in subsurface flow to the channel. The interrelationships of these mechanisms was the subject of a recent investigation by McDonell (1990).

2.1.3 Return Flow

There is a limit to the amount of subsurface flow which can pass downhill within the soil profile. Under Darcian assumptions this limit is governed by the hydraulic gradient, the hydraulic conductivity, and soil thickness. When this limit is exceeded water is forced to reemerge from the soil surface as return flow (Musgrave and Holtan, 1964; Dunne and Black, 1970a,b). This mechanism is most likely to occur where subsurface flow is forced to converge, or where the gradient, soil thickness, and hydraulic conductivity decrease (Dunne, 1990). These conditions are most common on footslopes and in swales. The contributing area of return flow could be expected to expand rapidly in areas where the capillary fringe is close to the surface (Beven, 1989b).

2.1.4 Saturation Overland Flow (SOF)

On some parts of a hillside, usually the lower portion of a concave hillslope, the soil may become saturated to the surface by a rising groundwater table, or by percolation above an impending horizon. Rain falling on these locations can not infiltrate but runs over the surface as saturation overland flow (Dunne and Black, 1970 a,b). Some of the water moving slowly through the topsoil may emerge and flow overland to the channel as return flow. Saturated

overland flow velocities, which may or may not include return flow, are typically between 9×10^{-5} and 3×10^{-2} m/s (Dunne, 1982).

Saturation overland flow tends to dominate storm runoff in landscapes with thin soils of low conductivity, high water tables, and long gentle concave hillslopes. During a storm the saturated zone may spread upslope into topographic hollows and zones of shallow, wet, or less permeable soil (Dunne, 1982). The areal extent of saturated zones expand and contract more slowly through the year in response to seasonal changes in soil moisture.

2.2 Quasi-Physics Based Hydrologic Models

2.2.1 Coupled Surface-Subsurface Flow Models

Physical modeling of coupled surface and subsurface flow processes have been made by Freeze (1972a,b), Smith and Hebbert (1983, 1984), and more recently by Binley et al. (1989a,b). However, detailed models of this type are confined to simple geometries at the elemental hillslope scale. Attempts to extend these models beyond the hillslope element scale, place huge demands on computer storage and execution time (Gan, 1988), making them impractical for routine application. The Systeme Hydrologique Europeen (SHE) model (Abbott et al., 1986) provides increased flexibility in how catchment characteristics can be represented. However, its general use is limited by large data input requirements and computational demand. This suite of models is still being developed and tested at a relatively small number of centers.

A simpler model for medium-sized catchments was developed by Beven and Kirkby (1979). They attempted to integrate the distributed effects of the basin into simple, lumped storage components for sub-basins linked together by a channel network. The subbasins are divided according to soil type and topography. For each subbasin, three basic flow mechanisms (HOF, SOF, and SSF) are generated by simplified physical and storage relations. When applied to an 8-km^2 catchment in England, the model produced satisfactory results. Since its development, the model has appeared in several forms (Beven, 1988a). Some model parameters lack physical basis, making the model inappropriate for describing smaller catchments prior to and when undergoing land-use change.

2.2.2 Process Models of Surface and Subsurface Flow

Process models deal with a specific process in the overall picture of watershed response. For instance, models of overland flow generally assume that flow depth, velocity, and discharge can be described by the classic shallow water equations. Frequently these flow equations are solved after simplification by means of the kinematic-wave approximation. Woolhiser and Liggett (1967) found this simplification to be valid under most circumstances. Kibler and Woolhiser (1970) used the kinematic approximation to simulate Horton overland flow on a "cascade" of impervious planes of different slopes and roughness. This approach was extended to a pervious surface by Smith and Woolhiser (1971), who used the one-dimensional form of Richard's equation (Richards, 1931) to describe infiltration.

Engman and Rogowski (1974) attempted to model Betson's (1964)

partial area concept by coupling Philip's (1969) approximate infiltration equation with the kinematic approximation for overland flow. Spatial variations of soil type, and hence infiltration, allowed simulated expansion of the watershed area contributing overland flow during a storm. Dawdy et al. (1978) used detailed kinematic wave routing of overland and channel flow coupled with the Green-Ampt infiltration equation.

Most subsurface flow models neglect the effects of macropores and assume flow in the soil matrix may be described by Richard's equation. Freeze (1971) used a finite-difference solution for three-dimensional, heterogeneous, isotropic, saturated-unsaturated, confined-unconfined flow. Binley et al. (1989a,b) have modeled three-dimensional flow through variably saturated soil using the Galerkin approximation to the finite element method. Two-dimensional, saturated-unsaturated flow models have been developed by Freeze (1972a,b), Neuman (1973), and Reeves and Duguid (1975). These types of models require that the geometry and hydraulic properties of the soil be known in considerable detail. Computational restraints generally only allow single, short-duration storms to be modeled at the elemental hillslope scale.

Beven (1981, 1982a) developed a computationally practical analytical, kinematic wave model to solve a simplified representation of subsurface flow. In his model, saturated hydraulic conductivity and saturated water content are assumed to decrease with depth. The model is restricted to a single rainfall event of constant intensity. The wetting and drying fronts are each represented by a moving sharp boundary (piston-type flow approximation). Beven's model was extended to a kinematic cascade by Park (1985). Hurley and Pantelis

(1985) further extended the kinematic approach to a curved hillslope profile (of unit width) and allowed downslope flow in the unsaturated zone. The resulting ordinary differential equations were solved numerically.

Sloan et al. (1983) and Sloan and Moore (1984) developed two simple storage-discharge subsurface flow models based on kinematic and Boussinesq assumptions. Their model results, particularly the kinematic assumption, compared favorably with more complex models when applied to field situations. In the kinematic storage model the entire hillslope segment is taken as a control volume, with an impermeable bed of slope α and length L, and soil thickness D (Figure 2.2). This model assumes that the water table has a constant slope between the upslope and downslope boundaries of the soil mass, and that the hydraulic gradient equals the slope of the impermeable bed. Discharge (q) at the downslope outlet is given by:

$$q = HK\alpha \tag{2-1}$$

where K is the soil saturated hydraulic conductivity and H is the saturated thickness at the outlet, measured normal to the hillslope. Combining these boundary conditions with a finite difference form of the continuity equation allows the hydraulic head at the outlet at the end of each time increment, Δt, to be expressed explicitly as:

$$H^{t+\Delta t} = \frac{H^t(L\gamma - K\alpha\Delta t) + 2Lp\Delta t}{(L\gamma + K\alpha\Delta t)} \tag{2-2}$$

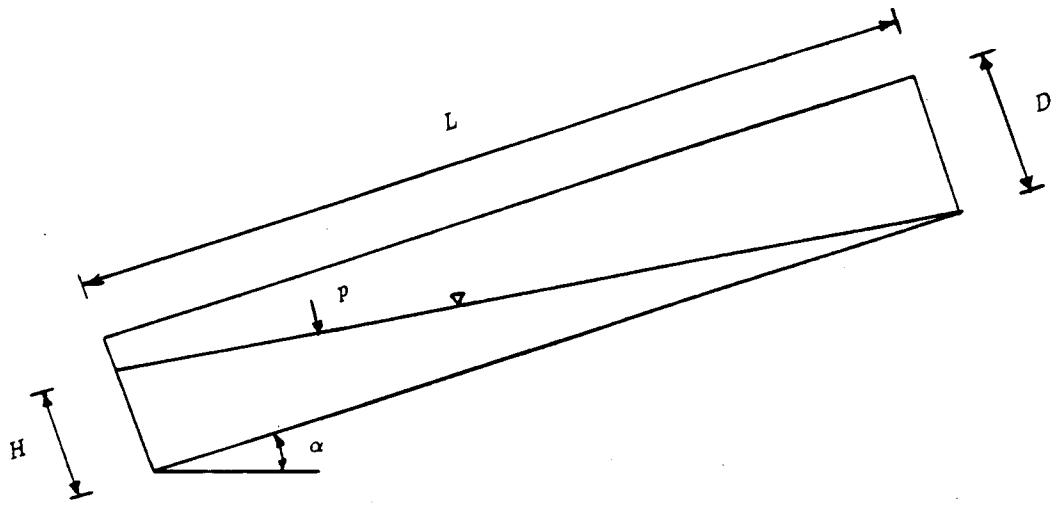

Fig. 2-2 Hillslope vertical section defining the symbols used in the kinematic storage model of Sloan and Moore (1984).

where γ is the drainable porosity of the soil, and p is the rate of water input from the unsaturated zone to the saturated zone. This input rate is taken as a function of the volume of water stored in the unsaturated zone, i.e.,

$$p = K(\theta) \tag{2.3}$$

where K is the unsaturated hydraulic conductivity associated with θ, the spatial average volumetric water content in the unsaturated zone at time t. The spatially averaged unsaturated zone moisture is determined through mass conservation.

Sloan et al. (1983) compared the drainage and cumulative drainage profiles of this model and four others. The additional models were Nieber and Walter's (1981) and Nieber's (1982) one- and two-dimensional finite element solutions of Richard's equation, Beven's kinematic wave model (1981, 1982a), and the Boussinesq storage model of Sloan et al. (1983). The application of each model was compared to the experimental results of Hewlett and Hibbert (1963) who used a concrete-lined soil trough to study the drainage characteristics of steep sloping forested watersheds. The 0.91 x 0.91 x 13.7 m (3 x 3 x 45 ft) trough was constructed on a 40 percent slope (4 vertical to 10 horizontal) and filled with a reconstructed forest soil (C Horizon of a Halewood sandy loam). The soil was soaked using sprinklers, covered with plastic to prevent evaporation, and allowed to drain.

Because the soil was mixed and compacted in the bed of the soil trough, the effects of macropores were removed. Water movement in homogeneous soils

with no macropores is the simplest physical subsurface flow system to represent. Therefore, Sloan et al. (1983) felt Hewlett and Hibbert's (1963) discharge data is "a logical place to begin testing and/or developing and validating physically based models of subsurface flow, since Hewlett's system represents the simplest *ideal* condition".

Predicted drainage from the five models is compared with the measurements of Hewlett and Hibbert (1963) in Figure 2-3. The predictive accuracy of the kinematic storage model appears to be as good or better than that of the more complex models, including those using Richard's equation. The kinematic storage model allowed an almost 300-fold decrease in computer CPU time relative to the one-dimensional finite element model.

Sloan et al. (1983) also evaluated Nieber's 1-D finite element model, the kinematic wave model, and the kinematic storage model by applying them to observed and calculated rainfall-runoff relationships for four storms on a steep forested test plot. Precipitation input for the 1-D model and the kinematic storage model had a 30-minute time increment. Since the kinematic wave model was not set up for variable rainfall a constant rate was used throughout the storm. Three levels of saturated hydraulic conductivity were selected a priori. The baseline conductivity was 0.12 m/hr, corresponding to the hillslope average based on 76 mm (3-inch) core permeameter measurements. The second and third levels were one and one and a half orders of magnitude above the baseline, 1.2 and 6 m/hr respectively.

The kinematic storage model was found to be more accurate than the one-dimensional finite element or kinematic wave models in simulating runoff

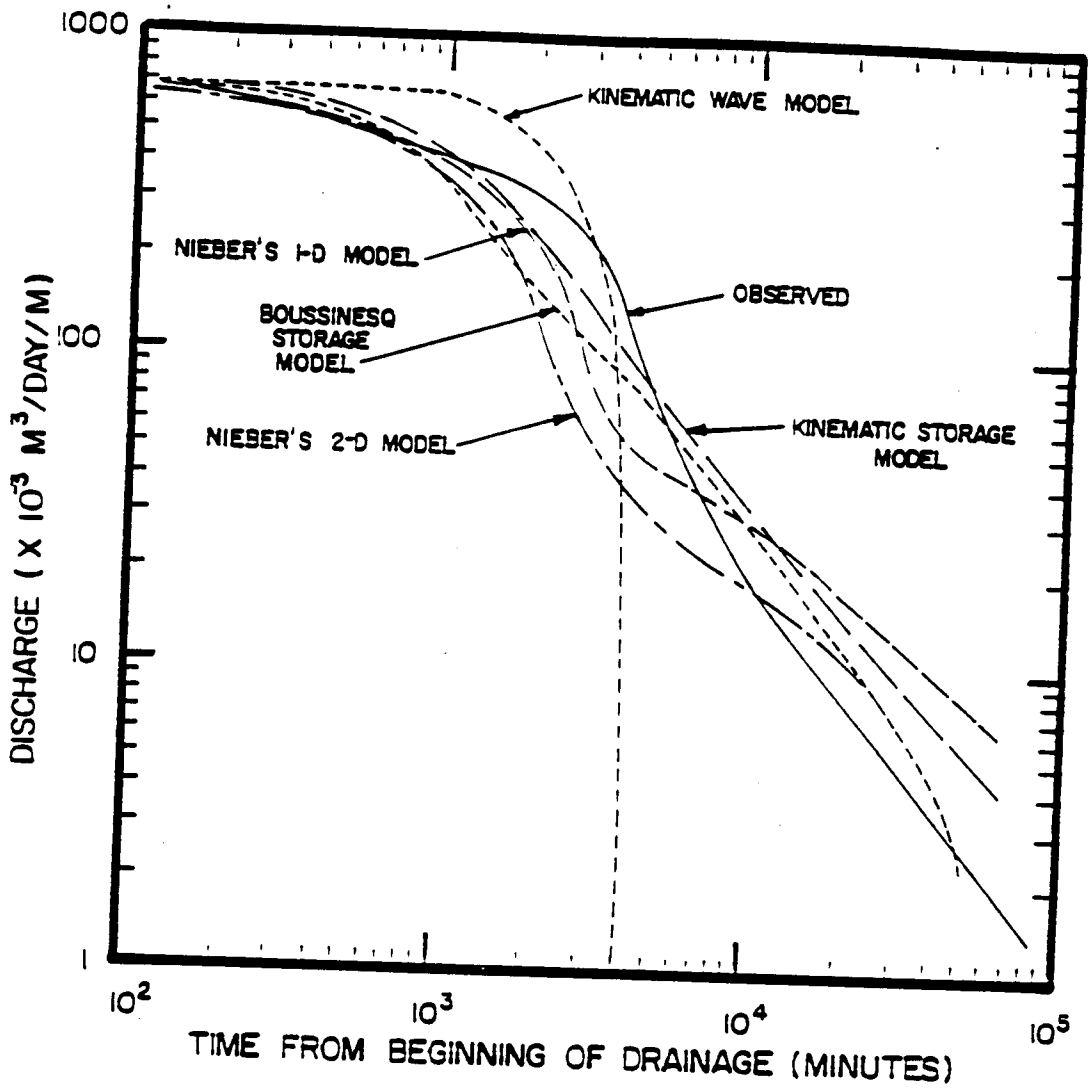

Fig. 2-3. Comparison of observed and predicted drainage hydrographs for Nieber's 1-D and 2-D models, the kinematic wave subsurface model, and the kinematic and Boussinesq storage models for a saturated conductivity of 16.8 cm/hr (from Sloan et al, 1983). (The maximum discharge was approximately 0.65 m^3/day/m.)

from the test plot. Sloan et al. felt that the kinematic storage model gave the best results because it's "assumption for stormflow through macropores and soil pipes is valid, while Darcian flow simulated by the 1-D model is not."

The kinematic storage model was initially run with the unsaturated storage input algorithm (2-3) that was used in the soil trough simulations. The agreement between simulated and observed hydrographs was poor. There was an excessive time lag and the unsaturated storage input zone dampened out the rainfall-runoff relationship. As the forest soil profile contains many macropores which allow quick vertical flow, Sloan et al. decided to test the model with no time delay between precipitation and input to the saturated zone. This greatly improved model results. In all cases the simulation improved as the hydraulic conductivity was increased.

Reddi et al. (1990) coupled Sloan and Moore's (1984) kinematic storage model with a three component unsaturated zone model. They also extended the model geometry to allow surface and subsurface topography to be represented by two sloping convergent planes. Simulated water table levels were compared to those of a more complex 2-dimensional finite difference model and to field measurements in a small drainage depression. In the finite difference model, flow in the unsaturated zone is ignored and it is assumed rainfall creates an instant recharge to the saturated zone. The authors found that the predictive accuracy of the Sloan and Moore based model was as good as the 2-dimensional model; however, there were noticeable differences between model predictions and field observations.

Ormsbee and Khan (1989) embedded Sloan and Moore's (1984)

kinematic storage model into the U.S Army Corps of Engineers HEC 1 model (1985) and applied it to four watersheds in West Virginia and eastern Kentucky. The model was calibrated to two winter and two summer storms in each watershed. The unsaturated zone was not modeled and model parameters (saturated hydraulic conductivity and effective porosity) were optimized for each storm. The model over-predicted storm volumes and substantially under-predicted the peak discharge.

Because of the marginal model performance a conceptual macropore component was added. The resulting model is composed of five storages and requires 12 parameters. Performance is substantially improved, however the model is quite conceptual in nature with many input parameters having no physical basis.

Ogawa and Ebisu (personnel communication, 1990) have developed a rain-runoff model in which hillslopes are represented by rectangular planes with 3 soil layers (designated from the surface downward, A, B, C). The model can generate Horton overland flow, saturation overland flow, and lateral subsurface flow in the A and B soil layers. These flows are modeled using a kinematic wave approximation. Flow is vertical within the C layer. General use of the model is limited by it's extensive data requirements.

The Hydrology Centre, Christchurch, New Zealand is developing a computer modeling system that utilizes a time-continuous saturated flow model based on Sloan and Moore's kinematic storage model (Ibbitt, 1989a). The unsaturated zone is modeled using a one-dimensional, piston flow approximation (Ibbitt, 1989b). Overland flows are routed across an infiltrating

plane using a kinematic wave method (Woods and Ibbitt, 1988). Hillslopes are approximated as sloping rectangular blocks of soil and reaches are modeled as wide rectangular channels of constant width.

The large data requirements and computational demand of complex finite difference models make them inappropriate for routine application. These models are presently restricted to simple geometries at the elemental hillslope scale. When applied to field situations some input parameters lose their physical representation and the results from complex models are generally no better than simulations from simpler models such as the kinematic storage model of Sloan and Moore (1984).

A new continuous simulation hydrologic model which was constructed to overcome the practical limitations of more complex models is presented in Chapter 4. The model is capable of simulating the four dominant runoff processes described in Section 2.1. All input parameters can be measured or estimated in the field, thereby avoiding the limitations of models that are structured conceptually. Topographic influences on runoff production are incorporated explicitly in the model. Catchment flow dynamics are represented using computationally efficient analytical and numerical approximations, allowing long-term continuous simulation on personal computers.

Chapter 3. Research Design

The need to develop suitable quantitative hydrologic tools for describing flow paths and fluxes that are important when considering alternative land-use measures is the primary focus of this work. Because change takes place incrementally, small catchments are the hydrologic units considered here. I have chosen to implement a systematic, adaptive combination of field mapping, simple hydrologic monitoring, and hydrologic modeling (combination methodology), to describe catchment states and fluxes. Land-use change in the form of urbanization was chosen for study because it generally results in the greatest alteration of internal catchment runoff production.

3.1 Research Tasks

The tasks carried out are summarized under four main categories:

1) Development of a relatively simple model to represent the broad spatial and temporal features of field observable flow processes;

2) Selection of and monitoring of two basins to evaluate the combination methodology for describing catchment states and fluxes under natural and under urbanized conditions;

3) Initial application and refinement of the combination methodology in the selected basins; and

4) Limited verification of the hydrologic simulation model.

Tasks 1 and 2 were undertaken concurrently. Both study catchments are underlain by glacial till and were chosen in part for their ability to be gaged and for remaining unchanged throughout the likely duration of observations. Boundary conditions (drainage area, soil depths, etc.) are well defined, allowing rigorous testing of the model. Tasks 1 and 3 were also carried out concurrently. Field measurements influenced me in deciding how to model various processes and were used to test the model structure. Examination of model simulations provided guidance in determining where additional field measurements were required, both for an increased understanding of basin hydrology and to test the model more thoroughly. The level of model detail and the scale of field measurements were consistent with the dominant hydrologic processes present at both catchments. This allowed a feedback between model development and the field program while increasing the understanding of catchment hydrology. The current model was verified in Task 4 using data which were not available in Task 3.

3.2 Methodology

The approaches used for each task are:

Task 1:

Field studies have shown that direct application of Darcian saturated and unsaturated flow concepts may not be realistic under many field conditions (Whipkey, 1965; Weyman, 1970; and Mosely, 1979; Sloan et al., 1983). As

pointed out by Beven (1988b), that while Richards (1931) equation is an adequate descriptor of unsaturated flow in homogeneous soil (in the laboratory), reality in the unsaturated zone is one of complexity and heterogeneity which does not conform to the assumptions underlying the equation's formulation. Based on a comparison of the predictions of five physically based subsurface flow models with observed data, Sloan and Moore (1984) concluded that the assumptions inherent in the development of more complex models "may be as limiting as the assumptions involved in the simpler models".

To address the limitations of both conceptual lumped-parameter models and highly complex physically-based distributed models (designed largely to address scientific questions about flow production), a relatively simple model that balances the above concerns and observations was developed (Chapter 4). The model uses commonly measured hydrologic fluxes (e.g., precipitation and channel flow) as well as easily obtainable supplemental spatial and point measures of hydrologic states (e.g., shallow water table elevations and the plan extent of saturation zones). While collected infrequently at present, these additional data will become essential components of catchment quantitative hydrologic data sets.

I am cognizant of previous and ongoing research concerning how to include spatial variation in field measured hydrologic quantities (e.g., saturated hydraulic conductivity) into models. For surface flow dominated situations, the degree of precision needed to represent the spatial distribution of bulk infiltration is a function of the relative amounts of infiltration and rain that reaches the ground surface. In situations where most rain enters the ground,

Binley et al. (1989a,b) have shown with theoretical simulations that detailed representation of spatial infiltration is needed to describe surface runoff. For lateral subsurface flow they found that an effective saturated hydraulic conductivity was suitable for describing flow rates; the findings for this case are consistent with simpler theoretical tests made by Bresler and Dagan (1983).

The model was designed specifically for application in "natural" catchments that will experience change and simulates Horton overland flow, subsurface flow, return flow, and saturation overland flow. It has 21 parameters (all with physical basis) to be estimated a priori or determined by calibration, preserves the affects of topography and the spatial variation of hydrologic properties, and is computationally efficient. Most input parameter values are estimated through simple field measurements.

Task 2:

Three criteria were used in selecting the study basins: 1) they must allow the combination methodology to be applied under natural conditions in one catchment and under urbanized conditions in the other; 2) they can be gaged accurately; and 3) boundary conditions can be defined properly to allow rigorous testing of the model during and after development.

A 37 ha forested catchment east of Lake Washington was selected to represent natural conditions and a 17 ha subbasin east of Lake Sammamish within the development known as "Klahanie" was chosen as representative of urbanized conditions (Figure 3-1). Housing densities, greenbelts, and the storm drainage system at Klahanie are typical of recent planned communities in King

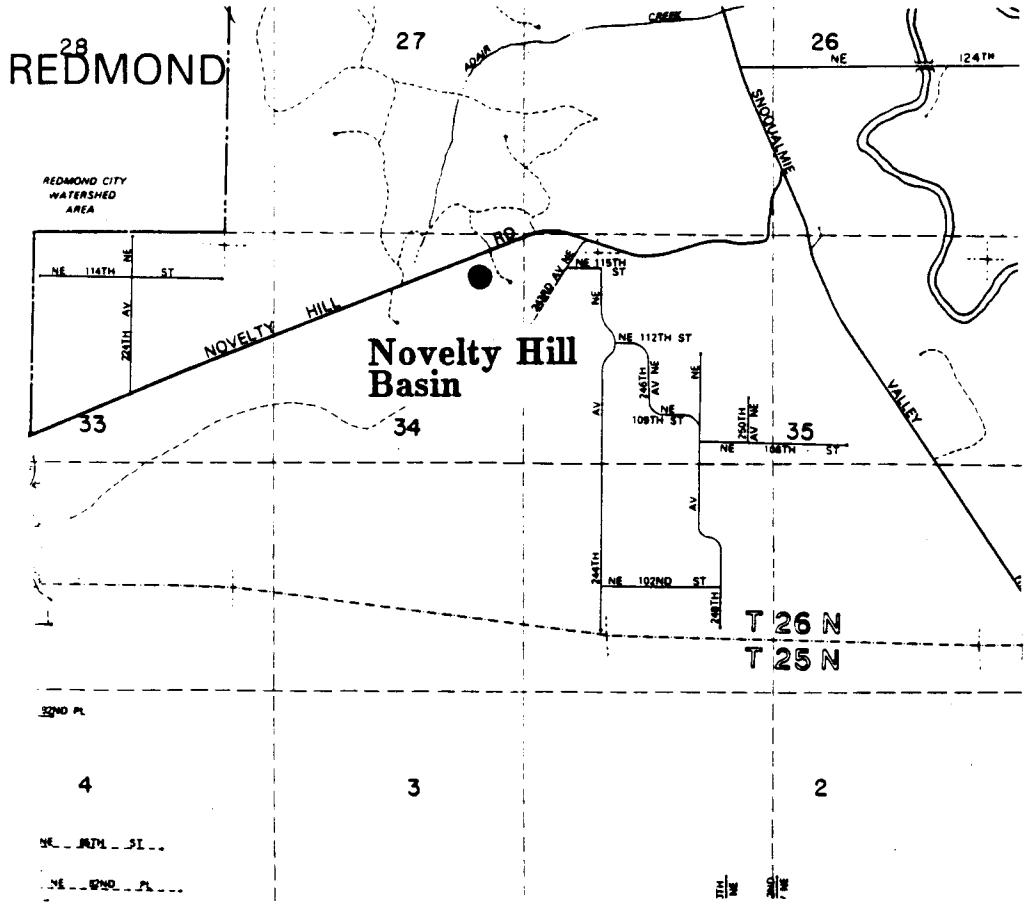

Fig. 3-1a. Location of the Novelty Hill, Washington (Forested) Test Basin.

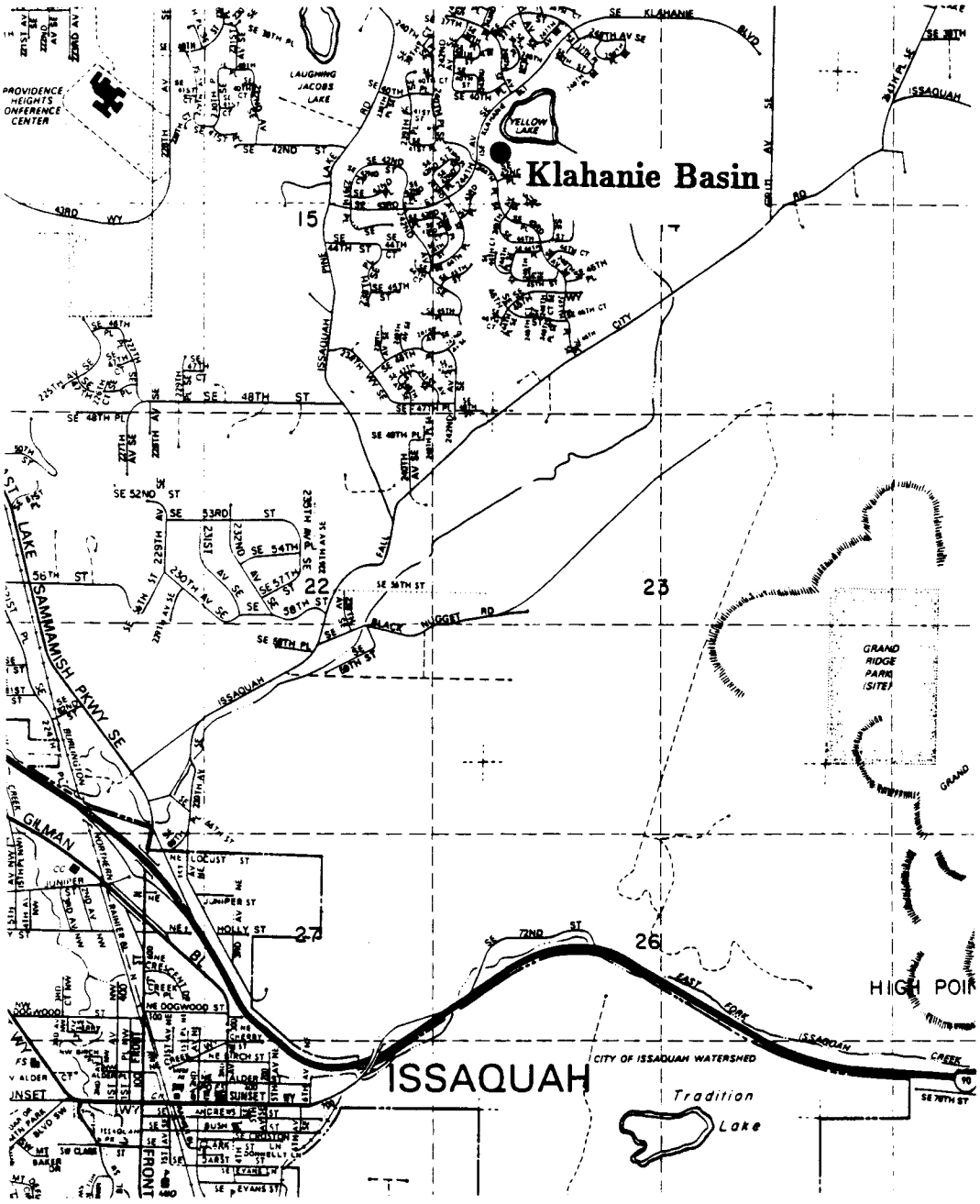

Fig. 3-1b. Location of the Klahanie, Washington (Urban) Test Basin.

County, Washington.

The two study basins were selected to demonstrate that any differences in runoff production could be attributed primarily to land use. Geologic conditions at the two sites are similar, both are contained within broad plateaus and are underlain by the Vashon glacial till - a dense, nonsorted, nonstratified deposit of silt, sand, and gravel. The soils in each catchment are classified as gravelly sandy loams. Prior to development, soil thickness at Klahanie was similar to that at the forested (Novelty Hill) site. The two basins also received nearly equal amounts of rainfall during the study period. Although the Klahanie site is generally steeper, most of the differences in runoff production and evapotranspiration between the two catchments results from land use.

The two catchments are zero-order and have relatively well defined boundary conditions. All flows leaving each basin appear to have been generated entirely within the basin; no inter-basin transfer of surface or subsurface flows is apparent either from process zones identified during field mapping or from analysis of recorded rainfall and streamflow. Basin boundaries are well defined, soil depths can be accurately measured, and the glacial till is continuous throughout the catchments, providing a lower boundary of relatively constant hydrologic properties.

Numerous zero-order forested catchments were investigated as possible study sites. Many of them would have been developed prior to completion of the study. Most of the remaining basins were drained by broad swales making them difficult to gage. The selected Novelty Hill site was logged near the beginning of the century and is presently covered with second-growth forest.

An abandoned railroad grade forms the lower basin boundary. Discharge from a swale flows through a culvert in the railroad grade, before being measured using a compound weir. The railroad grade rests on till and the weir is keyed into the till. As a result, nearly all surface and subsurface discharge leaving the catchment above the till layer is recorded. The combination sharp crested v-notch and rectangular weir was sized to allow accurate measurement of discharge over a wide range of flow rates.

In most of the urban catchments that have been investigated before selecting the Klahanie site surface flows are collected by the storm sewer system and leave the basin in a pipe. Flow in pipes is generally difficult and expensive to gage. In gaging just the outlet pipe it is possible to miss a large portion of the runoff generated on pervious areas which normally are not directly tied into the stormwater conveyance system. This results in a poorly defined boundary condition (an unknown percentage of flow is missing the gage) that limits model testing. The stormwater conveyance system at Klahanie discharges to a central engineered swale which was cut into the till layer. Pervious areas also discharge to the swale. A sharp crested low-flow v-notch weir and a high-flow sharp crested rectangular weir were used to measure discharge from the swale at the basin outlet. Both weirs are keyed into the till. As for the forested (Novelty Hill) site, nearly all surface and subsurface flow leaving the catchment above the till is measured at the weirs.

At both study sites rainfall and streamflow are measured at 15-minute intervals using solid-state data loggers. The rain gages are located away from buildings and trees so the catch is representative of the basin.

Task 3:

Initial application of the adaptive combination of field mapping, hydrologic monitoring, and hydrologic modeling began at Novelty Hill in October 1989 and continued through the remainder of Water Year 1990 (October 1, 1989 - September 30, 1990). Selection of the urban site was delayed, with initial application beginning in early October 1990. Each basin was field mapped for flow process zones following the techniques described by Dunne et al. (1975) and demonstrated in Burges et al. (1989). Aerial photos, 1.5-m (5-feet) contour maps, and soils maps were used in the mapping process. Basin boundaries were defined and soil depths were measured using a hand auger. Infiltration areas and locations that generate Horton overland flow were mapped. The seasonal extent of saturated areas was determined in the field from topography, soil morphology, and, to a lesser extent, vegetation. The maximum extents of saturated zones were defined from field observations during large storms.

Saturated zones occur where discharge from upslope contributing areas exceed the product of soil transmissivity and local hydraulic gradient. The model's representation of topography and subsurface flow paths was checked in part by its ability to model the locations of these zones. The observed locations and seasonal extent of saturated zones was also used to test the simulation of "time averaged flow dynamics" at various locations in each catchment.

In the Novelty Hill catchment a transect of six piezometers extending from the ridge crest to the valley bottom was installed in the upper basin to monitor shallow water table levels. One piezometer was instrumented to allow

measurements at 15-minute intervals. The five remaining piezometers contain crest gages to determine peak water depths. All piezometers were measured at about one-week intervals during Water Year 1990.

Field mapping and the first year of monitoring data at Novelty Hill were used to separate total basin outflow into flow components (surface, subsurface, etc.) at the annual scale and to estimate spatially averaged soil hydrologic properties. The piezometers recorded water table responses to rainfall. All of this information provided constraints during model simulations allowing a more complete test of the model structure (particularly subsurface components) than if just rainfall and integrated catchment outflow were used Model simulations provided an estimate of water loss through the glacial till, and helped refine field estimates of soil properties (saturated moisture content and field capacity). The simulations of flow components and spatial locations of process zones provided guidance in determining where additional monitoring stations were required; both for an increased understanding of catchment hydrology and to provide a more complete test of the model. Consequently, in November 1990 a second group of four piezometers was installed near the basin outlet.

Detailed field mapping at Klahanie provided the locations of impervious surfaces (roads, sidewalks, driveways, roofs, etc.) that are connected directly to the surface flow conveyance system. This information was used in conjunction with recorded rainfall and streamflow to separate the volumes of Horton overland flow generated on impervious surfaces from discharge originating in pervious areas of the catchment. This allowed model simulated runoff from pervious and impervious surfaces to te checked separately.

Model simulations and field measurements show pervious areas at Klahanie (approximately 70 percent of the basin area) contribute the majority of storm runoff. Field mapping and model runs suggest this rapid pervious area response is primarily subsurface. Additional field observations will be required during storms to define the runoff mechanism(s) more precisely. Such improved understanding of flow paths might be useful, for example, if the model were to be coupled with a model of geochemical processes governing water quality.

Task 4:

Task 3 was conducted at the Novelty Hill site during Water Year 1990 and from October 16, 1990 through May 15, 1991 at Klahanie. During this time the model was developed and calibrated under forested and urban conditions. The model was then verified at the Novelty Hill site using rainfall, streamflow, and piezometer measurements from the period October 1, 1990 through May 17, 1991.

Measurements used in this study were intentionally restricted to those methods which are simple, low cost, and manual or semi-automated (e.g. piezometers with crest gages), so that data collection time and expense are minimized, and do not require observers to be in the catchment during all storms. These requirements are typical of circumstances that would be experienced by personnel from public agencies and consulting firms (and many research scientists) who would subsequently use this or a similar approach. Such measurements are of great value in model validation because they provide

essential information about actual flow paths not contained in measured channel flow hydrographs. These types of measurements are not made frequently; I am not aware of any comprehensive model (including the suite of models contained in SHE) that makes direct use of such important and relatively easily obtainable information.

Chapter 4. Continuous Hydrologic Simulation Model

To evaluate the effects of land-use change in a natural catchment, and ultimately the possibility for mitigation, requires accurate quantitative representation of the mechanisms by which precipitation contributes to runoff in the natural (before) and changed (after) states. Any model developed to evaluate these effects at the small (zero to third order) catchment scale must be able to simulate explicitly the four primary runoff processes discussed in Chapter 2.

The land component of the model is composed of six major elements that simulate canopy and litter zone interception; evapotranspiration; infiltration; and surface, unsaturated, and saturated subsurface flow dynamics (Figure 4-1). The catchment to be modeled is divided into subareas based on soil type and depth, vegetation type, topography, and field-mapped hydrologic process zones. Spatial and temporal variations of Horton, subsurface, return, and saturation overland flow are simulated for land segments within each subbasin. Each subbasin is modeled separately, and the results from all subbasins are combined using a flexible channel routing scheme (Section 4.7).

Time series of precipitation and potential evapotranspiration drive the model. Calculations are made for all model elements on a finite time interval (normally 15- or 60-minutes) using updated rainfall and potential evapotranspiration amounts. Actual evapotranspiration is computed for each time step as a function of moisture conditions and the current potential evapotranspiration demand.

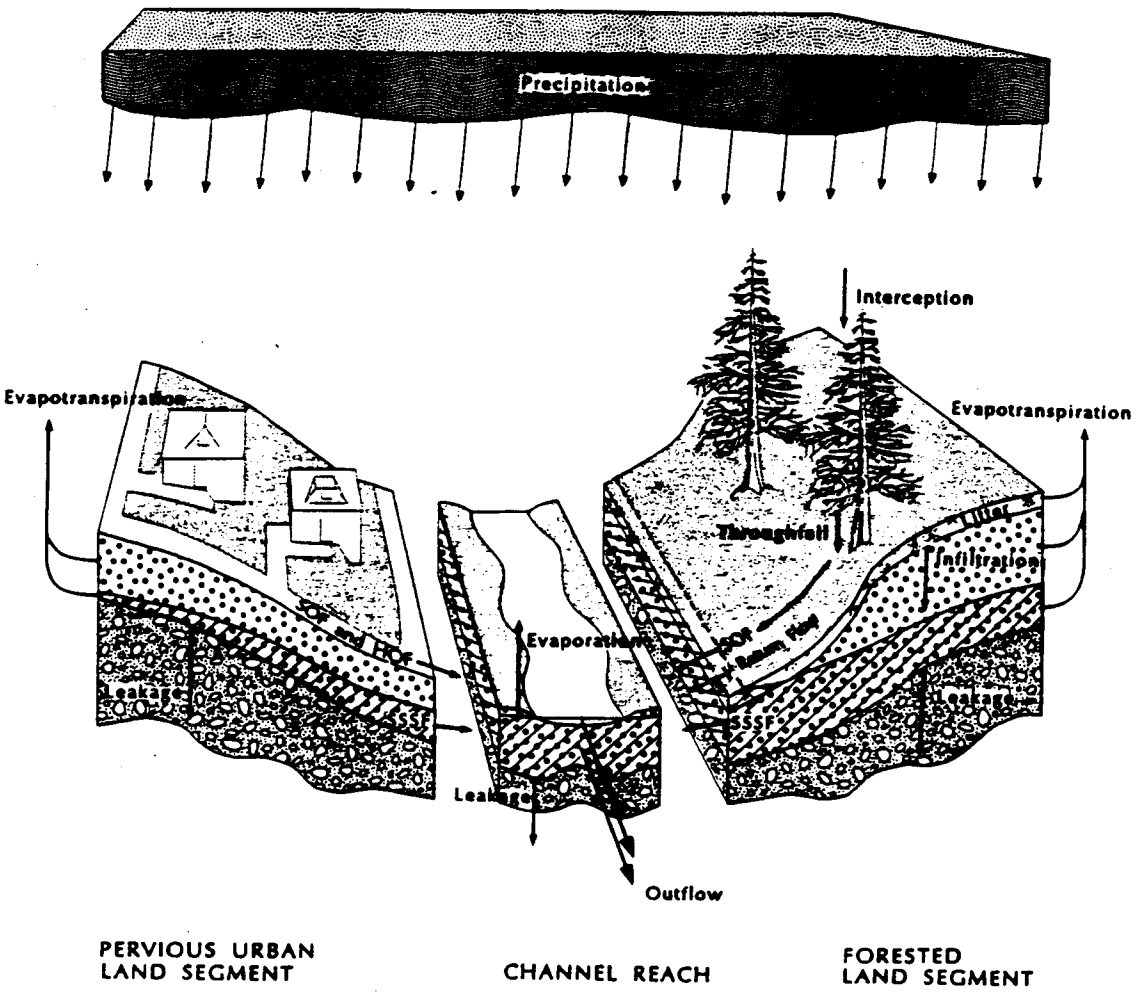

Fig. 4-1. Model representation of urban and forested land segments draining to a channel reach.

The influence of topography and soil characteristics on flow production are explicitly incorporated into the model as illustrated in Figure (4-1). Complex natural topography is disaggregated into independent hillslope segments. Each hillslope segment is modeled as a two-dimensional cross-section along a flow line down a valley side. A facility for convergence is also included, allowing the effect of flow convergence or divergence to be simulated. In plan view the hillslope segment consists of a quadrilateral which extends from ridge crest to valley bottom.

The surface soil is assumed to lie above a less permeable layer (bed). The slope of the ground surface and the lower layer, as well as soil thickness, may vary downslope. The soil saturated hydraulic conductivity may also change with depth and/or downslope distance. When vertical unsaturated flow in the upper soil exceeds the hydraulic conductivity of the lower layer, a perched water table forms. If this water table rises to intersect the ground surface, saturation overland flow and return flow may be generated.

4.1 Canopy and Litter Zone Interception

Canopy interception loss is simulated by an interception storage based on canopy type. All rainfall is assumed to enter interception storage until this storage is full. Excess rainfall is assumed to pass through the canopy with no change in intensity. Interception storage is depleted by evaporation at the potential rate until reduced to zero (Section 4.6). Thus interception may continue during a storm due to evaporation losses. Rainfall that is not intercepted (throughfall) may fall either on forest litter or directly on soil. The

impact of various forms of land use can be simulated by changing the vegetation cover or by completely removing the litter zone or changing its thickness. Throughfall landing on a saturated zone generates saturation overland flow. Throughfall which enters the litter zone is stored until the average volumetric moisture content reaches field capacity. Once field capacity has been reached, throughfall is assumed to pass through the litter zone with no attenuation. Water is continuously removed from the litter zone as a function of its current moisture content and the current potential evapotranspiration demand (Section 4.6).

4.2 Soil Infiltration

The amount of direct throughfall or litter-zone percolation that enters the soil profile is estimated by Philip's (1957, 1969) equation modified to allow for variable rainfall intensities (Chow et al., 1988, p. 141). When available input to the soil zone exceeds the infiltration capacity, percolation from the litter zone is restricted, or when no litter is present, Horton overland flow is generated (once surface detention has been exhausted). The modeled soil zone extends from the base of the litter zone to the lower layer (Figure 4-1). The infiltration rate, i, is

$$i(t) = K_z + S(\theta_i)\left[\frac{S(\theta_i) + \sqrt{S(\theta_i)^2 + K_z I(t)}}{4I(t)}\right] \qquad (4\text{-}1)$$

in which t is time, θ_i is the average unsaturated zone moisture content at the start of a storm, K_z is the component of saturated conductivity perpendicular

to the slope, I is the cumulative storm infiltration, and S is the soil sorptivity. Antecedent conditions are imposed through the sorptivity term, which is a function of soil type and moisture content at the start of a storm.

Sorptivity is updated prior to a storm using the average moisture content in the unsaturated zone. Sorptivity is assumed to remain constant during a storm. Cumulative infiltration is reset to zero between storms. This approach for modeling infiltration assumes that for a given soil, the infiltration capacity depends only on cumulative infiltration during the event and on initial conditions at the start of the event. This method is most valid for storms with relatively uniform rainfall intensities separated by inter-storm periods long enough to allow a return to nearly uniform soil moisture conditions. In general, thin coarse grained soils return to uniform moisture conditions more rapidly that deeper finer textured soils.

4.3 Unsaturated Zone Dynamics

A comparison of recorded precipitation and shallow water table fluctuations at the Novelty Hill site shows that under dry antecedent conditions very little of the rainfall recharges the saturated zone, while under wet soil conditions there is a very rapid water table response to precipitation. As a result, a relatively simple description of the unsaturated zone is incorporated in the model. When the average moisture content in the unsaturated zone (θ) is at, or below, the soils moisture content at field capacity (θ_{fc}) there is no discharge to the water table from the unsaturated zone. At moisture contents above field capacity infiltrated water moves through the unsaturated zone at a

constant velocity. The unsaturated discharge to the water table (p) is calculated as follows:

$$p^{t+\Delta t} = 0 \qquad \theta^t \leq \theta_{fc}$$
$$p^{t+\Delta t} = i^t - \kappa\Delta t \qquad \theta^t > \theta_{fc} \tag{4-2}$$

where i is the current rate of infiltration, κ is an unsaturated zone lag coefficient, and the superscripts t and $t+\Delta t$ refer to the beginning and end of the time period, respectively. The geometry of the unsaturated zone varies with time, depending on the current water table configuration. Moisture content is updated using mass conservation.

The product $\kappa\Delta t$ in (4-2) equals the average travel time of infiltrated water through the unsaturated zone. The coefficient κ is specified by the user and can be estimated from the timing of water table responses to rainfall (Section 5.5). It is assumed that a pulse of water infiltrated over the time period Δt moves independently through the unsaturated zone at a constant velocity and that spatial and temporal changes in water table depths can be ignored. These conditions are most likely to be met on long hillslopes with thin coarse grained soils.

4.4 Saturated Zone Dynamics

If steady-state saturated flow streamlines are assumed parallel to the local bedslope, discharge through a cross-section perpendicular to the bed (q_s)

can be calculated through the extended Dupuit-Forchheimer solution (Childs, 1971):

$$q_s(s,h) \;=\; -\,w(s)\;T(s,h)\;\zeta(s,h) \tag{4-3}$$

where s is the distance measured along the bed taken positive in the downslope direction (Figure 4-2), w is the local hillslope width, T is the local water table transmissivity, and ζ is the local hydraulic gradient. The hydraulic gradient is calculated by:

$$\zeta(s,h) \;=\; \frac{dh}{ds}\,cos\beta(s) \;+\; sin\beta(s) \tag{4-4}$$

where h is the local water table depth taken perpendicular to the bed and β is the local bed slope angle.

Beven (1982b) has provided evidence which suggests that saturated lateral conductivities for some soils exhibit a decrease with depth below the soil surface that can be approximated with a simple exponential function. This allows the soil transmissivity to be calculated as

$$T(s,h) \;=\; \int_{z\,=\,0}^{z\,=\,h} K_s(s)\,e^{fz}\,dz \;=\; K_s(s)\,\frac{\left[\,e^{fh(s)}-1\right]}{f} \tag{4-5}$$

where K_s is the local component of saturated soil conductivity parallel to the slope at the bed (z=0), and z is the perpendicular distance *above* the less permeable bed (Figure 4-2). Subsurface discharge at any downslope distance

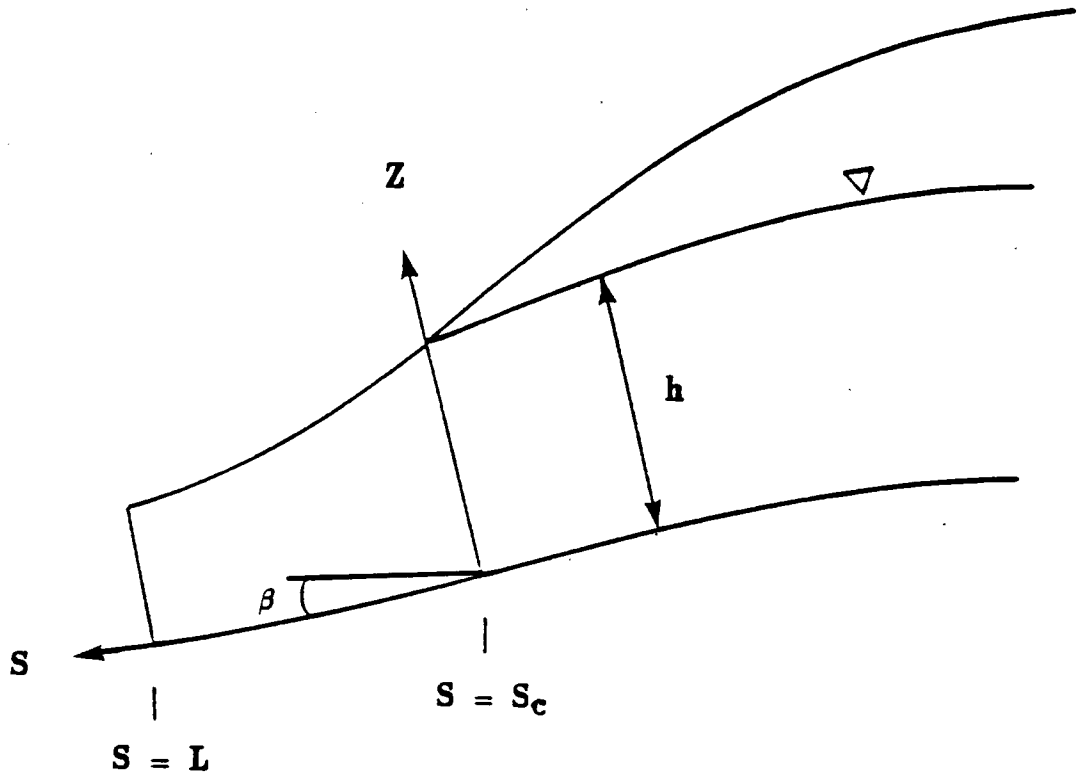

Fig. 4-2. Two-dimensional cross-section along a steady-state stream tube.

can be calculated as a function of saturated depth using (4-3), (4-4), and (4-5).

In regions where the water table intersects the ground surface both saturation overland flow and return flow may be generated. The flux rate of saturation overland flow (q_{sof}) available for surface routing (Section 4.5) is calculated as:

$$q_{sof} = \int_{s=s_c}^{s=L} R\, w(s)\, ds \tag{4-6}$$

where R is the current rate of throughfall, s_c is the downslope distance at which surface saturation begins (Figure 4-2), and L is the total hillslope length. Return flow (q_r) is obtained by taking the downslope integral of the divergence of the subsurface flux (Dietrich and Dunne, 1990):

$$q_r = \int_{s=s_c}^{s=L} -\frac{d}{ds}\left[q_s(s)\right] ds \tag{4-7}$$

The leakage rate through the lower layer is assumed to be equal to its spatially-averaged saturated hydraulic conductivity (K_l). When a perched water table exists the total slope leakage (q_l) is

$$q_l = \int_{s=0}^{s=L} K_l\, w(s)\, ds \tag{4-8}$$

All model parameters have a physical representation. The user specifies

the flow path width, ground surface slope, and bed slope at the top and bottom of each hillslope segment. Ground surface elevation, soil depth, and base lateral hydraulic conductivity (K_s in (4-5)) are supplied at selected downslope distances; the number and location of these points are determined by the user. Cubic spline interpolations are used to estimate hillslope properties between input locations. The hillslope is normally subdivided into 30 downslope points with cross-sectional width, soil depth, hydraulic conductivity, and bed and ground surface slopes calculated at each location.

It is assumed that hydraulic conditions within the seepage face at the base of the hillslope control the overall hillslope response, much as local hydraulic controls dictate upstream water surface elevations and discharge in open channel flow. The location of the hillslope cross-section that controls saturated zone discharge may vary in time depending on current water table conditions. When the water table remains *below* the ground surface over the entire land segment the control cross-section is taken at the bottom of the hillslope; hydraulic conditions at this location control the total hillslope discharge to the channel. If at a later time the water table rises to intersect the ground surface the control cross-section shifts to the upslope beginning of surface saturation (s_c in Figure 4-2) where the soil is saturated to the surface and subsurface discharge equals the maximum hydraulic conveyance of the cross-section. If this discharge exceeds the maximum conveyance of downslope cross-sections (due to a decrease in soil conductivity, soil depth, slope, etc.) some water will reemerge as return flow. Return flow and any throughfall landing on the zone of surface saturation are combined and routed to the

channel as overland flow.

The concept of a control cross-section is most valid when water table response is relatively uniform over the hillslope and the product of local soil transmissivity and hydraulic gradient is uniform or decreases downslope. Under these conditions the hillslope response is almost entirely dictated by water input rates and the down slope (seepage face) boundary conditions. These requirements are most likely to be met on plane or concave hillslopes, or the lower portion of convex-concave hillslopes where the concave section is adjacent to the channel. When the soil becomes saturated to the surface these conditions are met within the seepage face, and for some distance upslope.

When the water table remains below the ground surface there are only two subsurface related discharge components: saturated subsurface flow to the channel, and vertical leakage through the less pervious lower bed. It is necessary to determine the hydraulic gradient (the slope of the water table relative to the local bed slope) using (4-4) to calculate the saturated subsurface flow rate. This relative slope is given by:

$$\frac{dh}{ds} = tan\left[\alpha_w(s) - \alpha_b(s)\right] \tag{4-9}$$

where α_w and α_b are the local slopes of the water table and bed, respectively. It is assumed that when $h(s)$ equals zero the slope of the water table equals the local bed slope, i.e.:

$$\frac{dh}{ds} = 0 \qquad if \quad h(s) = 0 \tag{4-10a}$$

When the water table intersects the soil surface $h(s)$ equals the local soil depth ($D(s)$) and the slope of the water table *must equal* the local ground surface slope ($\alpha_t(s)$), as a result

$$\frac{dh}{ds} = tan\left[\alpha_t(s) - \alpha_b(s)\right] \qquad if \qquad h(s) = D(s) \qquad \text{(4-10b)}$$

If for simplicity one assumes a linear change between $h(s) = 0$ and $h(s) = D(s)$:

$$\frac{dh}{ds} = \frac{h(s)\ tan\left[\alpha_t(s) - \alpha_b(s)\right]}{D(s)} \qquad \text{(4-11)}$$

The hydraulic gradient can then be calculated by substituting (4-11) into (4-4):

$$\zeta(s,h) = \frac{h(s)\ tan\left[\alpha_t(s) - \alpha_b(s)\right]}{D(s)}\ cos\beta(s) + sin\beta(s) \qquad \text{(4-12)}$$

where $\alpha_t(s)$, $\alpha_b(s)$, $D(s)$, and $\beta(s)$ are provided by the cubic spline fit. The steady-state saturated subsurface discharge for any flow depth is calculated using (4-3), (4-5), and (4-12).

Based on a Dupuit approach the shape of the water table *upslope* of the seepage face is approximated as a parabola (within the seepage face the shape of the water table coincides with the ground surface topography). It is further assumed that conditions at the hillslope (downstream) control section dictate the geometry of the parabola at any given time.

For a plane slope with downslope distance s, the above assumptions allow water table depths to be calculated as

$$h(s) = B(s_c)s^2 + C(s_c)s \tag{4-13}$$

where B and C are coefficients related to aquifer properties at the control cross-section. At the downslope control section (s_c):

$$h(s_c) = B(s_c){s_c}^2 + C(s_c)s_c \tag{4-14}$$

and

$$\frac{dh(s_c)}{ds} = 2B(s_c)s_c + C(s_c) \tag{4-15}$$

Rearranging (4-15) yields

$$C(s_c) = \frac{dh(s_c)}{ds} - 2B(s_c)s_c \tag{4-16}$$

Substituting (4-16) for C in (4-14) yields $B(s_c)$ as:

$$B(s_c) = -\left[\frac{h(s_c) - \frac{dh(s_c)}{ds}s_c}{{s_c}^2}\right] \tag{4-17}$$

Water table heights can then be calculated as a function of s using (4-13), (4-16), and (4-17) where $\frac{dh(s_c)}{ds}$ is given as a function of water table depth by (4-11). In model application these water table depths are added to local bed elevations to yield elevations of the water table surface. This approach assumes the water table is strictly a function of conditions at the control cross-section.

When a perched water table exists the vertical leakage through the lower soil layer is determined from (4-8) as

$$q_l = K_l A_{bed} \tag{4-18}$$

where A_{bed} is the plan view area of the lower bed.

In locations where the water table intersects the ground surface ($h(s) = D(s)$) both return flow and saturation overland flow may be generated. For Dupuit-Forchheimer assumptions the total hillslope flux of return flow is determined using (4-7) as the difference in saturated subsurface discharge at the upslope extent of the seepage face ($s = s_c$) and subsurface discharge at the hillslope bottom($s = L$):

$$q_r = q_s\left[s_c, D(s_c)\right] - q_s\left[L, D(L)\right] \tag{4-19}$$

The total flux of saturation overland flow supplied to the surface routing algorithm is determined using (4-6) as

$$q_{sof} = RA_{sat} \tag{4-20}$$

where A_{sat} is the current areal extent of surface saturation.

Saturated zone dynamics are simulated using a simple mass-balance approach. A unique relationship between water table configuration, saturated zone volume, and steady-state subsurface discharge is assumed. This relationship is determined by evaluating the hillslope dynamics associated with different locations of the control cross-section (for example, at locations a and b in Figure 4-3 which depicts the results for a convex-concave hillslope profile). At each location the saturated zone volume is calculated from water table heights [(4-13)]. Corresponding values of lateral subsurface flow [(4-3), (4-5), and (4-12)], return flow [(4-19)], and leakage [(4-18)] are also computed. Calculations are performed for up to 20 water table heights when the control section is located at the downstream boundary and at approximately 30 upslope locations. An equivalent relationship is determined for the location and areal extent of surface saturation. These computations are only made once for each land segment, with the results saved in "look-up tables".

Land segment look-up tables are an integral part of the model. They provide information on subsurface dynamics and provide a link between surface and subsurface responses. Part of a typical land segment look-up table is presented in Table 4-1 and the complete table is shown graphically in Figure 4-3. Each row in the table corresponds to a specific water table configuration. All lengths are given in meters and all fluxes as liters per hour. Columns 2 through 10 provide, respectively: the saturated thickness at the lower boundary, the upslope extent of surface soil saturation (L_{eq}), the surface area available for

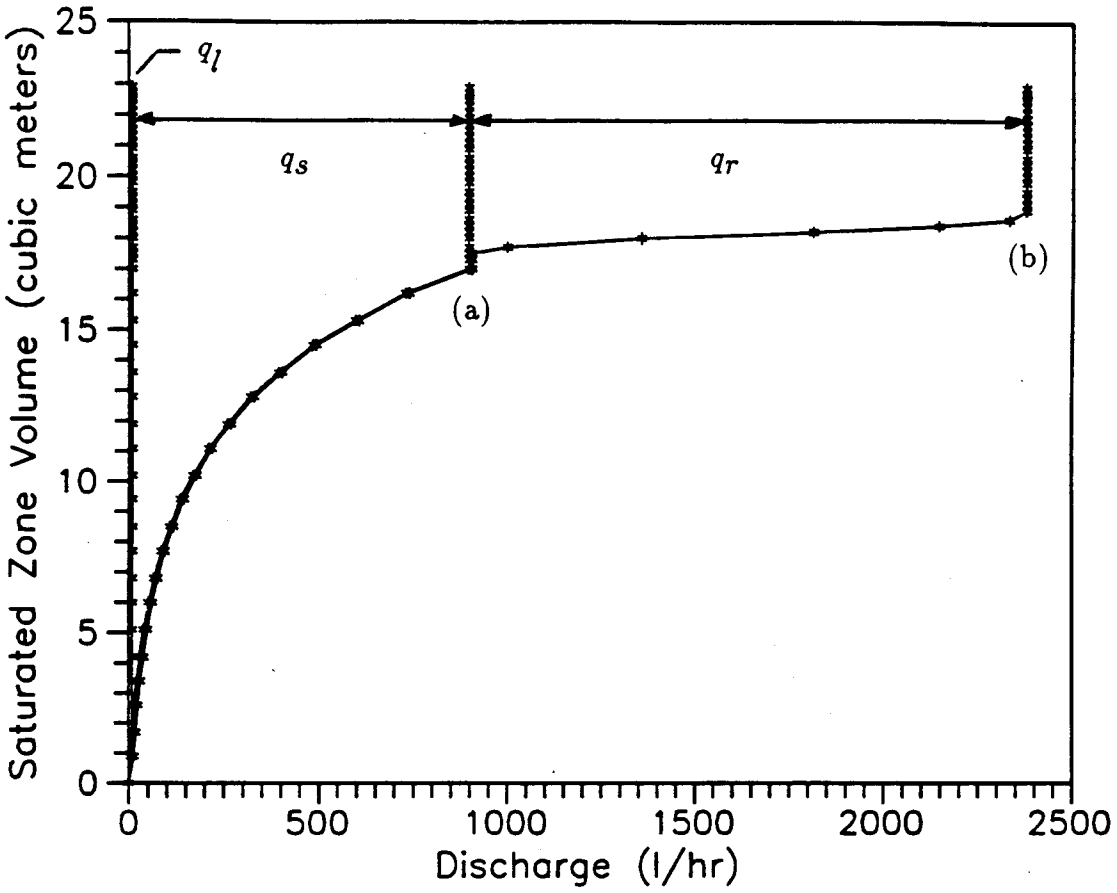

Fig. 4-3. "Look-up" table of saturated volume versus discharge for a convex-concave hillslope profile. The asterisks represent water table configurations where saturated volume and discharges are calculated. A linear interpolation is used between points. The farthest curve to the right gives total hillslope discharge (excluding SOF) and is composed of leakage (q_l), lateral subsurface flow (q_s), and return flow (q_r).

TABLE 4-1. Example from a Look-Up Table

Row (1)	h (2)	L_{eq} (3)	Infil Area (4)	Sat Vol (5)	q_s (6)	q_l (7)	q_r (8)	q_T (9)	α_e (10
10	0.43	0	155	8.5	107	10	0	117	0
11	0.48	0	155	9.4	135	10	0	145	0
12	0.52	0	155	10.2	169	10	0	179	0
13	0.56	0	155	11.1	209	10	0	219	0
14	0.61	0	155	11.9	259	10	0	269	0
15	0.65	0	155	12.8	320	10	0	330	0
16	0.69	0	155	13.6	394	10	0	404	0
17	0.74	0	155	14.5	484	10	0	494	0
18	0.78	0	155	15.3	598	10	0	608	0
19	0.83	0	155	16.2	731	10	0	741	0
20	0.87	0	155	17.0	898	10	0	908	0.0
21	0.87	4	151	17.3	898	10	0	908	0.0
22	0.87	8	147	17.5	898	10	0	908	0.0
23	0.87	13	142	17.7	898	10	93	1001	0.0
24	0.87	17	138	18.0	898	10	450	1358	0.0
25	0.87	21	134	18.2	898	10	906	1814	0.0
26	0.87	25	130	18.4	898	10	1238	2146	0.0
27	0.87	29	125	18.6	898	10	1424	2332	0.0

Length in m and discharge in l/hr

infiltration (area without ground surface saturation), soil water volume in the saturated zone, lateral subsurface flow (q_s), leakage (q_l), return flow (q_r), the total subsurface discharge (q_T), and an equivalent slope for the zone of surface soil saturation (α_{eq}). Information from columns 3 and 10 is used in overland flow routing (Section 4.5).

The subsurface information presented in Table 4-1 is shown graphically in Figure 4-3. The asterisks represent water table configurations where hillslope saturated volumes and discharge components were calculated (columns 5-9, Table 4-1). The curve farthest to the right gives total hillslope discharge (excluding any saturation overland flow) as a function of saturated zone volume. This discharge can be composed of leakage (q_l), lateral subsurface flow (q_s), and return flow (q_r) as shown in the upper portion of the figure. Prior to calculation point **a** (row 20, in Table 4-1), the water table remains below the ground surface over the entire hillslope and the total discharge is composed of leakage and lateral subsurface flow. The lateral subsurface discharge increases exponentially [via (4-5)] until the water table reaches the ground surface at the lower boundary (point **a**, Figure 4-3). Lateral subsurface discharge can not increase with saturated zone volume beyond this point.

The example hillslope has a convex upper portion and a concave footslope. As a result, if saturated conductivity is constant, return flow is generated when soil in the footslope area is saturated to the ground surface (beginning with row 23 in Table 4-1 and shown as the zone of q_r in upper right of Figure 4-3). If surface saturation extends upslope to the convex portion of the hillslope, conveyance does not decrease with downslope distance in this

region and no additional return flow is generated (point **b**, Figure 4-3).

The fluxes and volumes associated with the saturated zone are related through mass conservation:

$$V^{t+\Delta t} - V^t = I - ET_a - Q_{sub} \tag{4-22}$$

where V is the saturated zone water volume, I is the volume of water supplied from the unsaturated zone over the time period Δt, ET_a is the volume of water removed by evapotranspiration over the time period, Q_{sub} is the total volume of water removed by subsurface discharge, and the superscripts t and $t+\Delta t$ refer to the beginning and end of the time period, respectively. The volume of subsurface discharge lost from the hillslope during time period Δt is

$$Q_{sub} = \tfrac{1}{2}\left[{q_T}^t + {q_T}^{t+\Delta t}\right]\Delta t \tag{4-23}$$

where

$$q_T = q_s + q_l + q_r \tag{4-24}$$

is the total subsurface discharge.

The unsaturated flux volume (I) and the evapotranspiration demand (ET_a) are supplied from other model components (Sections 4.3 and 4.6). The only unknowns in (4-22) and (4-23) are the saturated volume and discharge rate at the end of the time period ($V^{t+\Delta t}$ and ${q_T}^{t+\Delta t}$). For any land segment

total subsurface discharges corresponding to specific saturated volumes are given in the previously described look-up tables (Table 4-1 and Figure 4-3). Linear interpolation between rows in a look-up table results in a piecewise continuous relation between total subsurface discharge and saturated volume. This relation allows $V^{t+\Delta t}$ and ${q_T}^{t+\Delta t}$ to be calculated for each time step through a simultaneous solution of equations (4-22) and (4-23). The solution is accomplished using the efficient numerical scheme presented in Johanson et al. (1984, pp. 231-235).

4.5 Overland Flow

The model allows overland flow to be generated by a single mechanism or a combination of mechanisms which include Horton overland flow, saturation overland flow, or return flow. For each land segment the user specifies a depth per unit area of surface depression storage. These depths are converted to volumes by the model. The volume of surface water must exceed the current available depression storage for overland flow to occur. Water is continuously removed from depression storage by evapotranspiration (Section 4.6) and, in the case of Horton overland flow, by infiltration at a rate determined using (4-1). Water in excess of that retained in depression storage is available for overland flow. This excess water is stored temporally in *surface detention* as it flows down the slope. Thus the total volume of surface water on the hillslope consists of water held in *depression storage* unavailable for routing and water temporally stored in *surface detention* as it moves over the hillslope. When the total volume of water on the ground surface falls below the depression storage

capacity surface discharge from the slope terminates.

Many methods for calculating unsteady overland flow were considered, including the finite difference methods described in chapter 2. These latter methods have a major disadvantage for long-term continuous simulation in that substantial amounts of computer time are needed for their solution. I have chosen to modify the nonlinear storage model developed for the Stanford Watershed Model by Crawford and Linsley (1966). This overland flow routing scheme is computationally efficient and has been verified against the experimental results of Izzard (1944, 1946) for flow over artificial slopes 22 m long.

For steady, turbulent, uniform flow the depth profile of overland flow on a plane is

$$y(s) = \left(\frac{r\,n}{\sqrt{\alpha_p}}\,s\right)^{0.6} \tag{4-25}$$

where $y(s)$ is the local flow depth, s is the downslope distance, r is the supply rate, n is Manning's roughness coefficient, and α_p is the slope. The volume of surface detention per unit width at equilibrium (D_e) is equal to

$$D_e = \int_{s=s_1}^{s=s_2} y(s)\,ds = \frac{5}{8}\left(\frac{r\,n}{\sqrt{\alpha_p}}\right)^{0.6}\left({s_2}^{1.6} - {s_1}^{1.6}\right) \tag{4-26}$$

For a single plane $s_1 = 0$ and $s_2 = L$, (4-26) reduces to

$$D_e = \frac{5}{8} \frac{r^{0.6}\, n^{0.6}\, L^{1.6}}{\alpha_p{}^{0.3}} \tag{4-27}$$

where L is the length of the plane.

The rate of discharge per unit width (q_o) from the plane, based on Manning's equation, is

$$q_o = \frac{1}{n}\, y(L)^{\frac{5}{3}}\, \alpha_p{}^{\frac{1}{2}} \tag{4-28}$$

To calculate continuous overland flow from surface detention storage, the depth, $y(L)$, must be related to surface detention storage. No fixed relation exists between detention storage and discharge from overland flow when the flow is unsteady. At equilibrium

$$y(L) = \frac{8}{5} \frac{D_e}{L} \tag{4-29}$$

but for other conditions some approximations are needed. Crawford and Linsley (1966) assume three general conditions will occur during a storm. Initially, as rain begins, the depth of overland flow will be uniform along the surface. This will be followed by a transition from a uniform depth to an equilibrium profile. Finally, when rainfall stops recession flow occurs from water in surface storage. Under these assumptions, $y(L)$ must be in the range

$$\frac{D_c}{L} \leq y(L) \leq \frac{8}{5} \frac{D_e}{L} \tag{4-30}$$

where D_c is the current detention storage per unit area. The current detention storage D_c, divided by the detention storage required at equilibrium D_e for the current rate of inflow, is used as an index to the distribution of water on the overland flow plane. Crawford and Linsley found that the most satisfactory empirical relationship between outflow depth and detention storage for reproducing experimental hydrographs was

$$y(L) = \frac{D_c}{L}\left(1.0 + 0.6\left[\frac{D_c}{D_e}\right]^3\right) \tag{4-31}$$

Substituting (4-31) in (4-28) allows the rate of discharge to be calculated as

$$q_o = \frac{1}{n}\ \alpha_p^{\frac{1}{2}}\left(\frac{D_c}{L}\right)^{\frac{5}{3}}\left(1.0 + 0.6\left[\frac{D_c}{D_e}\right]^3\right)^{\frac{5}{3}} \tag{4-32}$$

where D_e varies in time as a function of the current supply rate to overland flow and is calculated using (4-27). During recession flow when D_e is less than D_c the ratio $\frac{D_c}{D_e}$ is assumed to be one.

Crawford and Linsley developed equation (4-32) for a *plane on which the entire surface is generating overland flow.* It is necessary to modify this solution to allow for varying topography and local zones of surface flow whose lateral extent changes with time (i.e., zones of transient saturation overland flow or return flow). This was accomplished by representing the region of overland flow by a plane of "equivalent slope" whose slope and length change in

time with changes in the areal extent of overland flow production. The basin to be modeled is subdivided into hillslopes that can be considered homogeneous in terms of surface roughness and temporal infiltration rates.

The total equilibrium detention for a cascade of m planes is equal to the sum of their individual storages. For a spatially constant roughness and input rate this volume can be calculated using (4-26) as

$$D_e = \frac{5}{8} r^{0.6} n^{0.6} \sum_{j=1}^{m} \left({s_j}^{1.6} - {s_{j-1}}^{1.6} \right) / {\alpha_{p_j}}^{0.3} \tag{4-33}$$

In the context of Crawford and Linsley's overland flow routing scheme, a cascade of m planes will behave identically to a single plane with the same equilibrium surface detention for a given input rate. Setting the equilibrium detention of a single equivalent plane equal to the equilibrium detention of the cascade in (4-33) yields

$$\frac{{L_{eq}}^{1.6}}{{\alpha_{eq}}^{0.3}} = \sum_{j=1}^{m} \left({s_j}^{1.6} - {s_{j-1}}^{1.6} \right) / {\alpha_{p_j}}^{0.3} \tag{4-34}$$

The equivalent slope (α_{eq}) is

$$\alpha_{eq} = \left[\frac{{L_{eq}}^{1.6}}{\sum_{j=1}^{m} \left({s_j}^{1.6} - {s_{j-1}}^{1.6} \right) / {\alpha_{p_j}}^{0.3}} \right]^{\frac{10}{3}} \tag{4-35}$$

where L_{eq} is the length of the equivalent single plane (equal to the total length

of the cascade, s_j). Equation (4-35) allows a cascade of planes to be represented by a single equivalent plane of slope α_{eq}. The equivalent length and slope are used in (4-27) and (4-32) to calculate discharge from the cascade.

For overland flow routing the hillslope profile is represented by a cascade of planes whose lengths and slopes are determined from the cubic spline fit to user specified ground surface elevations. In most cases the cascade will be composed of about 30 planes. Starting at the hillslope bottom, equivalent slopes are calculated at each cubic spline interpolation point using (4-35). For example at calculation point (b) in Figure (4-3) L_{eq} is equal to the distance along the slope between the hillslope bottom and point (b). An equivalent slope is then determined for this distance using (4-35). This process is continued up the entire hillslope with the results stored in columns 3 and 10 of the land segment look-up table described in Section 4.4 (Table 4-1).

The look-up table provides a link between subsurface and surface dynamics. For example, prior to calculation point **a** in Figure 4-3 the water table remains below the ground surface over the entire hillslope. This corresponds to rows 10 - 19 in Table 4-1 which shows a saturated hillslope length of zero (column 3) and an infiltration area (column 4) equal to the surface area of the entire land segment. At point **a** in Figure 4-3 (row 20, Table 4-1) the water table intersects the ground surface at the lower boundary. Beyond this point surface saturation begins to expand upslope. The total hillslope surface area minus the infiltration area (column 4) gives the area of saturated ground (A_{sat} in (4-20)) available to generate saturation overland flow. Column 8 gives the flux of return flow [(4-19)] which must be routed as

overland flow, and columns 3 and 10 give the equivalent plane parameters for use in surface routing equations (4-25) and (4-30). During model use as the zone of surface saturation expands and contracts the length and slope of the equivalent plane is also adjusted via the look-up table.

4.6 Evapotranspiration

Actual evapotranspiration (ET_a) is computed for each time step as a function of moisture conditions and the current potential evapotranspiration demand (ET_p). Actual evapotranspiration can not exceed the potential demand. Water is removed from canopy interception, surface depression storage, and the saturated root zone at the potential rate. In the litter-zone and the unsaturated soil root-zone the relationship between actual and potential evapotranspiration is expressed as:

$$ET_a = cET_p \tag{4-36}$$

where

$$c = 1 \quad \text{if} \quad \theta' \geq \theta'_{fc} \tag{4-36a}$$

$$c = (a+b)\left(\frac{\theta' - \theta'_{wp}}{\theta'_{fc} - \theta'_{wp}}\right) \quad \text{if} \quad \theta_{wp} < \theta' < \theta'_{fc} \tag{4-36b}$$

$$c = 0 \quad \text{if} \quad \theta' \leq \theta'_{wp} \tag{4-36c}$$

where θ' is the average moisture content, θ'_{fc} is the field capacity moisture content, and θ'_{wp} is the wilting point moisture content. The coefficients a and b are used to describe the relationship between actual and potential evapotranspiration when moisture is limiting.

The relationship between actual and potential evapotranspiration when moisture is limiting is a function of several variables including soil texture, plant physiology, rooting characteristics, and the rate of evapotranspiration itself (Dunne and Leopold, 1978). Veihmeyer (1964) conducted a series of experiments in California and concluded that evapotranspiration proceeds at the potential rate until soil moisture is depleted to the wilting point. This is equivalent to taking $a = 1$ and $b = 0$ in (4-36b). Thornthwaite and Mather (1955), working on a loam in Nebraska, found that the ratio of actual to potential evapotranspiration decreases as a linear function of the amount of available water (represented by taking $a = 0$ and $b = 1$ in [4-36b]).

The coefficients a and b are assigned by the user based on soil type, climatic conditions, and land cover. Dunne and Leopold (1978) feel that the Veihmeyer and Thornthwaite models should be adequate approximations for sandy and clay rich-soils, respectively. In a sandy soil plants with a dense root system can withdraw water rapidly from the soil pores, and evapotranspiration may proceed at close to the potential rate until moisture content is close to the wilting point. In clay rich soils water is held more tightly and movement of water to the plant roots is slower. Under such circumstances moisture supply to the roots will not keep up with potential rates of loss, and actual

evapotranspiration rates will decline throughout most of the range of available water (Dunne and Leopold, 1978).

4.7 Channel Dynamics

The channel routing scheme presented below is an extension of the method used in the Hydrologic Simulation Program- Fortran (HSPF) (Johanson et al., 1984). Each subbasin is drained by its own reach of channel, which is part of the larger channel network. An individual reach is composed of a "channel" and it's associated floodplain (Figure 4-4). The fluxes and volumes within a reach satisfy mass conservation:

$$V_r^{t+\Delta t} - V_r^{t} = V_p + V_L + V_{in} - ET_a - V_{out} \qquad (4\text{-}37)$$

where V_r is the volume of water in the reach (including floodplain), V_p is the volume of rainfall on the reach, V_L is the volume of surface and subsurface discharge to the reach from subbasin land segments, V_{in} is the inflow volume from the adjacent upstream channel reach, ET_a is the volume of water removed by evapotranspiration, and V_{out} is the volume of water discharged from the reach over the time period Δt. The volume of reach discharge, V_{out}, is

$$V_{out} = \tfrac{1}{2}\left[q_{out}^{\,t} + q_{out}^{\,t+\Delta t}\right]\Delta t \qquad (4\text{-}38)$$

where

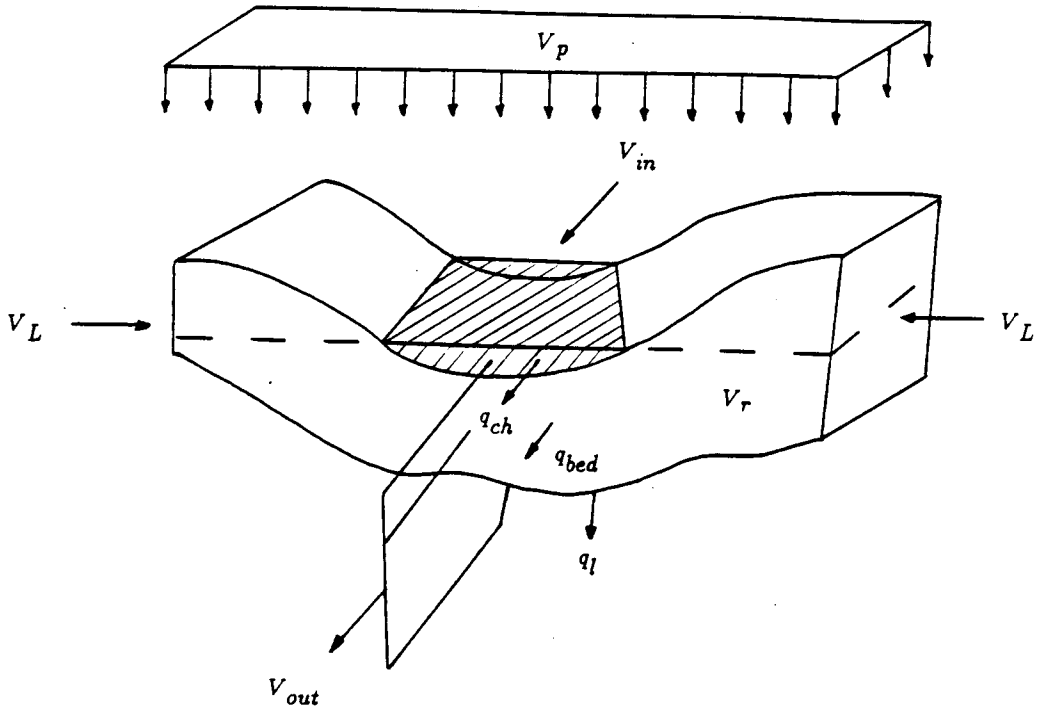

Fig. 4-4. Volumes and fluxes for a channel reach.

$$q_{out} = q_{ch} + q_{bed} + q_l \tag{4-39}$$

with q_{ch} equal to discharge from the channel (shaded region in Figure 4-7), q_{bed} is equal to subsurface outflow occurring below the channel bed, and q_l is leakage through the lower boundary. Channel discharge (q_{ch}) and q_{bed} are normally routed as inflow to the adjacent downstream reach.

While no assumptions are made regarding the shape of a channel reach, a unique relationship between stored water volume and discharge must be specified. The user specifies properties of the reach in a look-up table with columns for reach water volume (V_r), channel discharge, below-bed discharge, and leakage. Each row in the table contains values appropriate to a given water surface elevation. When the water table remains below the channel bed $q_{ch} = 0$ and q_{bed} and q_l can be computed from Darcy's Law. When the water table intersects the channel bed q_{ch} is calculated from hydraulic properties. For natural channels this discharge component can be calculated for various water surface elevations using surveyed channel cross-sections and Manning's equation. It is also possible to model channel reaches controlled by weirs or detention ponds with one or several orifices. Backwater effects can be incorporated by using steady-state backwater calculations determined by any suitable scheme to generate the look-up table.

The only unknowns in (4-37) and (4-38) are the reach volume ($V^{t+\Delta t}$) and discharge (${q_{out}}^{t+\Delta t}$) at the end of the time period, $t + \Delta t$. Discharges corresponding to specific volumes are available from the look-up table. Linear interpolation between rows in a look-up table result in a piecewise continuous

relation between total reach discharge and volume. This relation allows $V^{t+\Delta t}$ and ${q_{out}}^{t+\Delta t}$ to be calculated through simultaneous solution of (4-37) and (4-38) using the same numerical scheme that was required for subsurface flow in Section 4.4.

The continuous hydrologic simulation model described in Sections 4.1 through 4.7 was designed for application in natural catchments that will experience change and simulates Horton overland flow, subsurface flow, return flow, and saturation overland flow. The model preserves the effects of topography and the spatial variation of hydrologic properties, and is computationally efficient.

The model was developed so that physical processes are described with a minimal number of parameters (21), that all parameters have physical attributes, and that the model structure allow proper calibration and testing using relatively simple hydrologic measurements. The current model structure was influenced by measurements and observations in two study basins. Application of the combination methodology to a forested basin is described in chapter 5 and application to an urbanized catchment is given in chapter 6.

Chapter 5. Illustration of Methodology: Novelty Hill Catchment

Application of the combination methodology to the forested Novelty Hill catchment is discussed in this chapter. Physical features of the basin, field mapping, and a model-independent hydrological analysis of field measurements are presented in Sections 5.1, 5.2, and 5.3. Model representation of the catchment and model evaluation criteria are described in Sections 5.4 and 5.5. Model calibration and the results of limited model verification are discussed in Sections 5.6 and 5.7.

5.1 Physical Features

The 37 hectare Novelty Hill catchment is located approximately 6 km northeast of Redmond and 26 km northeast of Seattle in the Evans Creek drainage basin, King County WA. The basin is oblong in plan view (Figure 5-1), 1006 m long and an average of 366 m wide. The site is located entirely within a broad upland plateau with ground surface elevations ranging from 183 m at the crest of knolls in the northern portion of the site to about 168 m near the basin outlet. Side slopes within the northern portion of the site are between 3 and 5 percent. Within the lower third of the basin side slopes are between 1 and 2 percent. A central swale, with an average gradient of 0.9 percent, runs for approximately 800 m upstream from the outlet. A shallow seasonal wetland covering about 1.44 ha exists within the swale. The site was logged, probably around the beginning of this century, and now contains an extensive cover of second growth Douglas Fir (*Pseudotsuga menziesii*), Alder (*Alnus rubra*), Cottonwood (*Populus trichocarpa*), Western Red Cedar (*Thuja plicata*), Big

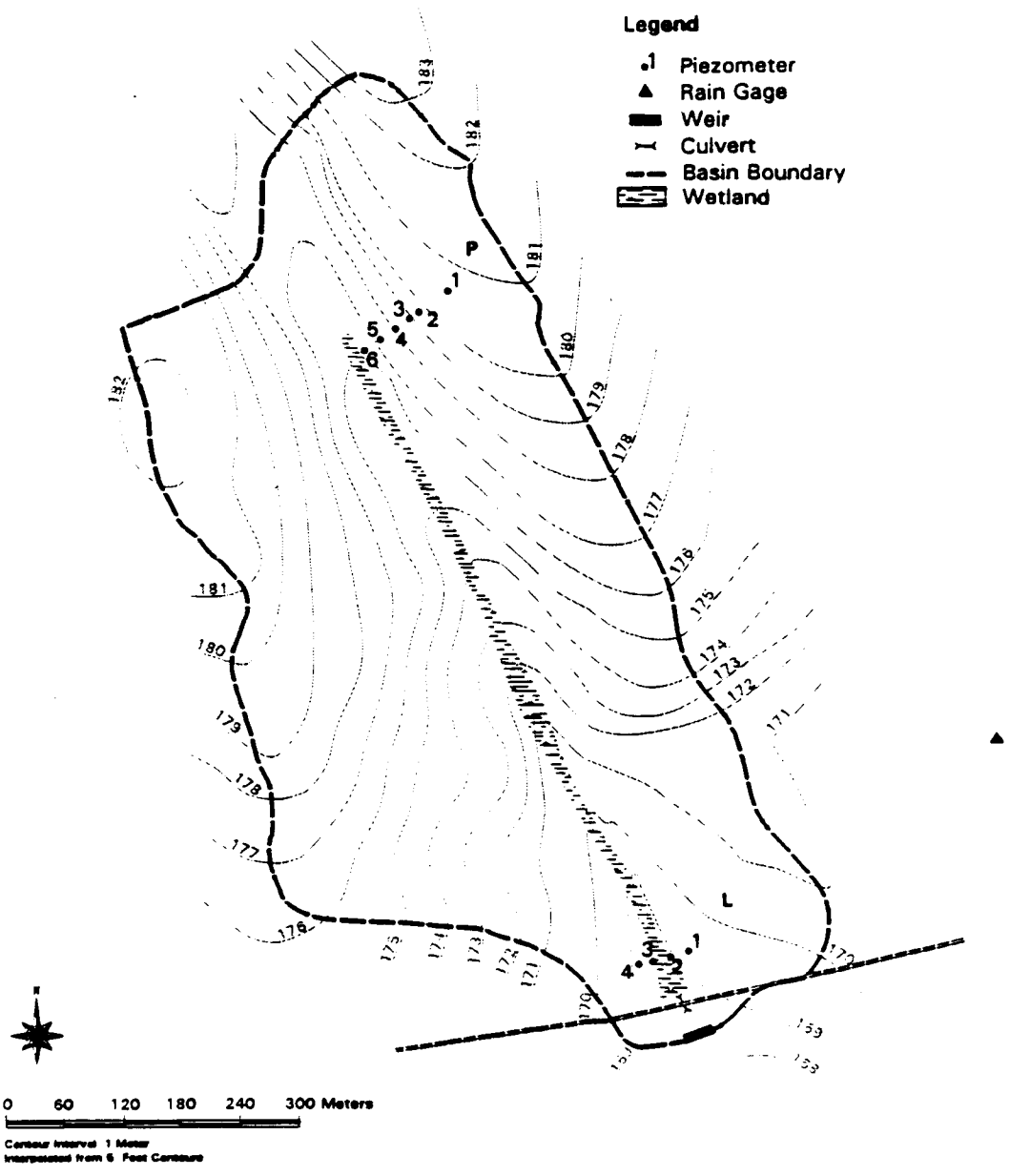

Fig. 5-1. Site map of the Novelty Hill basin showing the basin boundary and rain gage, piezometer, and weir locations.

Leaf Maple (*Acer macrophyllum*), and Vine Maple (*Acer cirinatum*). An abandoned narrow-gage railroad grade defines the eastern boundary. The catchment outlet is located at the southeast border, where discharge from the swale flows through a culvert passing under an abandoned railroad grade, before being measured using a compound weir.

Geologic conditions at the site are primarily the result of several regional glaciations, the most recent being the Vashon glaciation which ended approximately 10,000 years ago. Deposits include advance outwash, glacial till, and recessional drift. The entire site appears to be underlain at shallow depths by the Vashon till, a dense, nonsorted, non-stratified deposit of silt, sand, gravel, and cobbles.

Site soils are formed in the Vashon till layer and are classified as Alderwood gravelly sandy loam with a moderately rapid permeability of 0.05 to 0.15 m/hr (U.S. Dept. of Agriculture, Soil Conservation Service, 1973). Based on observations during piezometer installation and hand auger samples, a typical soil profile consists of forest litter and a dark brown organic layer about 0.15 m thick, underlain by brown sand to silty sand with minor amounts of gravel and cobbles. The sandy layer typically extends to a depth of 0.6 to 1 m and overlies the dense Vashon till. The saturated vertical hydraulic conductivity of the glacial till is very low, from 0.15 to 0.3 m per *year* (Olmsted, 1969). Plant roots extend to the till, however the root network thins rapidly at a depth of 0.4 to 0.6 m below the ground surface.

Average annual rainfall in the area is estimated to be between 1170 and 1300 mm, based on two weather stations within a 10 km radius of the site

(Burges et al., 1989) Most of the precipitation (70 to 80 percent) falls from October through May. Average annual evaporation from shallow lakes is estimated to be 635 mm (Linsley et al., 1982).

5.2 Field Mapping

The Novelty Hill site was field mapped using the methods described in Burges et al. (1989). Based on detailed field mapping and observations during site visits the seasonal wetland was found to be the only source of surface runoff generation. Discharge from the remainder of the site is in the form of subsurface flow. The detailed mapping was conducted on July 23, 1990. Wetland boundaries were determined using vegetation, local topography, and evidence of recent or seasonal soil saturation. The average wet-season areal extent of the wetland is 1.44 ha, approximately 3.9 percent of the total catchment area. The width varies from a few meters at the northern end to a maximum of 31 m, with a mean width of about 18 m. The maximum length is 808 m, about 80 percent of the total catchment length. The wetland reached its largest areal extent during heavy rainfall in January 1990. Based on swale topography, spot measurements, and personal observations, particularly those during the major January 1990 storm, it is estimated that the maximum areal extent of the wetland is no more than 50 percent greater than the mapped area (2.16 ha).

5.3 Model-Independent Hydrologic Analysis of Field Measurements

5.3.1 Hydrologic Instrumentation

One tipping-bucket rain gage, with a bucket capacity of 0.254 mm (0.01 inch) has been recording at 15-minute intervals continuously since October 1, 1989. The rain gage is located on the edge of a large wetland approximately 300 m east of the catchment boundary. Rainfall data for the period from May 4, 1990 to June 13, 1990 were lost. The missing record was filled in using data from a 15-minute gage located at a similar elevation about 1 km to the northeast.

Streamflow at the outlet of the catchment is measured at 15-minute intervals using a combination v-notch and sharp-crested rectangular weir located about 4 m downstream of an abandoned railroad grade (Figure 5-1). Flows from the swale pass under the railroad grade through a culvert before entering a pool upstream of the weir. Both the railroad fill and the weir act as barriers to lateral subsurface flow above the till layer. The weir is keyed into Vashon till at a depth of about 0.6 m and has been sealed using Portland cement grout. As a result, nearly all surface and subsurface discharge exiting the catchment *above* the till layer passes through the weir.

Water levels in the pool formed by the weir are recorded in 3.05 mm (0.01 foot) increments at 15-minute intervals using an Instrumentation Northwest PS-7000 pressure transducer. A transducer has been in place since October 1, 1989. The original transducer displayed excessive drift and was replaced on January 15, 1990. Although data from October 1, 1989 to January 14, 1990 had to be discarded, it was still possible to determine the date at which surface discharge began in Water Year 1990. The replacement

transducer has functioned properly since it was installed. The difference in discharge calculated using transducer data and values from 22 manual measurements is 0.28 l/s, with a standard deviation of 0.57 l/s. Weir specifications and the complete error analysis are presented in Appendix A.

Six piezometers were installed along a 176 m transect in the northeast corner of the basin on December 7, 1989 (Figure 5-1, Piezometer Group P). The transect extends from the ridge crest to the swale, perpendicular to the ground surface contours (presumably coincident with a local flow line). Each piezometer is made of 63.5-mm diameter PVC pipe with the lower 0.3 m slotted. All piezometers rest on glacial till at a depth of about 1 m. Piezometer No. 5 (P-5), located 155 m downslope from the ridge crest contains a Unidata capacitative sensor which records water table height in 3.05 mm (0.01 foot) increments at 15-minute intervals. The remaining piezometers each contain a small-diameter PVC crest gage to record peak water table heights between site inspections. The sensor was operated continuously between December 7, 1989 and May 18, 1990. Based on 19 measurements, the average difference between manual and sensor recorded water elevations is 6 mm, with a standard deviation of 12 mm.

A second set of four piezometers was installed in the southeastern portion of the basin (Figure 5-1, Piezometer Group L) on November 13, 1990. Two piezometers were completed to till on each side of the swale, about 50 m up from the basin outlet. All four piezometers contain a crest gage. These piezometers were installed for two reasons: to provide water table information lower in the basin where hillslope gradients are less; and to record or estimate

the maximum lateral extent of surface saturation. Water level data also allowed the simulation model to be tested at locations where data was unavailable during calibration. Piezometer details and the complete error analysis for piezometer P-5 are given in Appendix B.

5.3.2 Mass Balance

Twenty months (October 1, 1989 - April 28, 1991) of 15-minute rainfall and streamflow data, including two entire wet seasons, were used. These data are displayed graphically in Figure 5-2. It was necessary to fill in the weir discharge record during the period of incorrect sensor operation to compute an annual streamflow volume. As discharge did not begin until December 4, 1989, the actual period to be filled is from then to January 16, 1990. The record was filled using linear interpolation through discharge calculated from 14 manual stage measurements. This period of the record contains two storms, including the large January 1990 storm. Nine manual measurements were taken during the January storm including two on the day of peak flow, allowing adequate reconstruction of the hydrograph. Only five manual measurements were available for the early December 1989 storm. Although reconstruction of this storm is crude, an estimate of daily runoff volumes is possible. The estimated flow volume for the period December 4, 1989 - January 16, 1990 is 49 percent of the annual total.

During Water Year 1990 (October 1, 1989 to September 30, 1990), 1210 mm of precipitation were recorded resulting in 352 mm of runoff at the weir (Table 5-1). An estimate of the volume of saturation overland flow from the

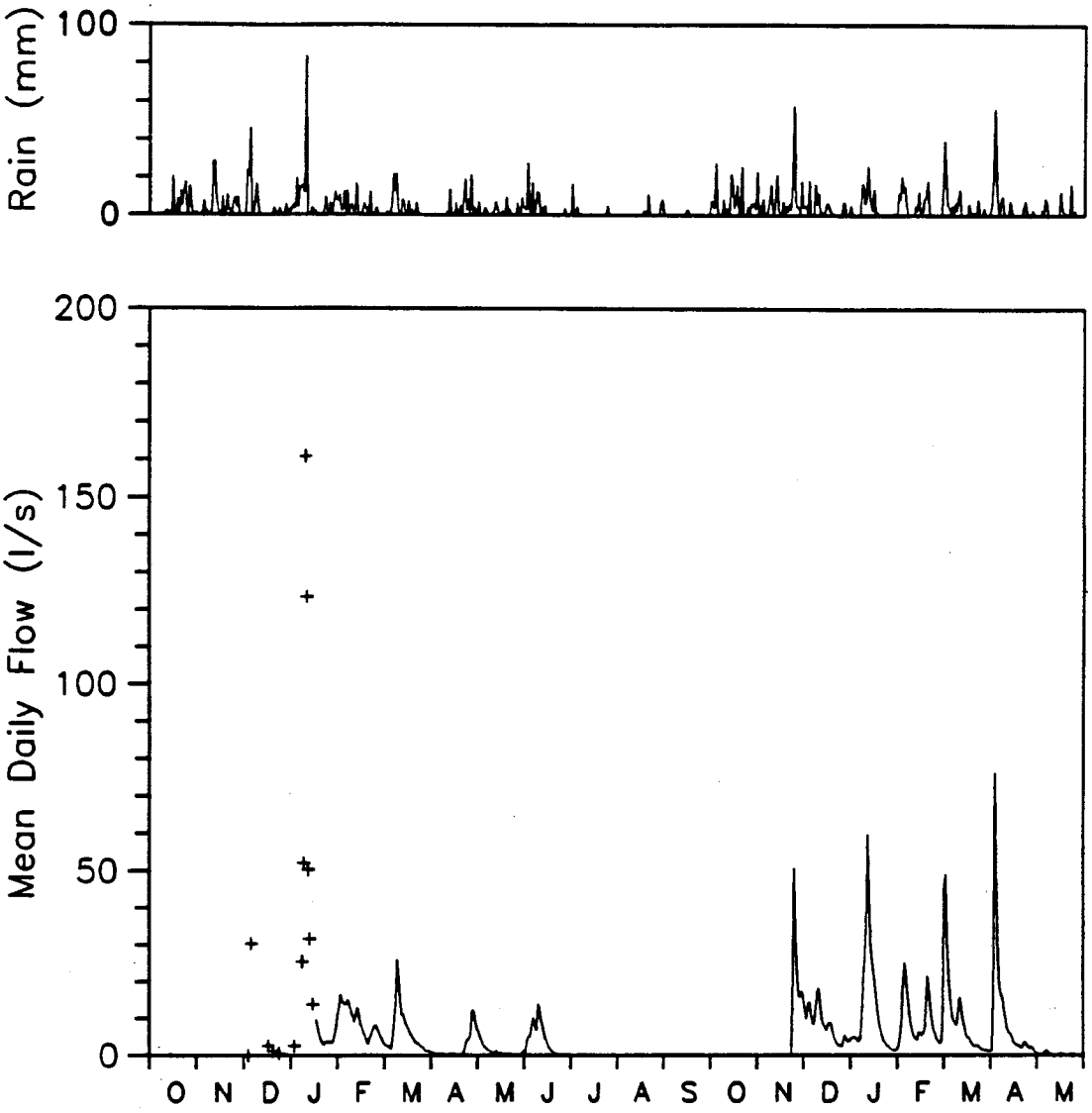

Fig. 5-2. Daily time series of rainfall and recorded streamflow for the 20-month study period from October 1, 1989 to May 26, 1991. Discharge calculated from manual stage measurements are shown as crosses.

TABLE 5-1. Novelty Hill Flow Components: Water Year 90

	Water Year 90		Wet Season (12/4/89 - 6/23/90)	
	(mm)	(percent)	(mm)	(percent)
Precipitation	1210	100	830	100
Weir Discharge	352	29	352	42
Swale SOF[1]	32	3	32	4
Lateral Subsurface	320	26	320	38
ET and Till Leakage[2]	858	71	478	58

1 Based on an average saturated area of 1.44 ha

2 Changes in soil moisture storage are neglected

wetland was made using rainfall volumes during the periods of swale discharge and an average wetland surface area of 1.44 ha. During the water year 29 percent of the precipitation discharges through the weir as streamflow. Lateral subsurface flow accounts for 91 percent of the total *streamflow*, while saturation overland flow (wet season precipitation times 1.44 ha) accounts for only 9 percent (26 and 3 percent of total precipitation respectively). Assuming no net change in soil water storage, evapotranspiration and leakage through the till total almost 858 mm (71 percent of the precipitation). This is in within the range of regional estimates of potential evapotranspiration (635 mm per year) and till conductivities (150 to 300 mm per year). Approximately 70 percent (830 mm) of the annual precipitation fell during the wet season (taken as the period of weir discharge; December 4, 1989 to June 23, 1990). Forty-two percent of this precipitation discharged through the weir as channel flow.

Flow components were also estimated for the first half of Water Year 1991 (from October 1, 1990 to April 28, 1991) including the entire wet season. Precipitation for this eight month period was 1195 mm (Table 5-2), nearly equal to the total for all of Water Year 1990. Of this precipitation, 854 mm fell during the period of weir discharge (November 24, 1990 - April 26, 1991). Weir discharge accounted for 47 percent of the wet season precipitation. Lateral subsurface discharge produced 88 percent of the total streamflow. It was not possible to separate evapotranspiration and till leakage from changes in soil water storage. The percent distribution of flow components shows good agreement with wet season 1990.

The above analysis demonstrates the value of a relatively simple

TABLE 5-2. Novelty Hill Flow Components:
October 1, 1990 - April 28, 1991

	Complete Record (10/1/90 - 5/28/91) (mm)	Wet Season (11/24/90 - 5/26/91) (mm)	Wet Season (11/24/90 - 5/26/91) (percent)
Precipitation	1195	854	100
Weir Discharge	402	402	47
Swale SOF*	33	33	5
Lateral Subsurface	369	369	42

* Based on an average saturated area of 1.44 ha

combination of rainfall and streamflow monitoring, along with field mapping, for evaluating current basin hydrology in the context of land-use change. Weir and precipitation gage installation required about 3 days, while field mapping was accomplished in a single day. From this information we know that during Water Year 1990, 71 percent of the precipitation does not reach the stream channel, 26 percent reaches the channel via subsurface flow, and only 3 percent of the rainfall supplies saturation overland flow to the channel. To avoid the stream channel and stream-side habitat degradation which normally accompanies a change in land use, it will be necessary to design mitigation strategies which result in a similar distribution of flow components. These observations are based on records for one year (with annual precipitation within the regional range based on 20-years of record).

5.3.3 Water Year 1990: Piezometer Analysis

Hillslope characteristics along the upper piezometer transect are typical of the northern two-thirds of the catchment. Ground surface slopes are 3 to 5 percent and soil depths range from 0.7 to 1 m. Most of the following discussion concerns piezometer P-5, which is located 155 m downslope from the ridge crest and contains a sensor that records water levels at 15-minute intervals. With the exception of the large January 1990 storm, there appears to be an almost linear relation between the piezometer measured water level and weir discharge (Figure 5-3). Even for the January storm the timing of the piezometer response agrees well with the weir response. The close relationship between piezometer

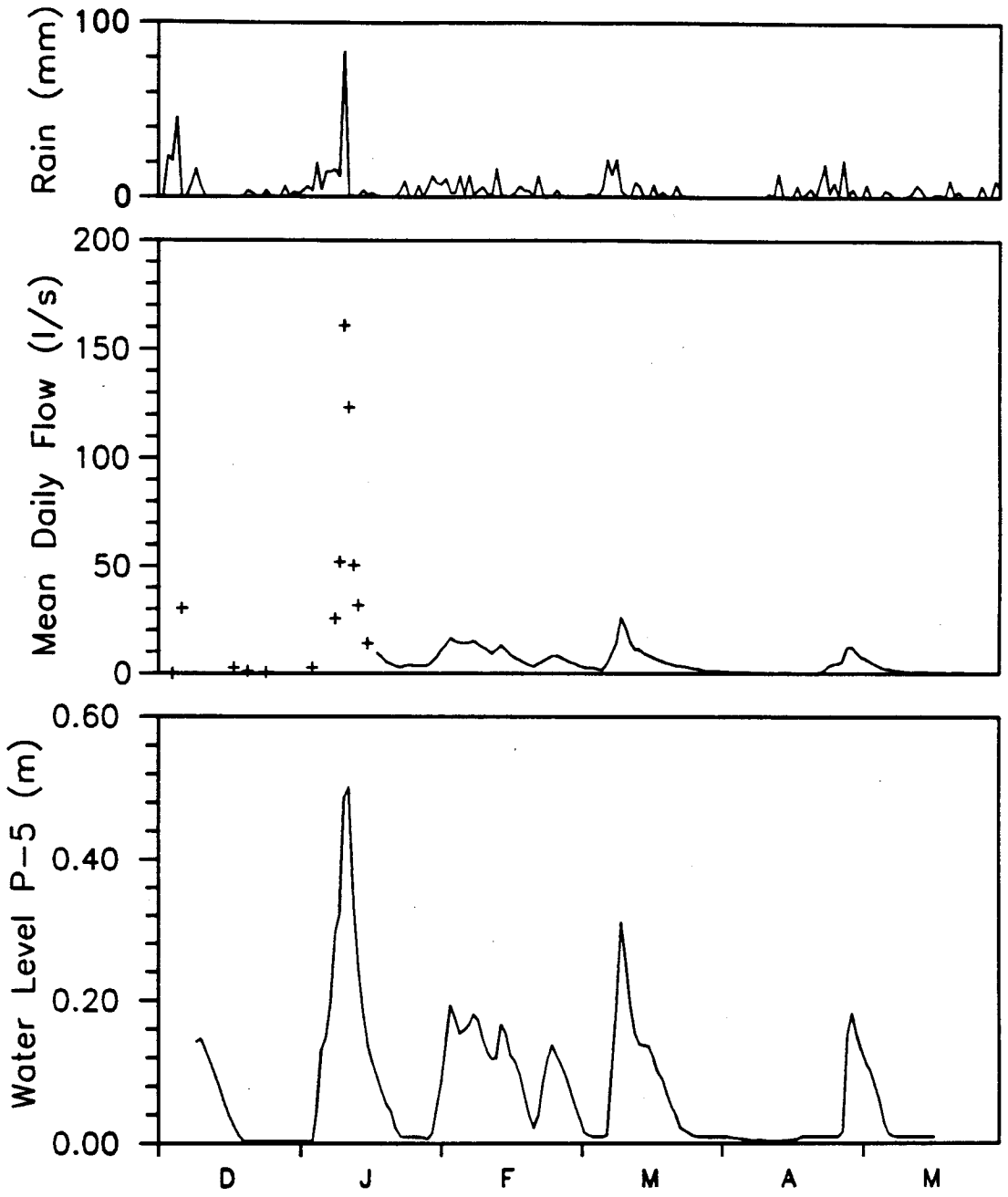

Fig. 5-3. Daily time series of rainfall, recorded streamflow, and water levels at piezometer P-5 for December 1, 1989 through May 17, 1990. Discharge calculated from manual stage measurements are shown as crosses. (With the exception of the large January storm, there is a nearly linear relationship between water levels and discharge.)

and weir responses indicates: 1) subsurface conditions control discharge at the weir, and 2) the response of piezometer P-5 appears to be representative of general water table response throughout the catchment.

Effective Soil Porosity

The response of piezometer P-5 to rainfall was used to estimate effective soil porosity and saturated lateral hydraulic conductivity. Maximum effective porosity (ϕ_e) was calculated for four unrelated storms as the total rainfall depth (P) divided by the corresponding water table rise at piezometer P-5 (Δh):

$$\phi_e = \frac{P}{\Delta h} \tag{5-1}$$

This method of analysis assumes that all storm rainfall enters the soil and contributes to the water table rise, so these estimates represent maximum values. Maximum effective porosities ranged from 0.13 to 0.27 (Table 5-3).

Spatially Averaged Saturated Lateral Hydraulic Conductivity

Several methods were used to estimate spatially-averaged saturated lateral hydraulic conductivity. An average saturated soil pore velocity (v_w) can be calculated by holding the saturated hydraulic conductivity constant and dividing equation (4-1) by the effective area of flow

$$v_w = \frac{\overline{K}\,\zeta(s,h)}{\phi_e} \tag{5-2}$$

TABLE 5-3. Calculation of Effective Porosity

Date of Storm	Precipitation (mm)	Piezometer Range* (m)	Effective Porosity (m^3/m^3)
1/03/90 - 1/08/90	81	0.003 - 0.335	0.24
1/08/90 - 1/10/90	90	0.305 - 0.640	0.27
3/06/90 - 3/10/90	64	0.009 - 0.335	0.19
4/27/90 - 4/28/90	23	0.009 - 0.189	0.13

* From start of storm to peak

where $\overline{K}$ is an average saturated hydraulic conductivity. The hydraulic gradient, $\zeta(s,h)$ will be taken equal to 0.03, the median water table gradient at piezometer P-5. If the recession time from piezometer peak to pre-storm water levels (ΔT_r) represents the time required to drain the entire saturated zone upslope from piezometer P-5, an average flow velocity can be calculated as the upslope distance (155 m) divided by ΔT_r. Setting this velocity equal to v_w in (5-2) allows average saturated conductivities to be calculated from effective porosity (Table 5-3) and piezometer recession time. This analysis was performed for three storms (Table 5-4) yielding average saturated conductivities of 2.7, 3.1, and 5.2 m/hr.

The average velocity method for determining saturated hydraulic conductivity depends on an accurate estimation of effective porosity. To avoid this requirement conductivities were also calculated through a mass balance approach. If it is assumed that all storm precipitation which fell upslope of piezometer P-5 discharges past the piezometer, the following relation holds:

$$V_{pz} = \overline{K}\ \overline{h}\ \overline{\zeta}\ \Delta t_s \qquad (5\text{-}3)$$

where V_{pz} is the volume of storm rainfall per unit width upslope of the piezometer, $\overline{h}$ an average saturated depth, $\overline{\zeta}$ an average hydraulic gradient, and Δt_s is the time from the *beginning* of storm rainfall to the time when the piezometer returns to pre-storm levels. In the remaining calculations it is the hydraulic gradient at piezometer P-5 which is of interest; a median value of 0.03 will again be used.

TABLE 5-4 Saturated Conductivity Calculated by Average Velocity

Piezometer Range (m)	Duration (hr)	Average Velocity (m/hr)	Effective Porosity (m^3/m^3)	Saturated Conductivity (m/hr)
0.640 - 0.009	276	0.56	0.27	5.2
0.335 - 0.009	375	0.41	0.19	2.7
0.189 - 0.009	213	0.71	0.13	3.1

In (5-3) it is assumed that the amount of water stored in the unsaturated zone is the same at the beginning and end of the time period. To approach this condition, the analysis is continued until the water table returns to its pre-storm level. Obviously during this time period some water will be lost to evapotranspiration and leakage through the till. This loss of volume, estimated from the wet season mass balance calculations for Water Year 1990, is 0.37 m^2/day per unit width above piezometer P-5. Average values of saturated hydraulic conductivity are calculated for five storms and are presented in Table 5-5. When no water is assumed lost to evapotranspiration or till leakage saturated lateral hydraulic conductivity values range from 7.9 to 14.9 m/hr. With water loss, saturated hydraulic conductivity values are between 4.3 and 14.0 m/hr.

With the exception of the January 1990 storm there is a nearly linear relation between the water table height at piezometer P-5 and discharge at the weir (Figure 5-3). If it is assumed that the piezometer response at P-5 is representative of average water table conditions through out the entire catchment, then under conditions where subsurface flow dominates:

$$Q_w(t) \simeq 0.03\, \overline{w}\, \overline{T}(h) \tag{5-4}$$

where Q_w is the weir discharge, $\overline{w}$ is the representative seepage face width, $\overline{K}$ is the catchment-averaged saturated lateral hydraulic conductivity, and h is the transient water table height at piezometer P-5. The hydraulic gradient is again taken as 0.03. The representative width is calculated as the total basin area

TABLE 5-5. Mass Balance Calculation of Saturated Conductivity

Start of Storm	Duration (hr)	Average Piezometer Height (m)	Volume* (m^2)	Average Discharge (m^2/hr)	Saturated Conductivity (m/hr)
1/08/90	68	0.460	14.03	0.67	14.9
			13.84	0.64	14.0
1/03/90	429	0.204	27.96	0.21	10.7
			21.46	0.15	8.2
1/28/90	553	0.122	18.95	0.12	9.4
			10.50	0.06	5.2
4/27/90	168	0.134	5.39	0.09	7.9
			2.79	0.06	4.3

* First row volume uncorrected for leakage and evapotranspiration
Second row volume corrected for leakage and evapotranspiration

(36.8 ha) divided by the downslope distance to piezometer P-5 (155 m) and is equal to 2374 m (36.8 ha/155 m).

Various values of saturated hydraulic conductivity were used in (5-4) to calculate discharge at the weir. Calculated discharges were compared to recorded discharge over the period when both piezometer and weir sensors were operational (January 15, 1990 to May 18, 1990). The saturated thickness at piezometer P-5 remained below 0.34 m for the entire time period. Saturated lateral hydraulic conductivity was optimized based on the root-mean-squared-error (RMSE) between calculated and recorded flows. A vertically-constant saturated lateral hydraulic conductivity of 4.0 m/hr produced the best results having a RMSE of 1.7 l/s (Figure 5-4a). However, this saturated hydraulic conductivity produces a peak weir discharge during the large January storm of 51 l/s, well below the value of 201 l/s calculated from a manual stage measurement (Figure 5-4b). Stage was increasing at the time of this measurement, therefore the peak discharge must have been greater than 201 l/s.

The timing of the water table rise and recession at piezometer P-5 agreed well with hydrograph timing at the weir (Figure 5-3). It was first assumed that the peak weir discharge of January 9-10 was produced by precipitation falling directly on an expanding saturated area (primarily in the lower catchment where the lowest gradients occur). However, measurements and field evidence do not support this hypothesis. The rainfall peak of 11 mm/hr occurred on January 9, 1990 at 0900 PST. Discharge at the weir was increasing at the time of the manual stage measurement on January 9, 1990 at 1800 PST, therefore the weir peak must have occurred between this time and

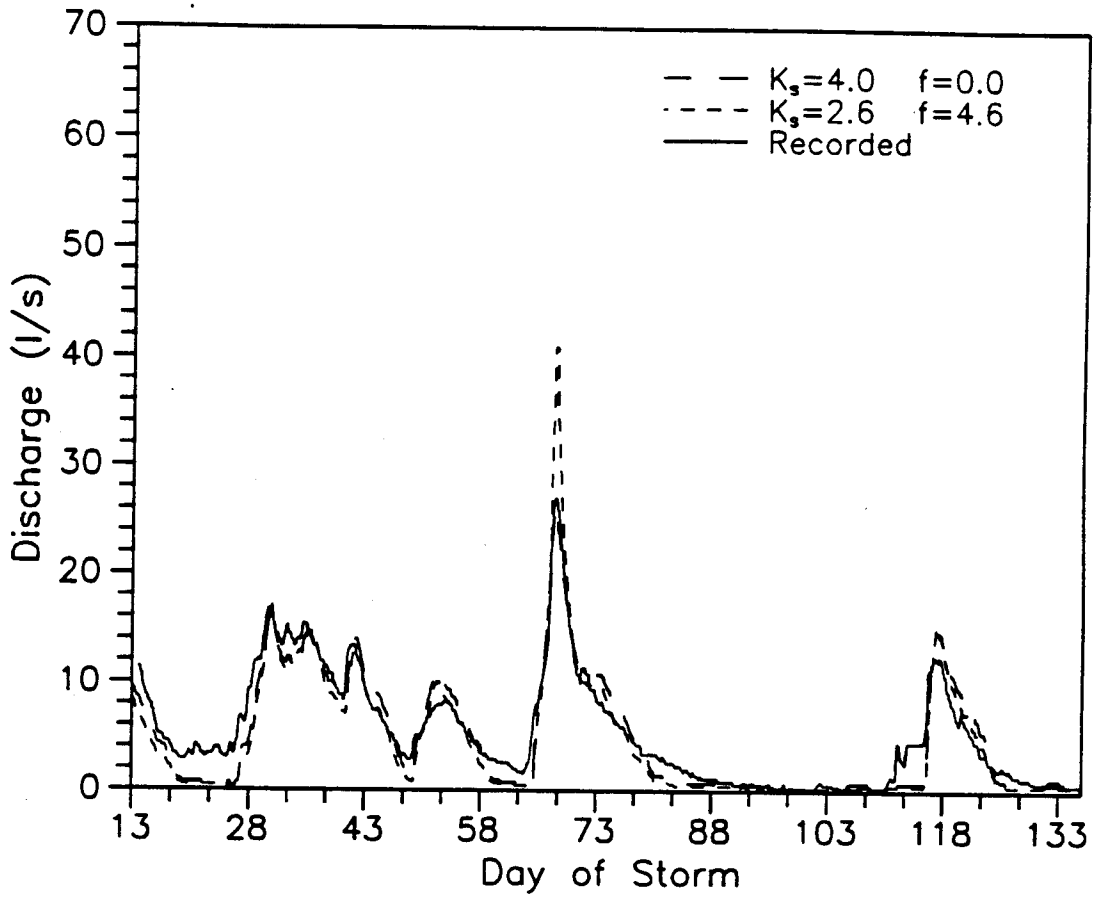

Fig. 5-4a. Mean hourly discharge recorded at the weir and discharge calculated using an effective channel width and hydraulic conditions at piezometer P-5. Calculated discharge is shown for two vertical distributions of saturated lateral conductivity for the period January 15, 1990 through May 17, 1990.

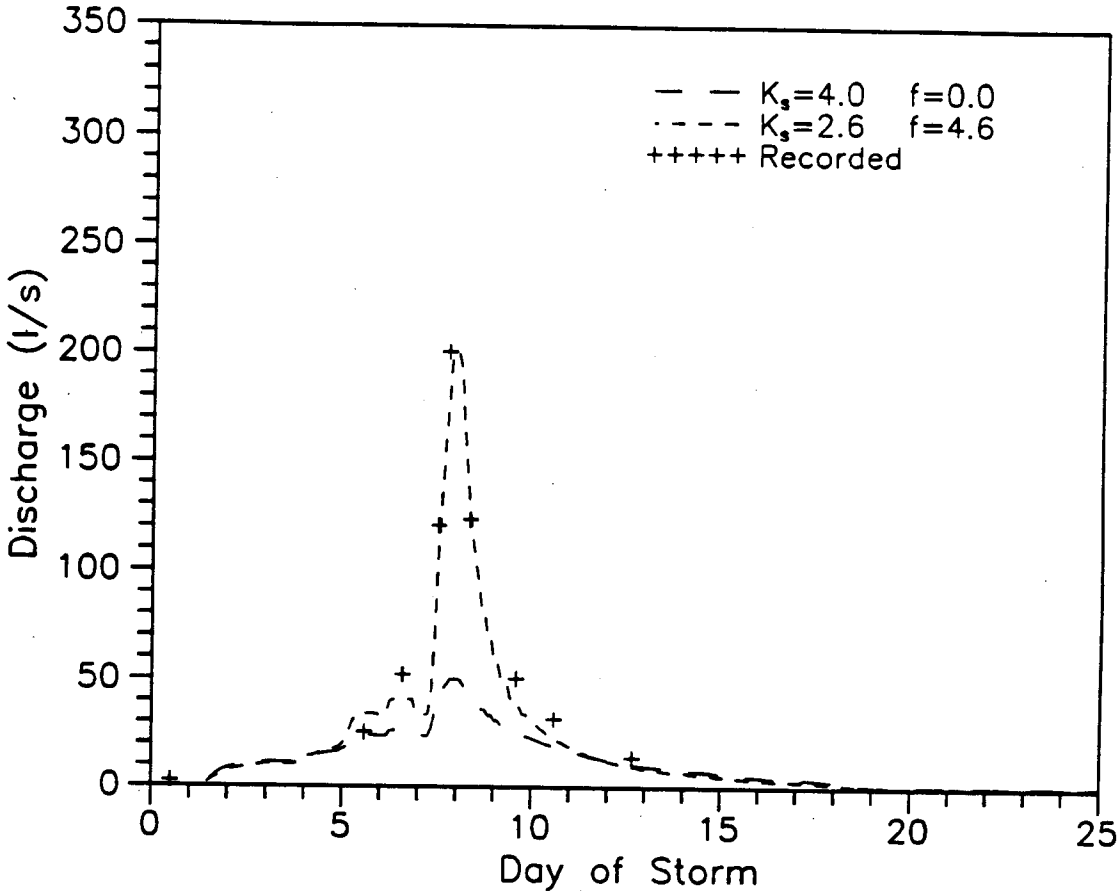

Fig. 5-4b. Mean hourly discharge recorded at the weir and discharge calculated using an effective channel width and hydraulic conditions at piezometer P-5. Calculated discharge is shown for two vertical distributions of saturated lateral conductivity for the period January 2, 1990 through January 24, 1991.

the next stage measurement on January 10, 1990 at 0930 PST. Assuming average flow velocities in the swale of 0.15 to 0.3 m/s, the channel lag is between 0.7 and 1.5 hours. This is much less than the minimum 9 hour delay between rainfall and weir peaks.

If the previously calculated, vertically-constant saturated lateral hydraulic conductivity of 4 m/hr is correct, depending on the water table height, saturation overland flow must account for all weir discharge exceeding about 30 to 60 l/s (Figure 5-5). This occurs for the entire 71 hour period between hand measurements on January 8, 1990 at 1315 PST and January 11, 1990 at 1315 PST (and for about one-half the time between January 7, 1990 at 1515 PST and January 12, 1990 at 1505 PST). The total discharge volume over this 71 hour period is about 14,440 m^3. Precipitation during this period totaled 91 mm. A saturated area of 15.8 ha would be required to generate 14,440 m^3 of runoff from 91 mm of rainfall. This would require surface saturation over 40 percent of the basin. Field observations and measurements indicate that the actual saturated area was much *lower* than this, probably no more than 4 to 6 percent of the basin. This indicates that much of the peak weir discharge results from rapid subsurface flow and that there may be an increase in saturated lateral hydraulic conductivity with distance above the till layer.

There is a nearly linear relation between water levels at piezometer P-5 and weir discharge for water table heights below 0.3 m. At heights greater than 0.3 m, the preceding analysis supports a non-linear relationship between subsurface discharge and saturated depth, indicating an increase in effective saturated hydraulic conductivity. Based on soil conditions this change may be

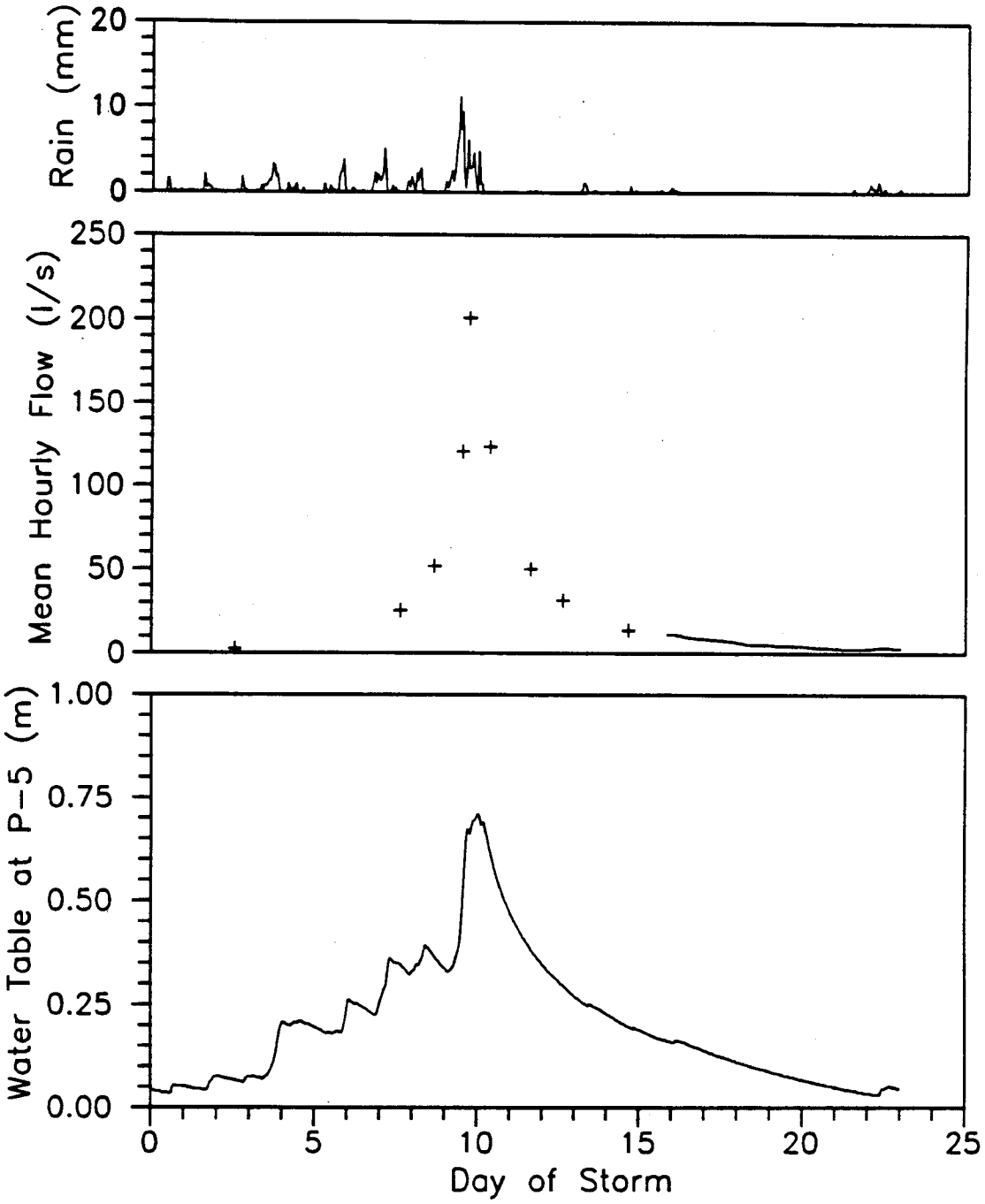

Fig. 5-5. Hourly rainfall, streamflow, and water levels at piezometer P-5 for the period December 31, 1989 through January 22, 1990. Discharge calculated from manual stage measurements are shown as crosses.

expected. At most locations within the catchment the densest vegetative root network extends to a depth 0.4 to 0.6 m below the soil surface; about 0.3 m above the till layer. When saturated thickness at piezometer P-5 is plotted against weir discharge (Figure 5-6) there is an obvious break in slope near this depth. Within this root zone, one would expect flow velocity to increase with water table height (saturated thickness) due to the greater availability of macropores.

To test the above hypothesis, the exponential saturated hydraulic conductivity relation incorporated in equation (4-1) was used to calculate transmissivity in (5-4). The best correspondence between calculated and observed discharge occurs with a base saturated hydraulic conductivity of K=2.6 m/hr and f = 4.6. The RMSE of 2.0 l/s is nearly the same as obtained using a constant saturated hydraulic conductivity of 4 m/hr. However, the exponential hydraulic conductivity distribution produces a better fit to the January 9-10 storm (not used in the RMSE calculation) (Figure 5-4b) with a peak discharge of 201 l/s (at the peak recorded water table depth of .64 m).

The field estimates of saturated lateral hydraulic conductivity are summarized in Table 5-6. Estimates of vertically-averaged saturated hydraulic conductivity show remarkably good agreement when the average saturated thickness at Piezometer P-5 is 0.3 m or less, ranging between 2.7 and 10.7 m/hr depending on the method used. When the saturated thickness exceeds 0.3 m hydraulic conductivity estimates range between 8.9 and 14.9 m/hr, suggesting an increase in saturated lateral hydraulic conductivity with distance above the till layer.

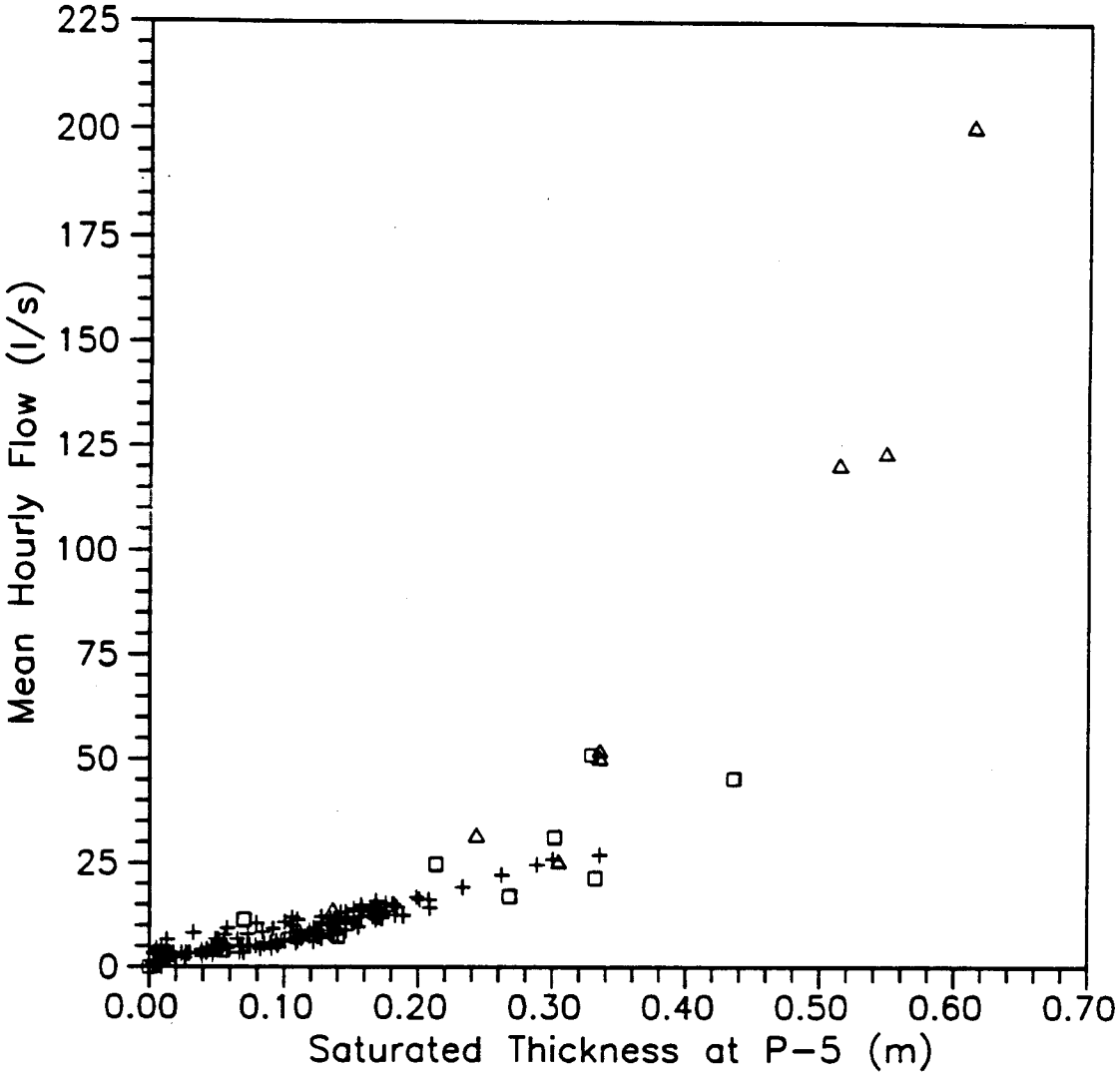

Fig 5-6. Mean hourly weir discharge as a function of saturated zone thickness at piezometer P-5. There is a break in slope at a saturated thickness of 0.30 - 0.35 m. Data for the period when both the weir and piezometer sensors were operational are shown as crosses. Weir discharge calculated from manual stage measurements in Water Year 1990 are shown as triangles. Squares represent manual measurements of water table levels in Water Year 1991.

TABLE 5-6. Summary of Field Estimates of Spatially Averaged Saturated Conductivity (m/hr)

Method	Average Saturated Thickness at Piezometer No. 5	
	< 0.3 m	> 0.3 m
Local Average		
Bail Test	3.7	--------
Hillslope Average		
Average Velocity	2.7 - 5.2	
Mass Balance[1]	7.9 - 10.7	14.9
Mass Balance[2]	4.3 - 8.2	14.0
Catchment Average		
Exponential f=0.0	4.0	--------
Exponential[3] f=4.6	3.6	8.9

1 Uncorrected for ET and leakage loss

2 Corrected for ET and leakage loss

3 K=2.6 m/hr, h=the average depth of Hillslope calculations (0.14 and 0.46)

The Novelty Hill catchment has relatively homogeneous hydrologic properties, side slopes are between 1 and 5 percent, soil depths are consistent at 0.6 to 1 m, and soil texture and surface cover on the forested hillslopes appear to be generally uniform throughout the basin. All of these features contribute to the close agreement in field estimates of saturated lateral hydraulic conductivity. In a more hydrologically heterogeneous catchment separate field estimates might be required for each type of runoff production zone.

5.3.4 Potential Evapotranspiration

Potential evapotranspiration is assumed equal to the potential evaporation from a free water surface. Daily values of potential evapotranspiration were estimated using data from a "Rain Bird WS-100 weather station" operated by the City of Redmond, Washington. The station is operated by the City Parks Department to determine park irrigation requirements. Daily values of total incoming solar radiation, percent relative humidity, average wind speed, rain fall, and maximum and minimum temperature were available from October 1, 1989 to the present.

Potential evapotranspiration was calculated using Penman's (1948) equation

$$E = \frac{\Delta}{\Delta + \gamma} Q_n + \frac{\gamma}{\Delta + \gamma} E_a \qquad (5\text{-}5)$$

where E is the potential evaporation from a thin free water surface, Δ is the slope of the curve relating saturation vapor pressure to temperature, γ is the

psychometric constant, Q_n is the net radiation exchange, and E_a describes the contribution of mass-transfer to evaporation. The last term was calculated through the empirical relation (Dunne and Leopold, 1978, p. 114)

$$E_a = (0.013 + 0.00016u_2)(e_{sa} - e_a) \tag{5-6}$$

where E_a is in cm/day, u_2 is the wind speed (km/day) measured at a height of two meters from the ground, e_{sa} (mb) is the saturation vapor pressure of a water surface at the air temperature, and e_a (mb) is the atmospheric vapor pressure at a height of 2 meters. The City of Redmond anemometer is positioned three meters above the ground. Wind speed was corrected to an elevation of two meters (z_2) assuming a log profile

$$\frac{u_2}{u_3} = \frac{ln\left(z_2/z_o\right)}{ln\left(z_3/z_o\right)} \tag{5-7}$$

where u_3 is the wind speed at three meters (z_3) and z_o is the roughness length taken equal to 0.7cm (corresponding to the grass height below the weather station of about 3 cm).

Linsley et al. (1982) present equations which allow $\frac{\Delta}{\Delta+\gamma}$, $\frac{\gamma}{\Delta+\gamma}$, and e_{sa} in (5-5) and (5-6) to be calculated from air temperature (T_a), and Q_n to be estimated from air temperature and daily solar radiation. The atmospheric vapor pressure (e_a) was calculated from saturation vapor pressure and recorded relative humidity. A complete description of evaporation calculations is given in Appendix C.

There were 42 days of missing data in the 20 month study period, all in Water Year 1990. The largest gap occurred from December 28, 1989 to January 28, 1990. These data were replaced with measurements from the Seattle-Tacoma Airport (Sea-Tac) weather station located 26 km to the southwest. Incoming solar radiation is not measured at Sea-Tac and was estimated following the procedure of Ducken (1990). Insolation (solar radiation at the outer atmosphere) was calculated based on date and location, and then attenuated by optical air mass, molecular scattering, albedo, and cloud cover to provide an estimate of incoming solar radiation at the land surface.

One is fortunate to find a relatively complete weather station within 6 km of a study site. However, there are several potential problems in using evaporation calculated at Redmond to estimate potential evapotranspiration at the Novelty Hill site. The weather station appears to be partially protected from the wind by buildings 4 to 5 m in height located to the south and to the west (prevailing wind direction), and by a strip of 15 to 20 m high trees to the north. It is not possible to determine the effect of these obstructions on recorded wind velocities. It is expected that recorded wind velocities will be lower than those over the forest canopy at the Novelty Hill site. The instrument station is contained within an approximately 6 m X 6 m grassed area. The lawn is watered during the summer months to simulate an irrigated park environment. No attempt was made to quantify the effect of watering on recorded air temperature and relative humidity. Irrigation of the grass beneath the instrument station may cause evaporation to be under estimated in the summer.

Early simulations of the hydrologic fluxes for the catchment indicated that potential evapotranspiration supplied to the model from the Penman calculations was low. This was confirmed by a model-independent mass balance calculation of actual evapotranspiration. Flow over the weir ceased at the Novelty Hill site on June 23, 1990; flow resumed on November 24, 1990. Over this period of time 445 mm of precipitation were recorded at the Novelty Hill site. During this period there was no evidence of soil water saturation, therefore leakage through the till should be near zero. Water storage in the canopy, litter, and soil should be about the same when the weir begins to flow as it was when the weir stopped discharging. As a result, the *actual* evapotranspiration over this time period should be about the same as the total precipitation of 445 mm. Potential evapotranspiration could not be quantified but should be greater. For the same period of time potential evapotranspiration calculated from Penman's equation using the City of Redmond data was 378 mm. To adjust for this difference, values of daily potential evapotranspiration calculated using Penman's equation were multiplied by

$$\frac{\text{445 mm actual evapotranspiration}}{\text{378 mm Penman}} = 1.18$$

Potential evapotranspiration should exceed actual evapotranspiration resulting in a coefficient greater than 1.18. However, it was not possible to quantify the amount of potential evapotranspiration between June 23 and November 24, 1990. Therefore the calculated coefficient of 1.18 was used. This coefficient was determined independently of the simulation model and makes no assumptions regarding the physical properties (soil depths and characteristics, canopy

storage capacity, etc) of the catchment. The resulting time series of daily potential evapotranspiration was applied to both land segments and channel reaches.

5.4 Model Representation

The Novelty Hill site contains two main hydrologic process zones: forested hillslopes that generate rapid subsurface flow; and a central swale with a dynamic zone of surface saturation that produces saturation overland flow. The hillslopes are generally homogeneous in terms of soil type and vegetation cover. For modeling purposes, the site was subdivided into 10 forested land segments based on topography and soil depth (Figure 5-7). The land segments are from 0.5 to 6.2 ha in size.

The central swale was modeled as a series of 5 channel reaches. Plan view areas were determined from field mapping. Flow conveyance was estimated from Manning's equation using surveyed channel cross-sections, channel slope and a roughness coefficient of 0.15. There is approximately 0.5 m of fine grained, dark, organic-rich soil between the swale bed and the underlying glacial till. This soil was assumed to have a water-holding capacity of 0.30 m per meter of soil.

The values of most model input parameters used to represent the basin were measured in the field or estimated from the literature (Table 5-7). Topographic information was taken from a 1.5-m (5-feet) contour map and supplemented with field surveys. Litter zone thickness and soil depths were based on 144 measurements throughout the basin. Values for canopy storage,

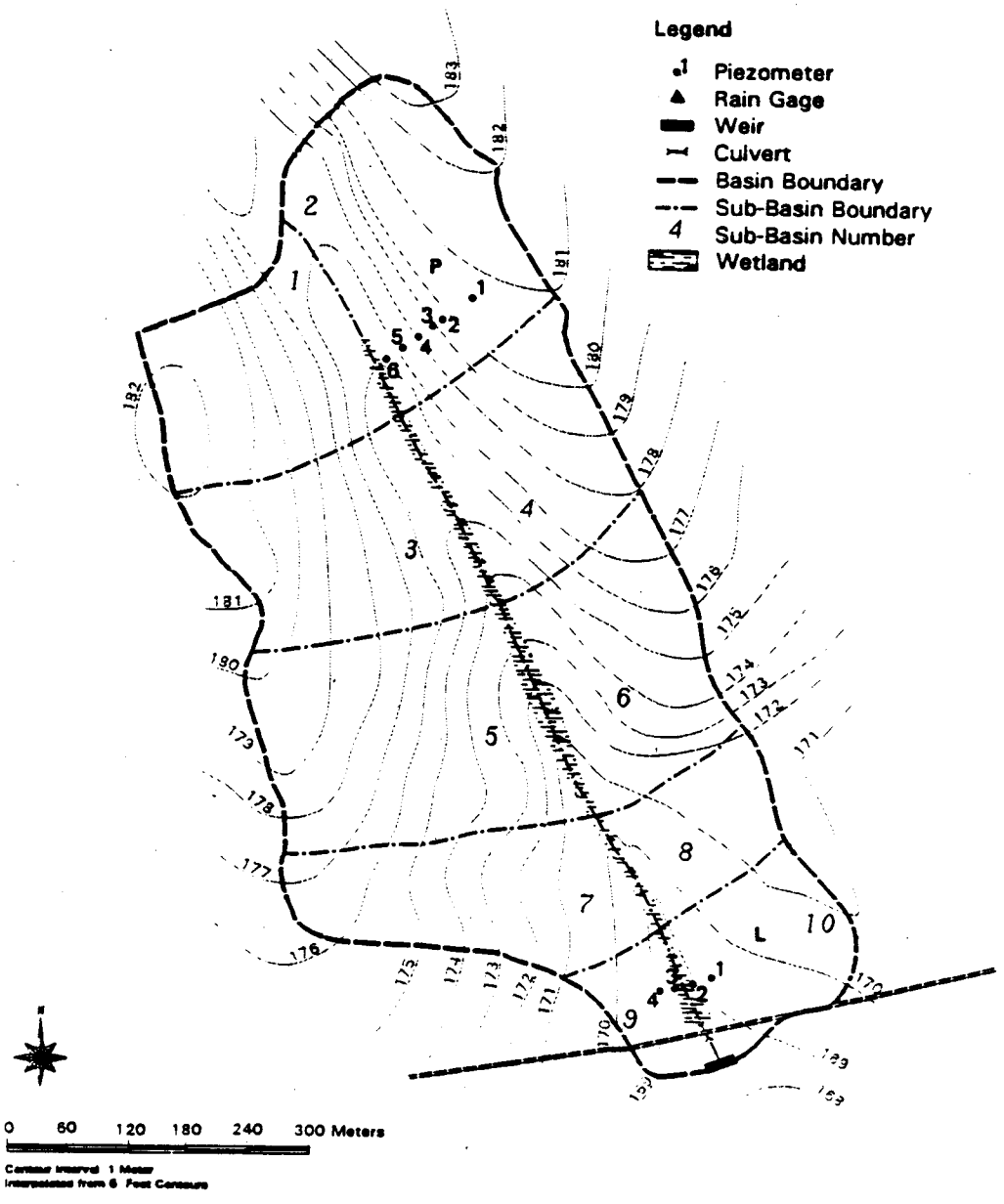

Fig 5-7. Subdivision of Novelty Hill basin into 10 land segments and 5 channel reaches.

TABLE 5-7 Model Input Parameters for the Novelty Hill Basin

Input Parameter	Value	Source
Topography		
Ground Surface Elevations	Variable	FM
Hillslope Top Width	Variable	FM
Hillslope Bottom Width	Variable	FM
Hillslope Length	Variable	FM
Canopy and Litter Zone		
Canopy Storage	6.1 mm	LIT[1]
Litter Zone Thickness	Variable	FM
Litter Zone Field Capacity	0.21	LIT[2]
Soil Characteristics		
Soil Depths	Variable	FM
Sat. Conductivity Coefficient	2.56 m/hr	FE
Sat. Conductivity Exponent	4.60	FE
Moist. Content at Wilting Point	0.10	LIT[3]

FM: Field Measurement
LIT: Literature
FE: Field Estimate

1 Dinicola, 1990
2 Balci(1964)
3 For a Sandy Loam, Rawls and Brakensiek (1989,p. 283)

litter zone field capacity, and the soil wilting point moisture content were taken from the literature and assumed *constant* over the catchment. There were insufficient field data to quantify any spatial changes in soil hydrologic properties. Therefore, in all land segments, the coefficient and exponent of saturated lateral conductivity (K_s and f) were taken equal to the catchment average field estimates of 2.6 m/hr and 4.6. Minimum soil infiltration capacities exceed the most extreme rainfall intensities. As a result, the model components for infiltration and overland flow were not used for the Novelty Hill simulations. Four input parameters were adjusted during calibration: the soil saturated moisture content, the soil field capacity, the unsaturated zone flow velocity, and the lower boundary (till) saturated vertical hydraulic conductivity.

5.5 Model Evaluation Criteria

A combination of statistical and graphical methods were employed to demonstrate differences between simulated (Q_s) and recorded (Q_r) time series. For daily time increments mean flow ($\bar{Q}$) and total volume (expressed as mm over the basin) were determined for Q_s and Q_r. Several measures were also used for the analysis of residues:

Root Mean Square Error, RMSE,

$$\text{RMSE} = \sqrt{\frac{\sum_{j=1}^{N}\left(Q_{sj} - Q_{rj}\right)^2}{N}} \tag{5-8}$$

Percent Root Mean Square Error, % RMSE,

$$\% \text{ RMSE} = \text{RMSE}\left(\frac{100}{\bar{Q}_r}\right) \tag{5-9}$$

Coefficient of determination, R^2,

$$R^2 = \frac{\sum_{j=1}^{N}\left(Q_{rj} - \bar{Q}_r\right)^2}{\sum_{j=1}^{N}\left(Q_{sj} - \bar{Q}_r\right)^2} \tag{5-10}$$

Modeling Efficiency, E_f,

$$E_f = 1 - \frac{\sum_{j=1}^{N}\left(Q_{sj} - Q_{rj}\right)^2}{\sum_{j=1}^{N}\left(Q_{rj} - \bar{Q}_r\right)^2} \tag{5-11}$$

where N is the number of discrete time increments. The coefficient of determination measures the proportion of the total variance of recorded data explained by the simulation model. The modeling efficiency is a measure used to describe the relative agreement between two time series (Nash and Sutcliffe, 1970; Gan and Burges, 1990). A perfect agreement between time series yields an efficiency of 1.0. A negative value of E_f represents a lack of agreement worse than if Q_s were replaced by its mean.

Two graphical displays are used to illustrate mean daily flows: a simple scattergram of simulated versus recorded flows, and a plot showing, from top to

bottom, daily rainfall depth, recorded stream flow, and the corresponding time series of $Q_s - Q_r$. Hydrographs resulting from large storms are illustrated by plotting mean hourly simulated and recorded streamflow on the same time series axis. Hourly rainfall totals are plotted above the hydrographs. Simulated and recorded water table elevations are analyzed statistically and graphically in the same manner as streamflow.

5.6 Model Calibration

Data from Water Year 1990 were available for model calibration. Unfortunately, the timing of individual instrument failures (Section 5.3.1) reduced the amount of 15-minute data used for calibration to the period from December 8, 1989 through May 3, 1990 for piezometer P-5, and from January 16, 1990 through May 3, 1990 for the weir.

At the start of model calibration runs canopy and litter zone water contents were assumed to be zero and the initial soil moisture content was taken equal to the wilting point. The model was driven using rainfall and potential evapotranspiration data for the period from October 1, 1989 through May 3, 1990. The simulations were started on October 1 to allow for the effects of assumed initial conditions to be removed by the start of recorded data at piezometer P-5 on December 8, 1989.

No attempts were made to gather data to permit modeling of spatial changes in soil hydrologic properties because, while the model is capable of such simulations, the required measurements are unlikely to be made by potential users of this type of model. As a result, hydrologic soil properties are assumed

constant throughout the basin, although topography and soil depths varied.

The physical basis of model parameters allow the model to be calibrated using a systematic approach. First the soil field capacity, saturation moisture content, and unsaturated zone velocity were calibrated by comparing simulated water table fluctuations at piezometer P-5 with recorded. The three soil parameter values were then used in all ten land segments and a single value for the saturated vertical hydraulic conductivity of the till was determined based on mass balance at the weir.

The product of soil depth and field capacity determines the volume of water that can be stored in the soil before a saturated zone forms on the hillslope and subsurface discharge to the swale begins. During calibration the field capacity was adjusted until the timing of simulated initial water table formation and weir discharge agreed with observed (which occurred on December 4, 1989). The final field capacity value of 0.43 was held constant through the remainder of the calibration.

How a water table responds to input from the unsaturated zone is primarily a function of the soil's saturated hydraulic conductivity and the current effective porosity $(\theta_s - \theta_{fc})$. Generally, the influence of effective porosity is most noticeable on the magnitude of piezometer rise, while saturated hydraulic conductivity controls the rate of recession. The vertical distribution of saturated lateral hydraulic conductivity has been estimated from field measurements and was not adjusted during calibration. As a result, during calibration the effective porosity controlled water table response to unsaturated zone input. The saturated moisture content was adjusted until simulated water

table fluctuations at piezometer P-5 were in agreement with recorded. A saturated moisture content of 0.62 produced the most satisfactory results. The resulting effective porosity of 0.19 is within the range of field estimates (0.13 - 0.27).

The unsaturated flow velocity determines the unsaturated zone lag, and therefore the timing of *initial* water table rise. A lag time of 5 hours was determined by comparing the timing of simulated water table rise with recorded at Piezometer P-5. Based on the average unsaturated zone thickness of 0.74 m, this results in an unsaturated flow velocity of 0.15 m/hr. The same four calibrated input parameter values were then used in all ten land segments and the saturated vertical hydraulic conductivity of the till layer was adjusted until the total simulated discharge volume at the weir was in general agreement with the recorded volume.

The soil property values obtained through calibration are in general agreement with the results of other studies conducted within forested watersheds in the Pacific Northwest. Buchanan et al. (1990) found soil porosities between 0.39 and 0.57 at their study site in Whatcom County, Washington. The soils average 0.7 m in depth and range from gravelly sands and poorly graded sands to silty sands. Measured soil field capacities are from 0.19 to 0.37. With the exception of one sample set, Buchanan et al. (1990) measured effective porosities ($\theta_s - \theta_{fc}$) between 0.16 and 0.33, with a mean of 0.21. The remaining sample set had a much lower effective porosity of 0.012. The authors also list soil porosities obtained from other regional studies by: Megahan and Clayton, 1983 (Idaho) 0.35-0.40; Humphrey, 1982 (Oregon) 0.6-

0.7; Harr 1977 (Oregon) 0.55-0.63; and O'Loughlin, 1972 (British Columbia) 0.55. Saturated moisture contents of about 0.6 were determined for forested soils at the University of Washington's experimental forest near Eatonville, Washington (Jackson, personnel communication, 1991). Laboratory measurements yields effective porosities around 0.2, while field estimates using (5-1) produce values closer to 0.06.

The final calibration results for water levels at piezometer P-5 are presented in Figures 5-8 through 5-11. The model consistently over-simulates saturated zone thickness, by an average of 0.015 m (Figure 5-8). This bias appears uniform over the entire range of saturated depths (R^2=0.95) (Figure 5-9). The timing and shapes of simulated water table fluctuations are adequate, having a RMSE of 0.034 m (Figure 5-10). However, simulated piezometer peaks are too high and recession times too long. Water table response to the large January 1990 storm is show in Figure 5-11. The simulated water table begins to rise early, although the timing and shape of the peak is good. The time scale of piezometer recession is again too long. The simulation could be improved considerably by increasing the saturated lateral hydraulic conductivity above the catchment average value. This would allow more rapid lateral discharge, reducing simulated piezometer peaks and decreasing recession times. Although field estimates yield hillslope average saturated hydraulic conductivities above piezometer P-5 greater that the catchment average (Table 5-6), the size of the area over which these values would apply is not known. Therefore, lateral saturated hydraulic conductivity was held to the catchment average in all forested land segments.

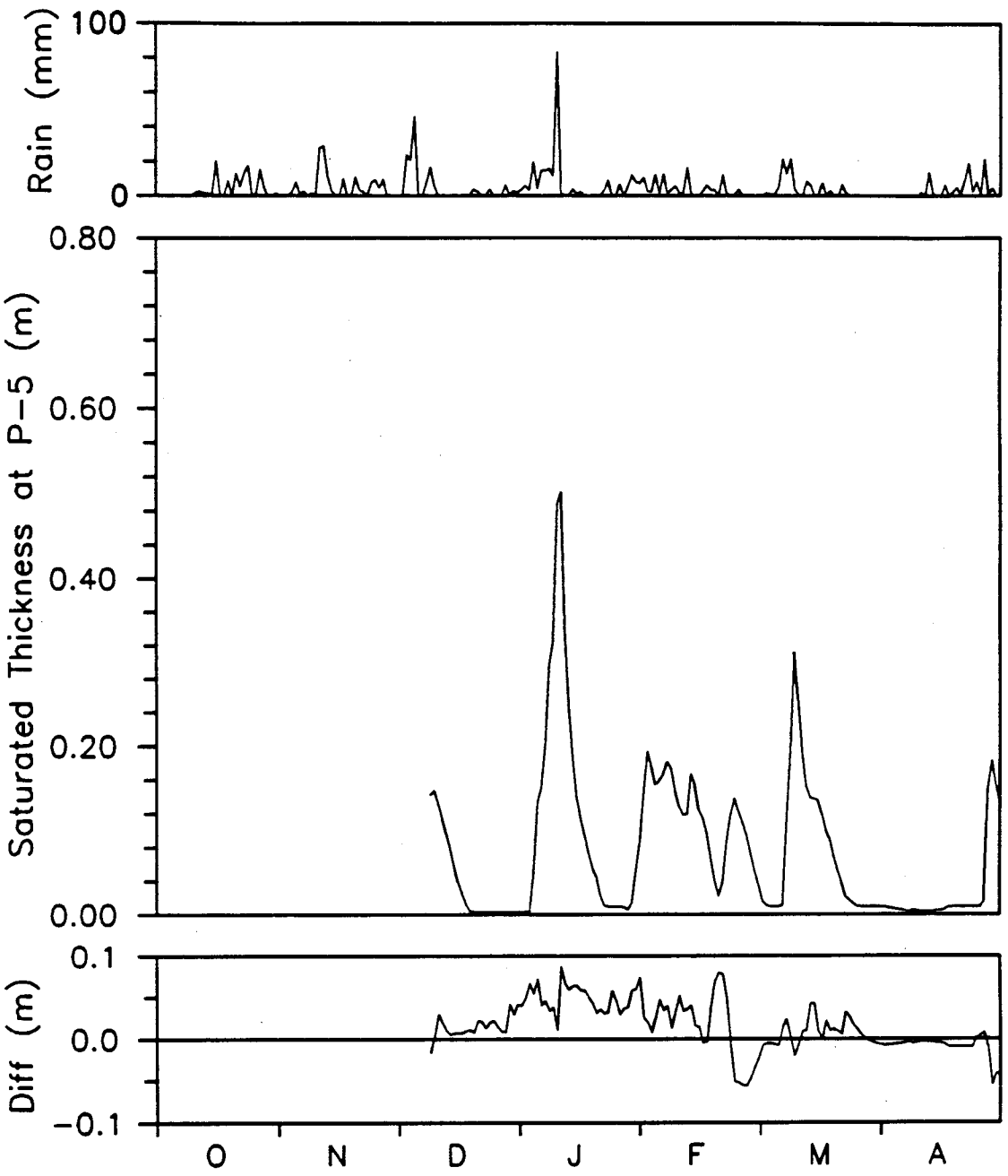

Fig 5-8. Daily time series of rainfall, recorded saturated zone thickness at piezometer P-5, and simulated minus recorded water levels for the period from October 1989 through April 1990.

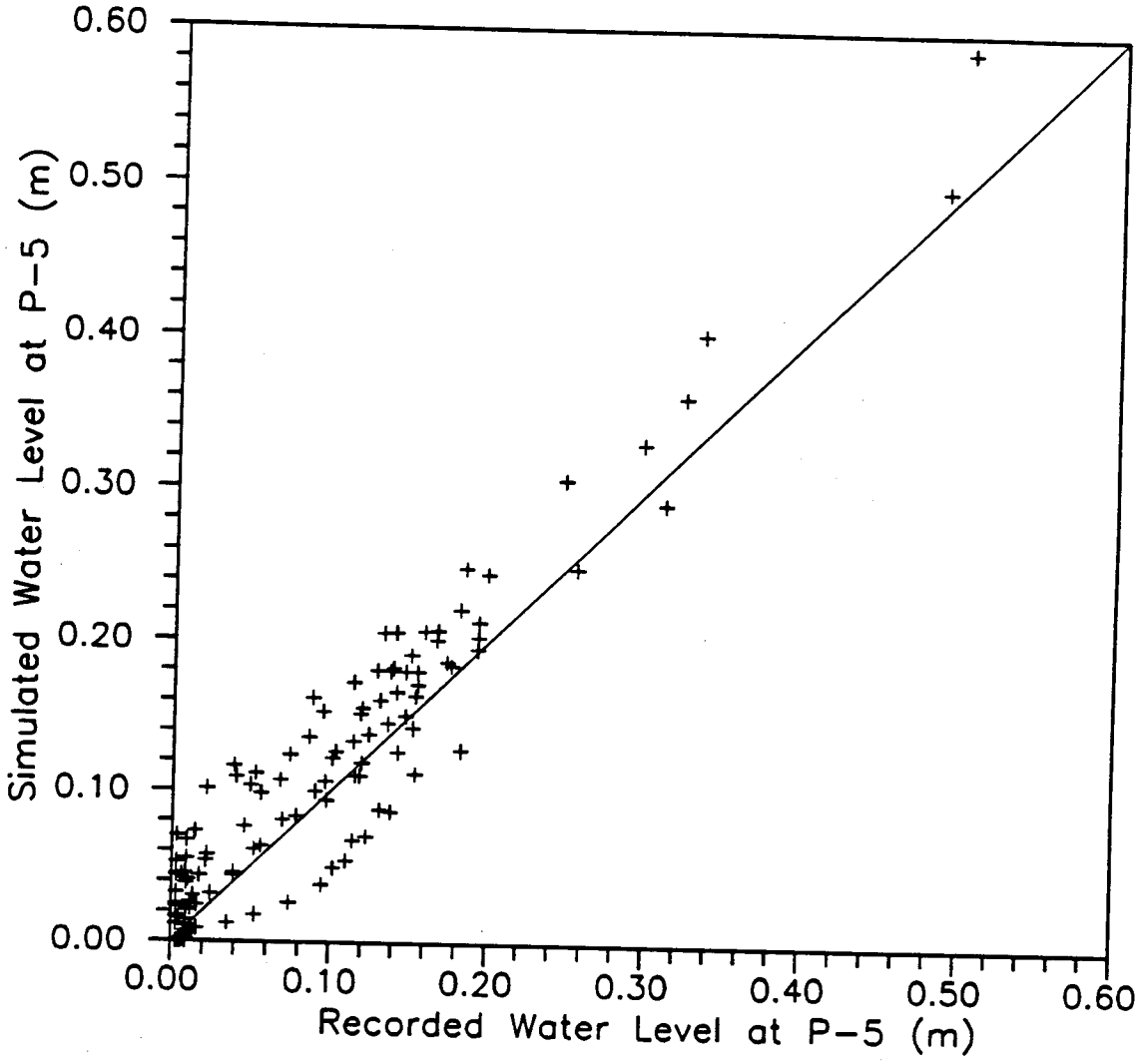

Fig. 5-9. Daily values of simulated versus recorded water levels at piezometer P-5 for the period December 8, 1989 through May 3, 1990.

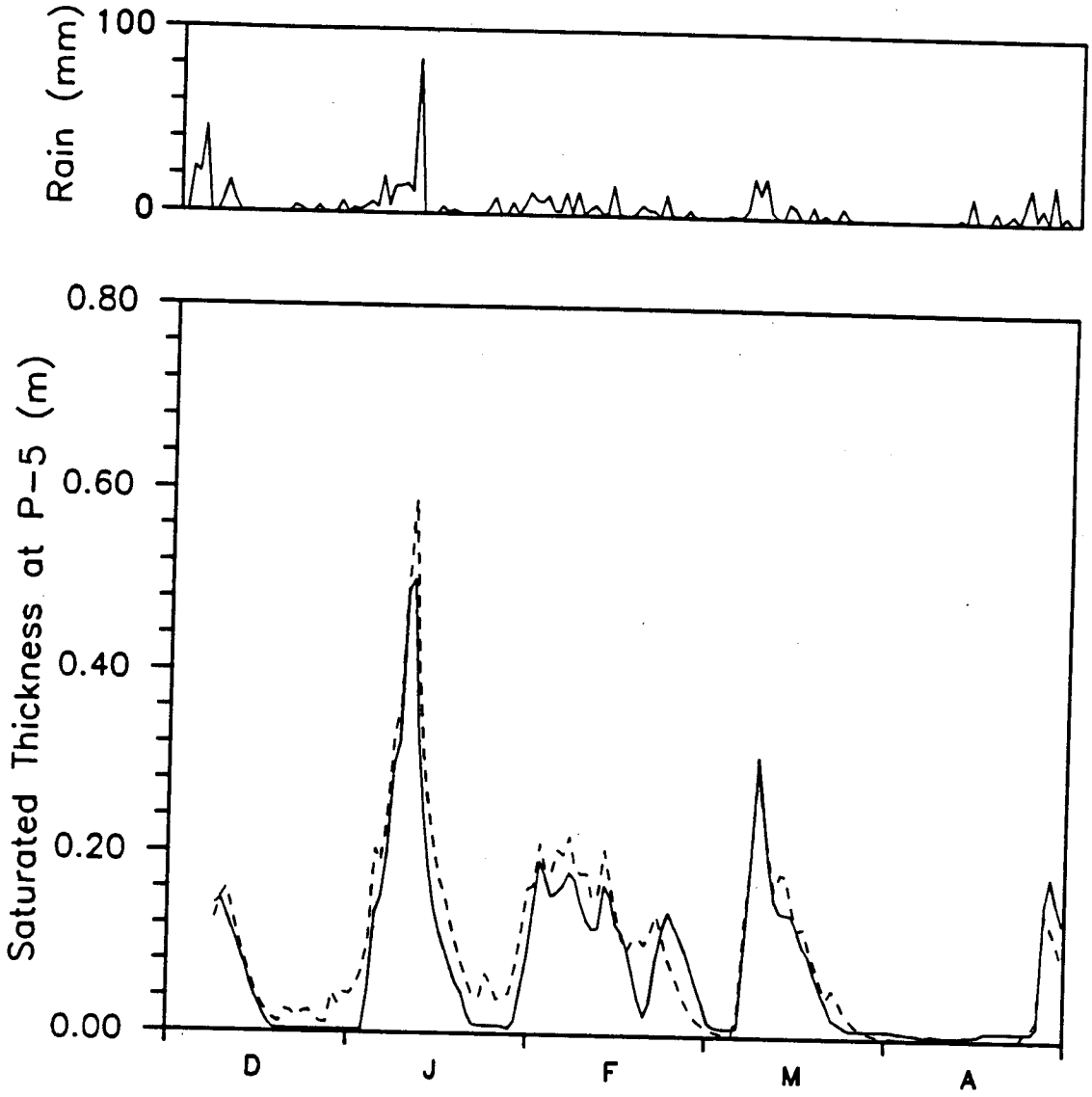

Fig. 5-10. Daily time series of rainfall, and recorded (solid line) and simulated (dashed line) saturated zone thickness at piezometer P-5. Data are for the period December 1989 - April 1990.

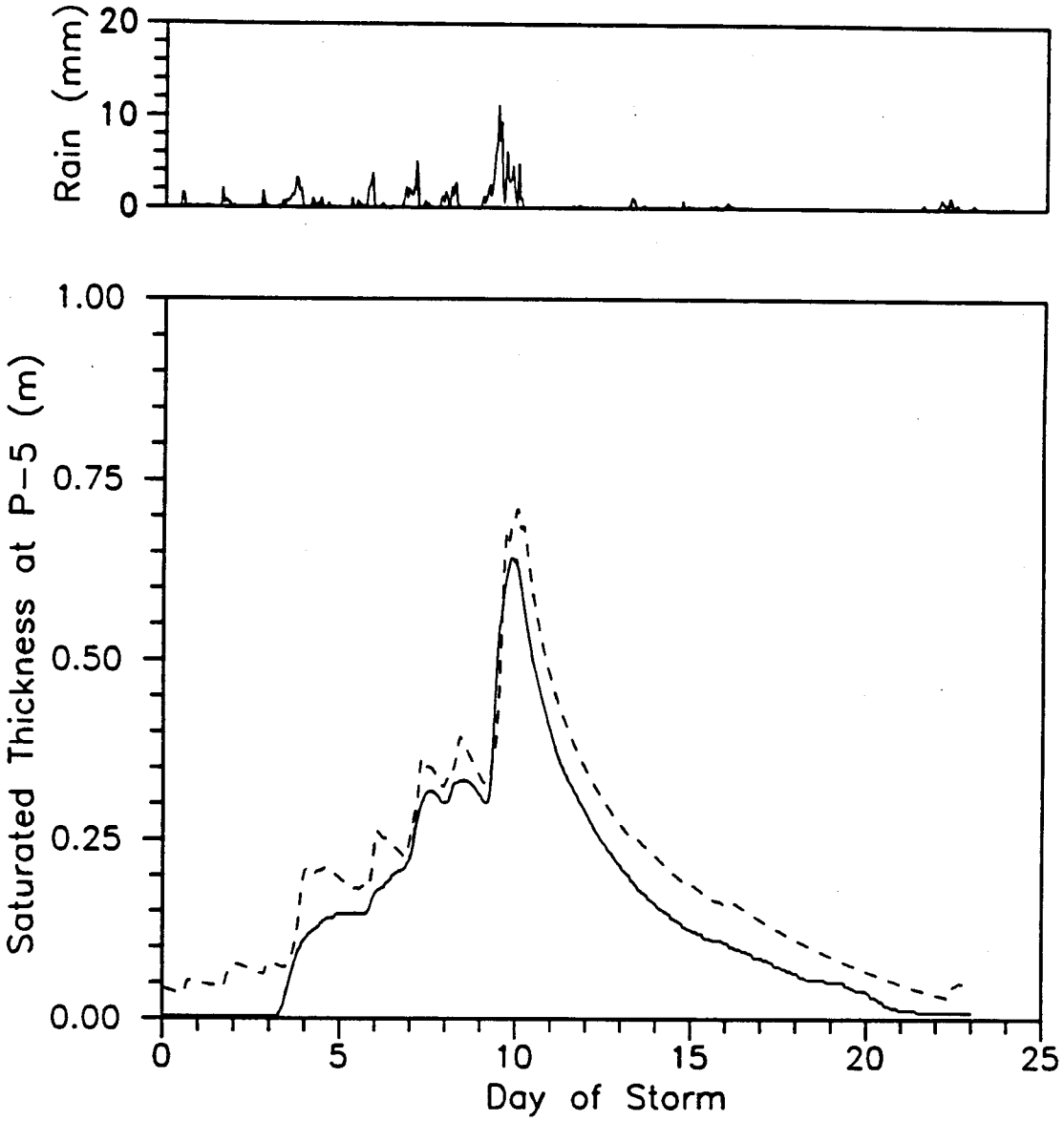

Fig. 5-11. Hourly time series of rainfall, and recorded (solid line) and simulated (dashed line) saturated zone thickness at piezometer P-5. Data are for the period December 31, 1989 - January 22, 1990.

Simulated and recorded weir discharge for Water Year 1990 are shown in Figure 5-12. There is no apparent model bias during the period of swale discharge when both the site rain gage and weir stage recorder were operational (calibration period from January 16, 1990 through May 3, 1990) (Figure 5-13). The model over-simulates discharge during the wet months of February and March, but under-simulates discharge from the April storm. Recorded and simulated flow means for the calibration period are within 0.02 l/s and total runoff volumes (expressed as depth over the catchment) are within 0.6 mm (Table 5-8, col. 1). The model simulation during the calibration period results in a coefficient of determination equal to 0.94 and a RMSE of 2.07 l/s.

The largest storm in Water Year 1990 occurred in January. The weir sensor was inoperative during most of the discharge hydrograph, however, point values of discharge were calculated from nine manual stage measurements (Figure 5-14). The general shape of the simulated hydrograph shows good agreement with the point discharge values. The timing and rise of simulated flows is good and the recession merges well with recorded flows.

Simulated discharge for all of Water Year 1990 is 331 mm, about 6 percent below recorded. During this period 49 percent of the recorded volume was estimated from manually determined weir stage measurements. There were 791 mm of potential evapotranspiration calculated from Penman's equation, resulting in 694 mm of actual evapotranspiration (57 percent of the rainfall). A total of 184 mm of water was simulated as lost through the till layer, which is consistent with the regional estimate of 150 - 300 mm.

The RMSE needs to be viewed in context of measurement accuracy. A

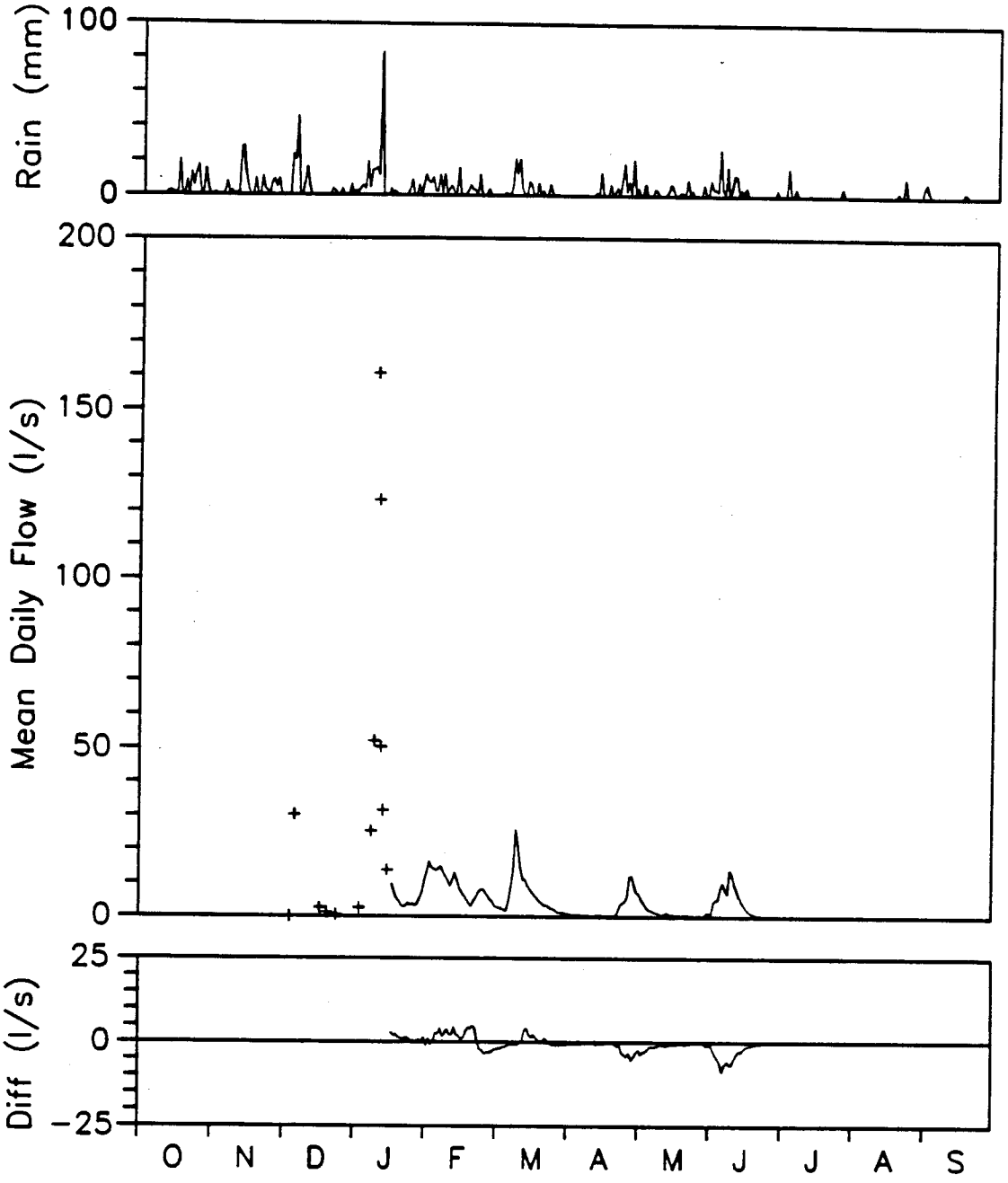

Fig 5-12. Daily time series of rainfall, recorded streamflow, and simulated minus recorded discharge ($Q_s - Q_r$) for Water Year 1990. Discharge calculated from manual stage measurements are shown as crosses.

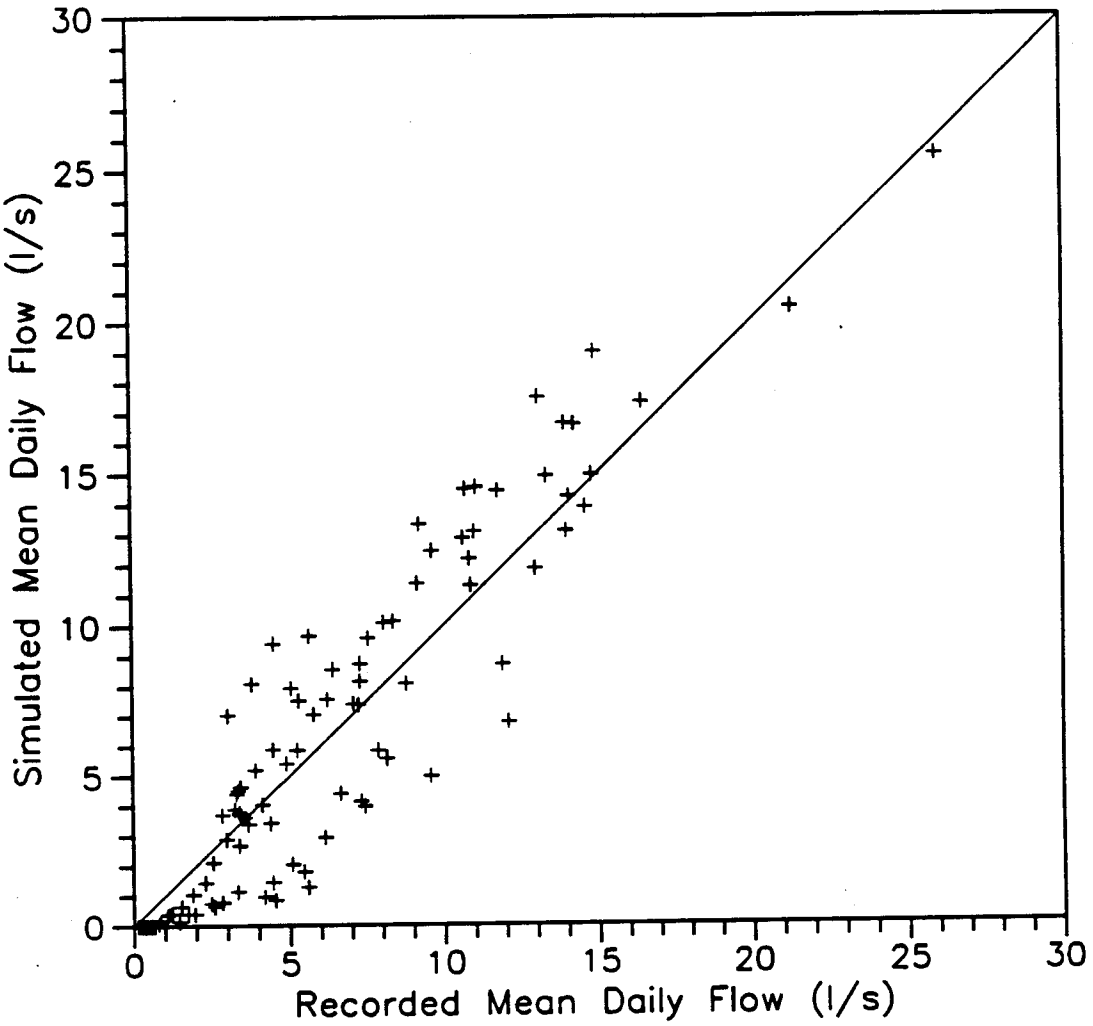

Fig. 5-13. Daily values of simulated versus recorded streamflow for the period January 16, 1990 - May 3, 1990.

TABLE 5-8. Summary Statistics for Weir Discharge

Statistic	Calibration[1]	Verification[2]		20-Month[3]
		WS	WY	
RMSE (l/s)	2.07	3.80	3.77	2.69
% RMSE	35.8	40.8	46.8	53.9
R^2	0.94	0.95	0.95	0.95
E_f	0.83	0.89	0.90	0.90
Mean Rec. (l/s)	5.78	9.32	7.20	5.00
Mean Sim. (l/s)	5.80	9.43	7.39	4.89
Rec. Vol. (mm)	146.4	402.0	402.0	581.5
Sim. Vol. (mm)	147.0	406.6	412.8	568.8

1 Period of Calibration: January 16, 1990 - May 3, 1990

2 Verification WS: Wet Season, November 24, 1990 - May 26, 1991
WY: Water Year, October 1, 1990 - May 26, 1991

3 January 16, 1990 - May 26, 1991

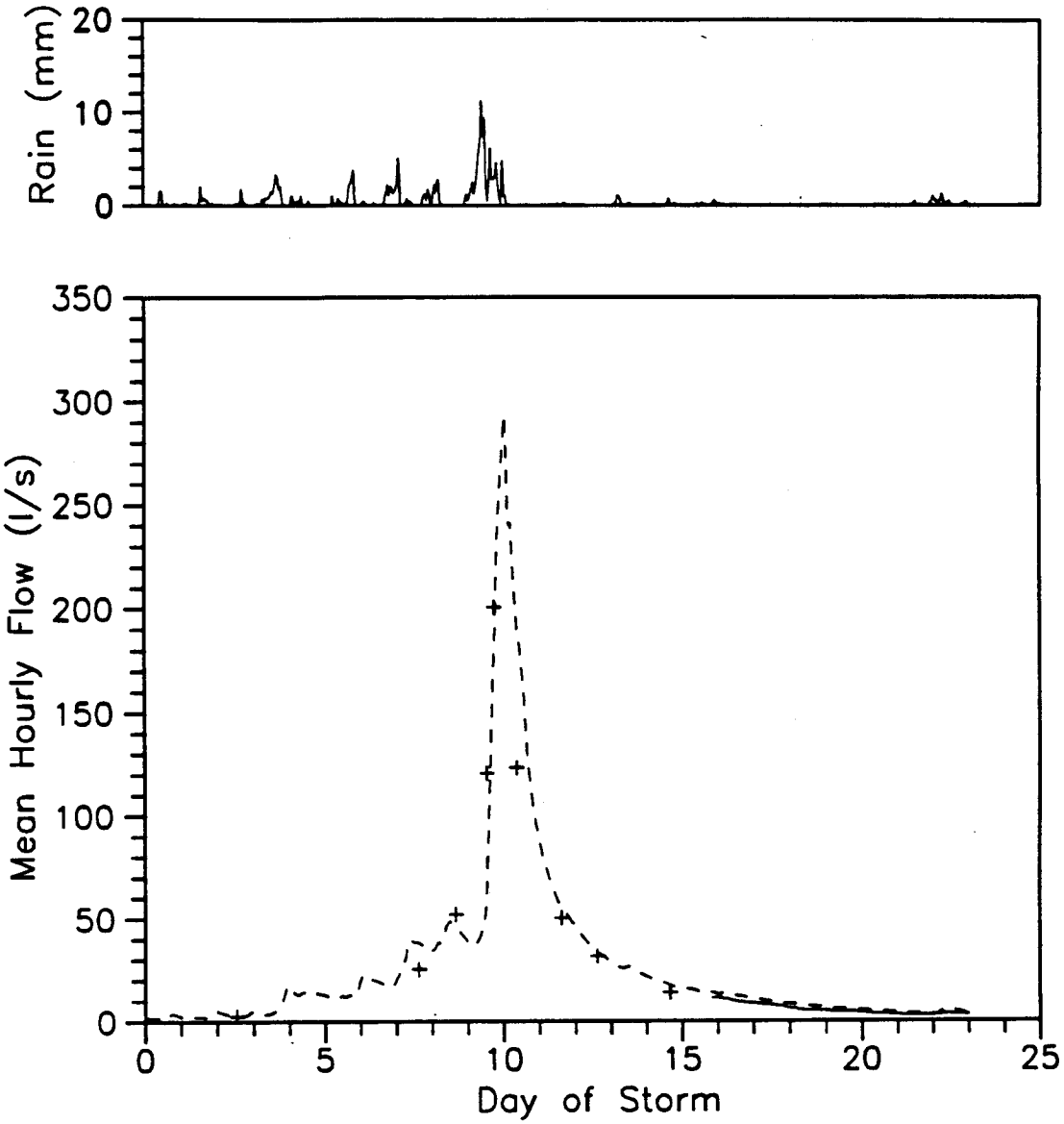

Fig. 5-14. Hourly time series of rainfall, and recorded (solid line) and simulated (dashed line) streamflow for the period December 31, 1989 - January 22, 1990. Discharge calculated from manual stage measurements are shown as crosses.

volumetric rain gage was placed next to the weir on January 11, 1991 and was measured 5 times between this date and March 20, 1991. The total depth of rainfall (338 mm) was about 3 percent less than the corresponding total of 349 mm recorded at the rain gage, excellent agreement under field conditions. The catch of the volumetric gage would be influenced by the presence of trees; the recording gage was located to minimize tree influence. If this relationship holds true over the entire simulation period, the effect of rainfall on simulated mean flows and on total runoff volume should be minor. This appears to be the case, as simulated mean flow and total volume are in excellent agreement with recorded.

The maximum difference in rainfall depths occurred between manual measurements on March 3 hr 12:30 and March 20 hr 14:30 when the rain gage recorded 6.1 mm more precipitation than at the weir. This corresponds to a difference of 0.359 mm/day. A small difference, especially when compared to the rain gage bucket capacity of 0.254 mm. However, the calibration RMSE of 2.07 l/s is equal to 0.485 mm/day of water over the catchment. The RMSE associated with the model is similar in size to potential errors in transferring rainfall measurements to the catchment.

5.7 Model Verification

Recorded and simulated discharge for the entire 20-month study period is presented in Figure 5-15. The model was verified using data from the final 8 months, in particular the period of swale discharge from November 24, 1990 through May 26, 1991. Several inches of snow fell and remained on the ground

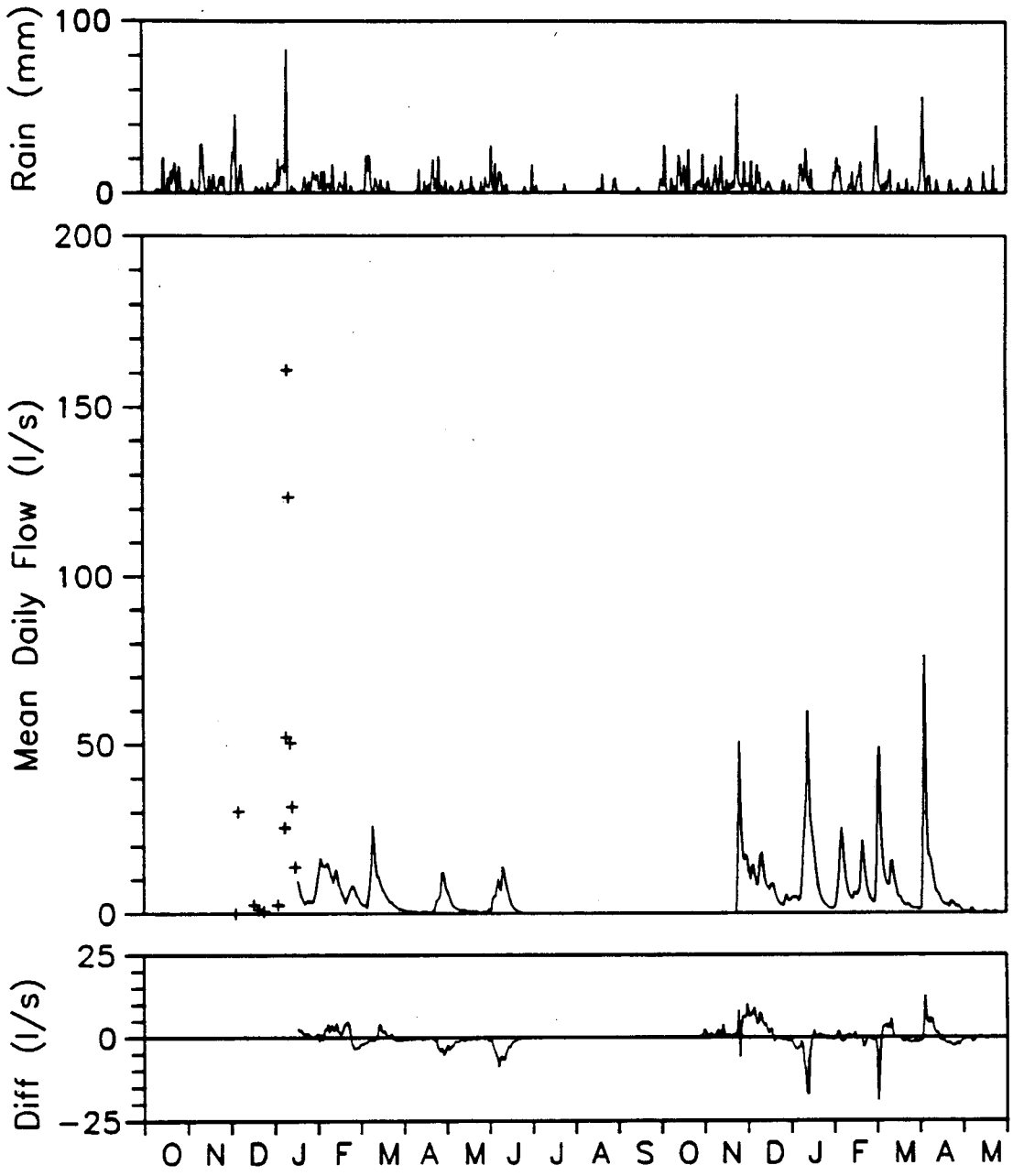

Fig 5-15. Daily time series of rainfall, recorded streamflow, and simulated minus recorded discharge ($Q_s - Q_r$) for the 20-month study period. Discharge calculated from manual stage measurements are shown as crosses.

from December 19 through December 31, 1990. Some of this snow would have accumulated on the rain gage and would have been recorded as precipitation during the melt beginning January 1. It is not possible to determine how well the timing and volume of the recorded snow melt represents the actual snow-on-the-ground melt. It seems probable that the depth of snow on the gage was less than on the ground and recorded volumes are low.

Model simulations show no systematic bias during the verification period (Figure 5-16). Storm flows are over-simulated in November, early December, January, and April, and under-simulated in February and March. The under-simulation in January may be related to an inaccurate recording of precipitation in the form of snow. Mean recorded and simulated flows are within 0.14 l/s and total runoff volumes are within 1 percent (Table 5-8, col. 2). These results are similar to the calibration period. The RMSE of 3.8 l/s is greater than for the calibration period, but the mean flow rate is also higher. The coefficient of modeling efficiency and the coefficient of determination are 0.89 and 0.95 respectively, both higher than for calibration. The RMSE increase of 1.73 l/s over calibration is equivalent to 0.40 mm/day, similar to the potential error in rain fall measurement.

The swale remained dry for about four and one-half months between late June and early November 1990 (Figure 5-15). The swale began to discharge again during the large storm of late November (Figure 5-17). The model accurately simulates the timing and shape of the rising limb of this storm hydrograph. Simulated peak discharge is within 5 percent of recorded. This reflects well on the model's ability to simulate evapotranspiration during the

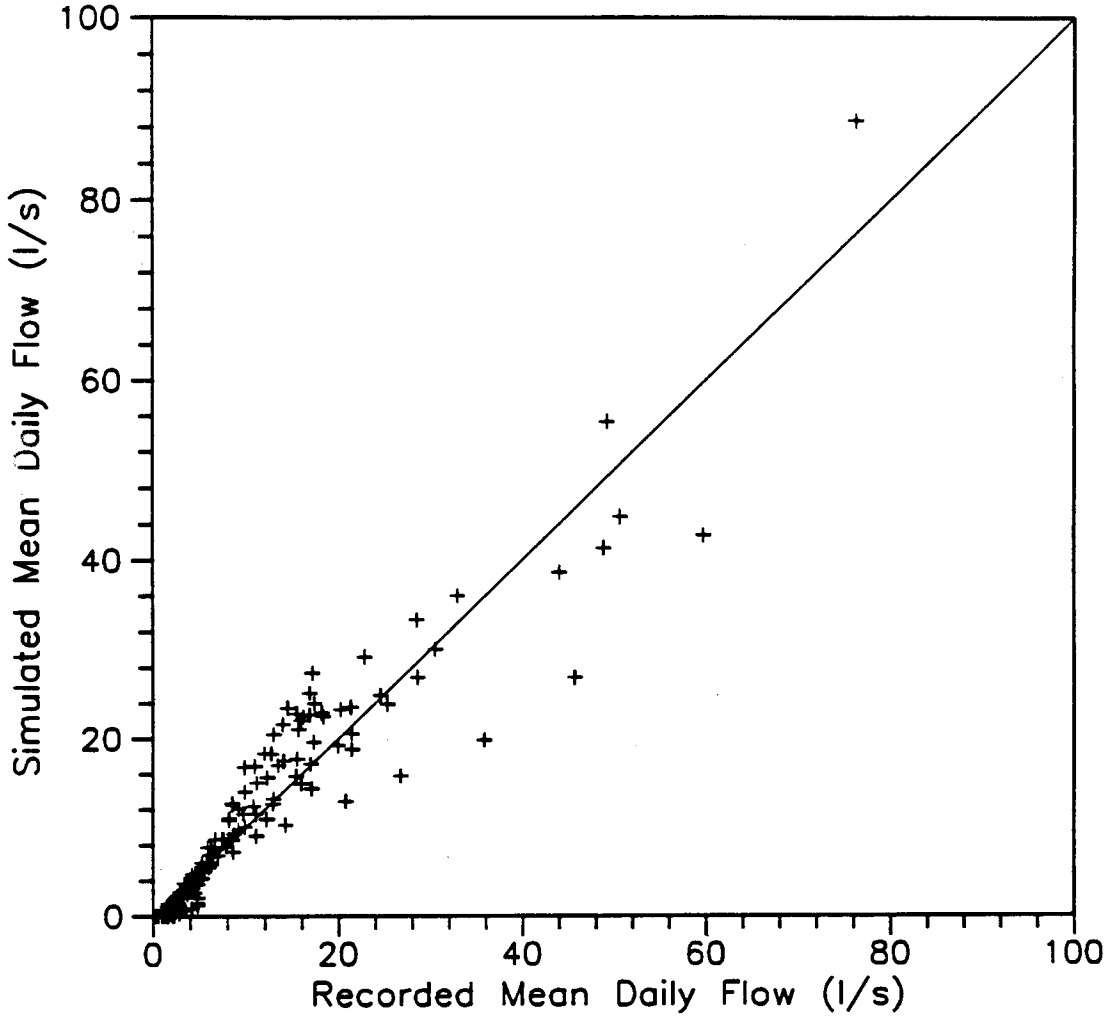

Fig. 5-16. Daily values of simulated versus recorded streamflow for the period of weir discharge, November 24, 1990 - May 26, 1991.

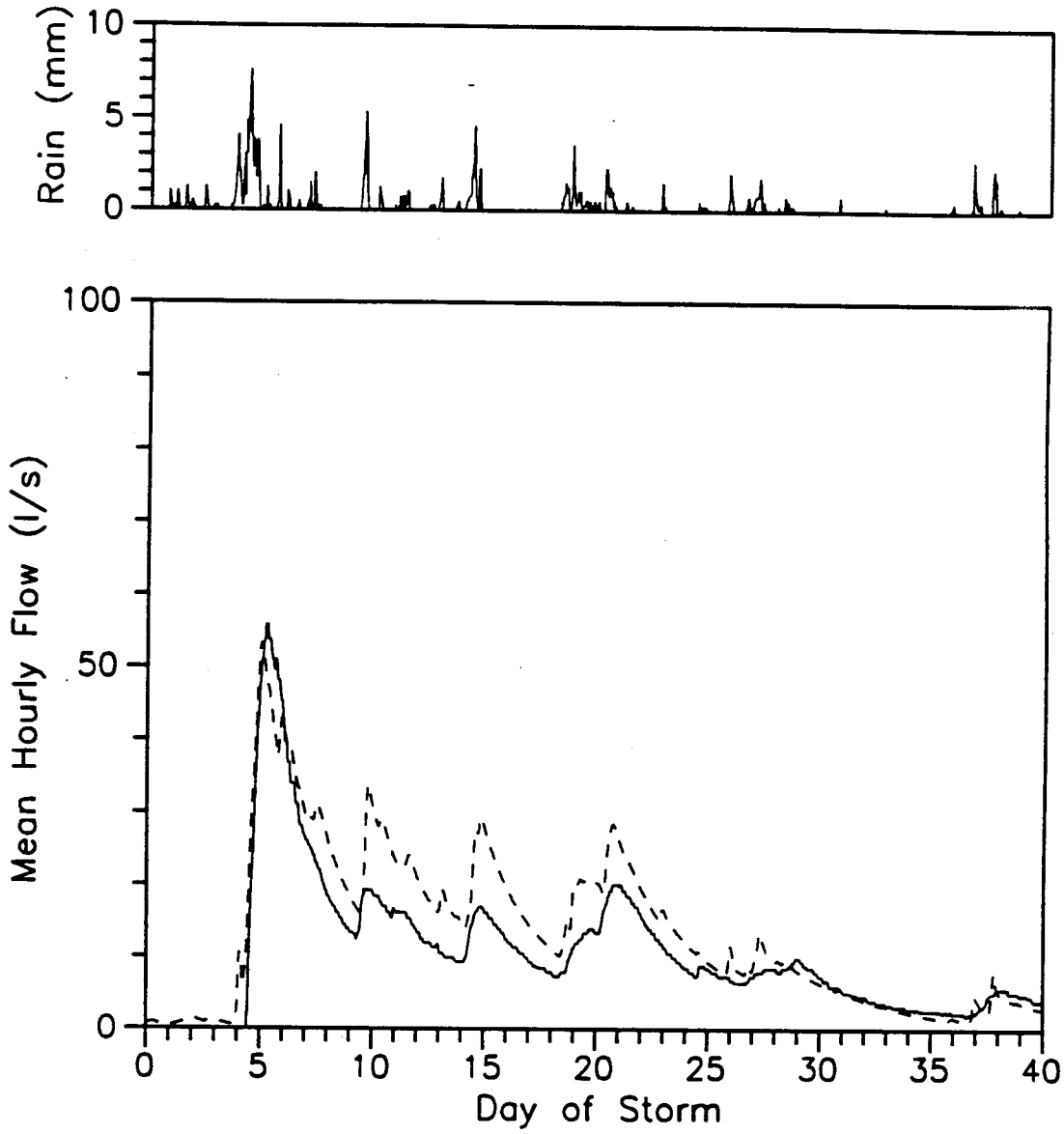

Fig. 5-17. Hourly time series of rainfall, and recorded (solid line) and simulated (dashed line) streamflow for the period November 20, 1990 - December 29, 1990.

preceding period of no flow, and on the calibrated value of field capacity which, along with the measured soil depths, determines the available soil storage that must be exhausted before discharge can occur. Simulation of the storm hydrograph recession is poor, with volumes of the three trailing storms over-simulated by a total of 27 percent.

Three distinct storms moved across the catchment between late January and the end of March (Figure 5-18). Model simulation of the first two moderate storms is excellent. Simulated hydrograph shapes are good and peak discharges are within 1- 2 percent of recorded. Model simulation of the March storm is less accurate, the peak discharge is under estimated by 22 percent and discharge is high early in the recession. The total simulated runoff volume for this period is within 4 percent of recorded.

The largest storm of the verification period occurred in April 1991 (Figure 5-19). The timing and general shape of the simulated hydrograph for this storm is good. However, the peak discharge is over-simulated by 23 percent and the recession is too long. Runoff volume is over-simulated by 10 percent.

Manual measurements of saturated thickness are available for piezometer P-5 and for piezometers on the lower transect. Simulated hourly water table fluctuations at P-5 generally are in good agreement with recorded (Figure 5-20). There is a slight under-simulation of peak saturated thickness in February and March, but the March recession is good.

The two lower transect piezometers adjacent to the swale were backwatered by the swale for parts of the winter. As a result, data from the

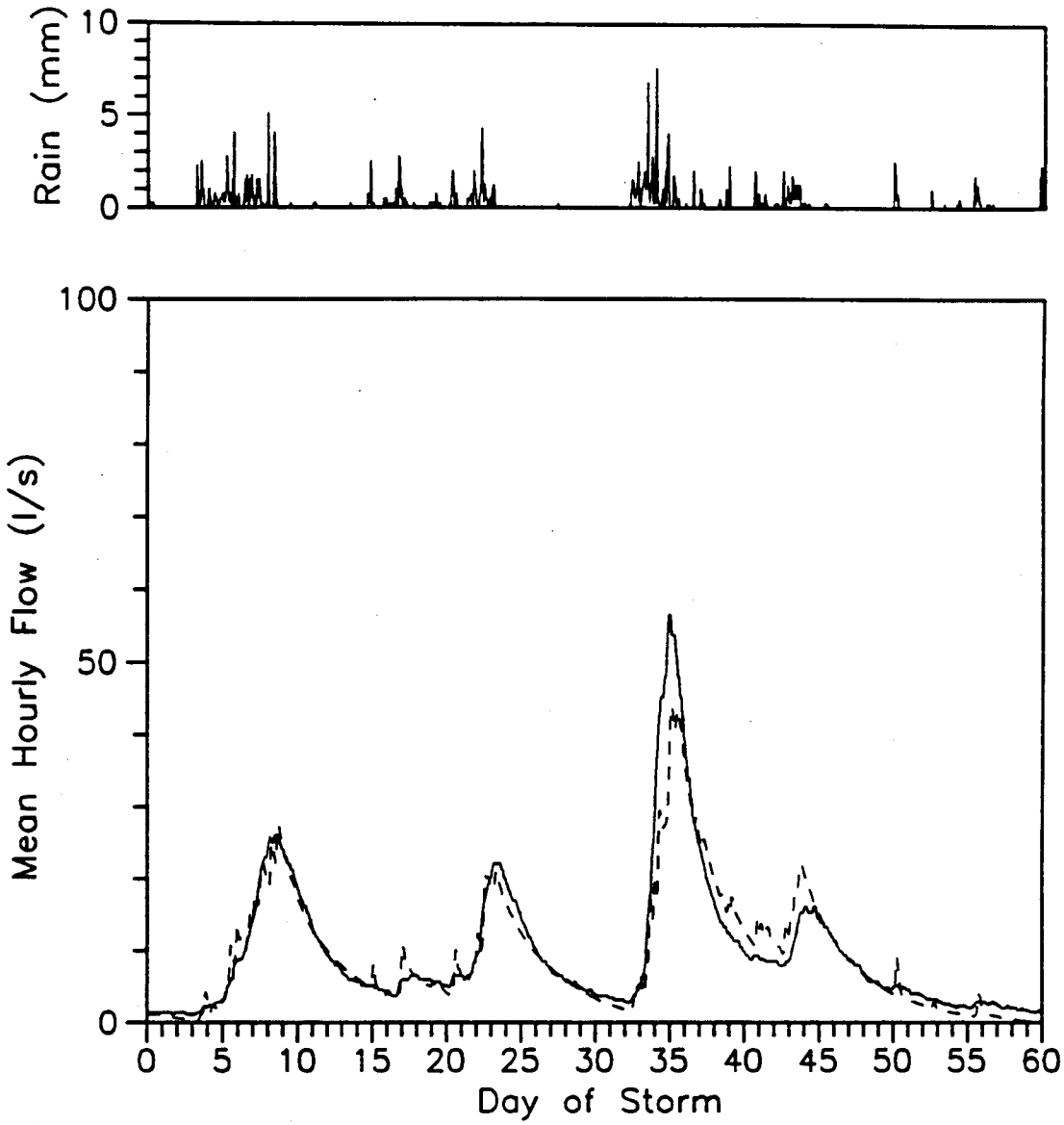

Fig. 5-18. Hourly time series of rainfall, and recorded (solid line) and simulated (dashed line) streamflow for the period January 28, 1991 - March 28, 1991.

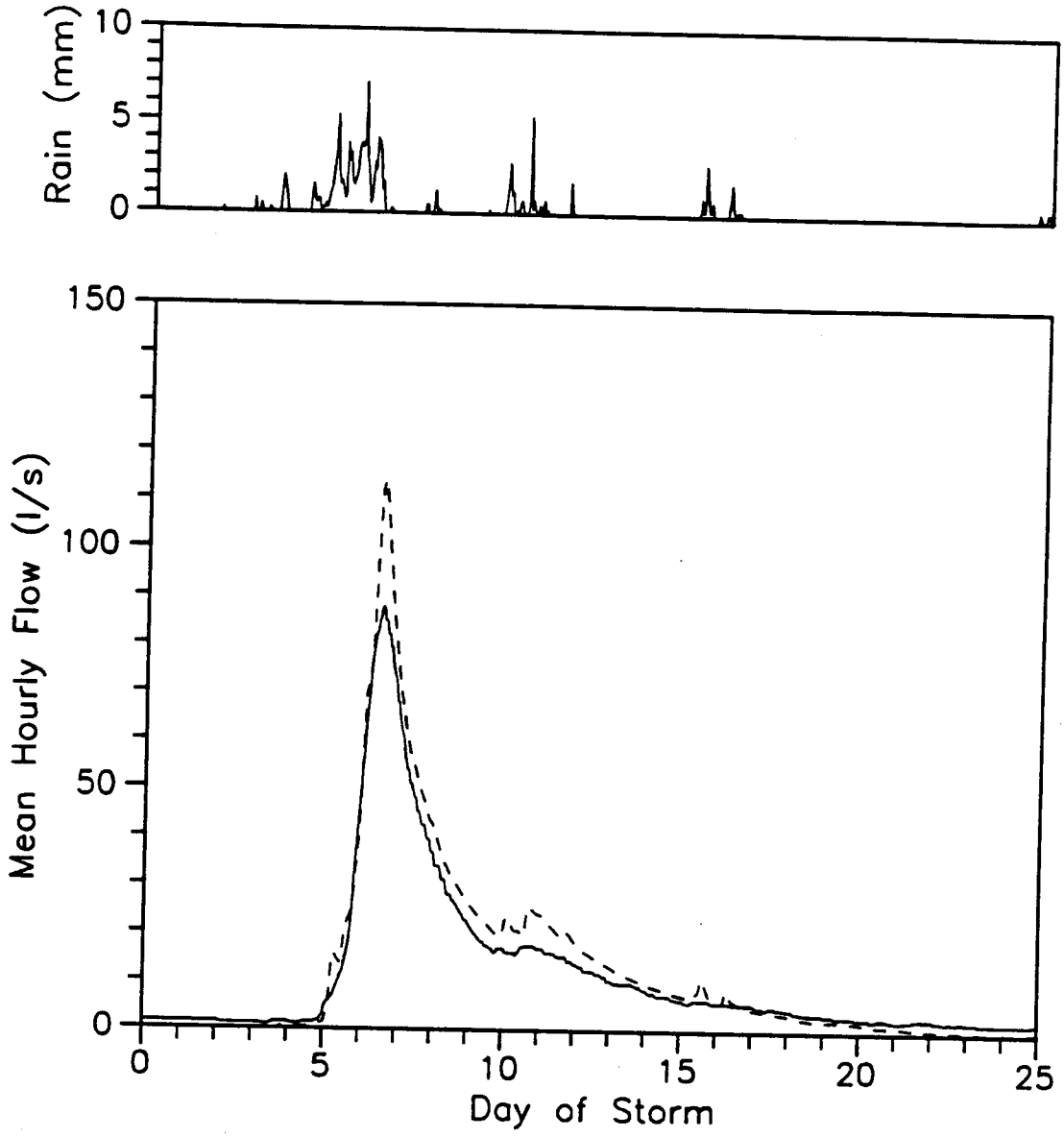

Fig. 5-19. Hourly time series of rainfall, and recorded (solid line) and simulated (dashed line) streamflow for the period March 30, 1990 - April 24, 1990.

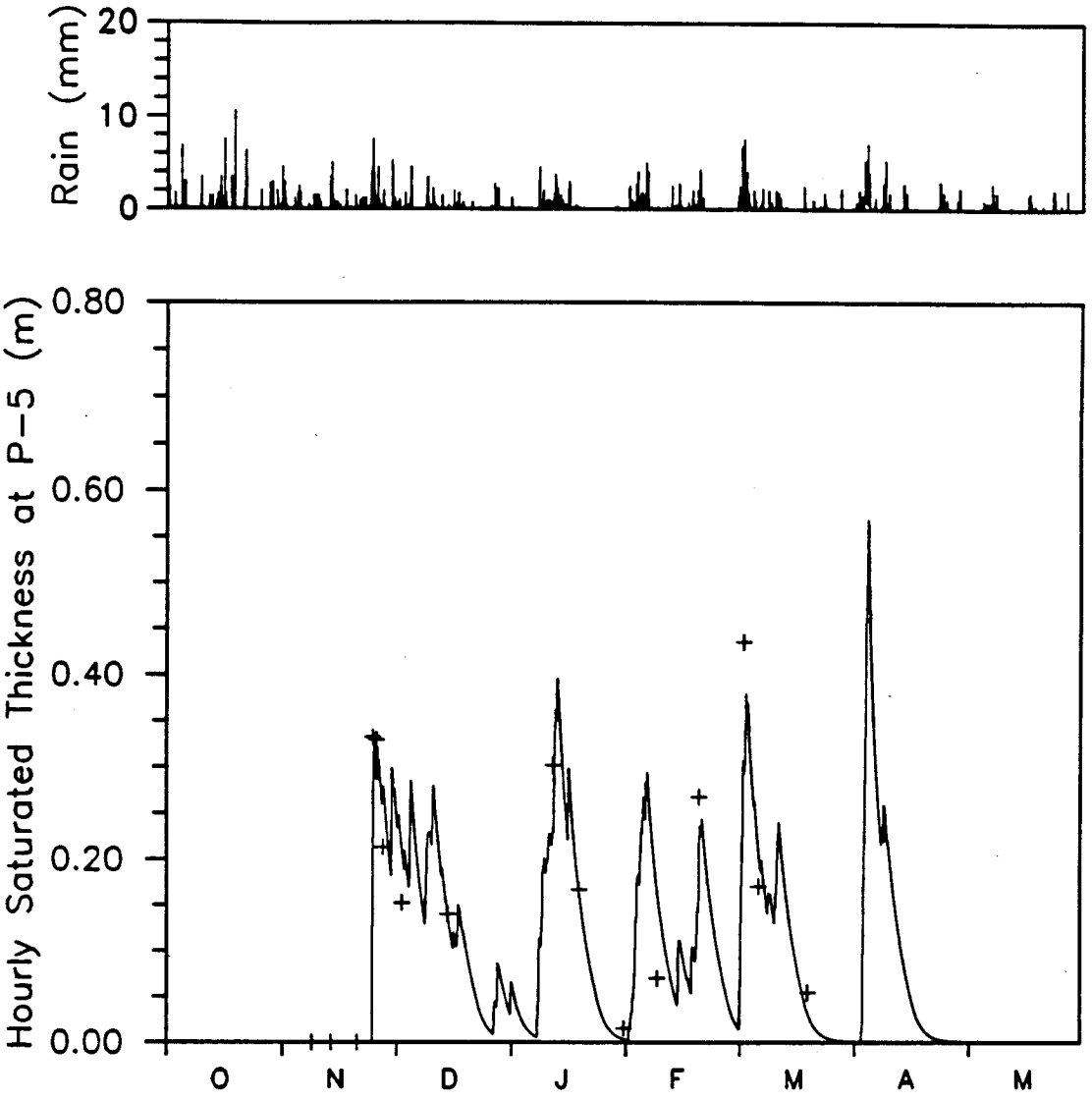

Fig. 5-20. Hourly rainfall, and recorded (crosses) and simulated (solid line) saturated zone thickness at piezometer P-5 for the period October 1, 1990 through May 26, 1991.

two outer most piezometers were used to test the model. Water table elevations at the western most piezometer (L-4) are shown in Figure 5-21. Simulated water levels are in very good agreement with recorded during November, December, and January. The model simulation is less satisfactory in February and March when simulated saturated thickness is generally less than recorded. Water table elevations at the eastern piezometer (L-1) are presented in Figure 5-22. The timing of the initial water table rise is good, however saturated zone thickness is grossly over-simulated in December. Simulation results for January, February, and March are excellent.

The calibration and verification results are encouraging, especially considering that during calibration there were only three and one-half months when the rain gage, piezometer, and weir sensors were operational concurrently. The largest storm hydrograph during this period of concurrent instrument operation was exceeded four times during verification.

5.8 Summary

The combination methodology was applied to the 37 ha, forested Novelty Hill basin. Based on detailed field mapping and observations during site visits it was found that surface runoff generation is confined to a seasonal wetland that occupies about 4 percent of the basin area. During the study period swale discharge accounted for 29 percent of annual precipitation and 42 to 47 percent of wet season precipitation. Saturation overland flow represents 9 to 12 percent of this discharge. Subsurface flow is the dominant runoff mechanism during storms. The majority of rainfall is removed from the catchment via

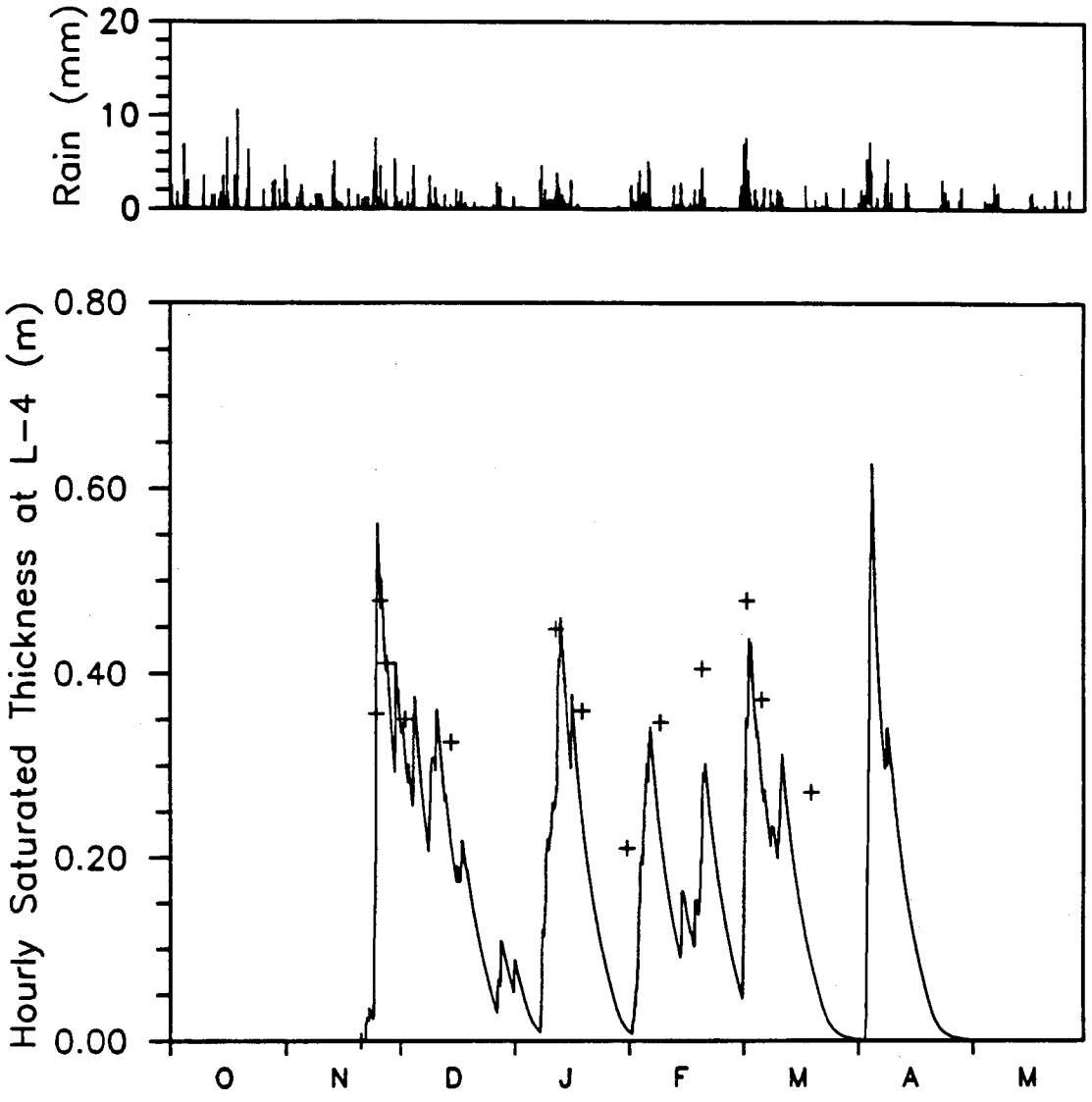

Fig. 5-21. Hourly rainfall, and recorded (crosses) and simulated (solid line) saturated zone thickness at piezometer L-4 for the period October 1, 1990 through May 26, 1991.

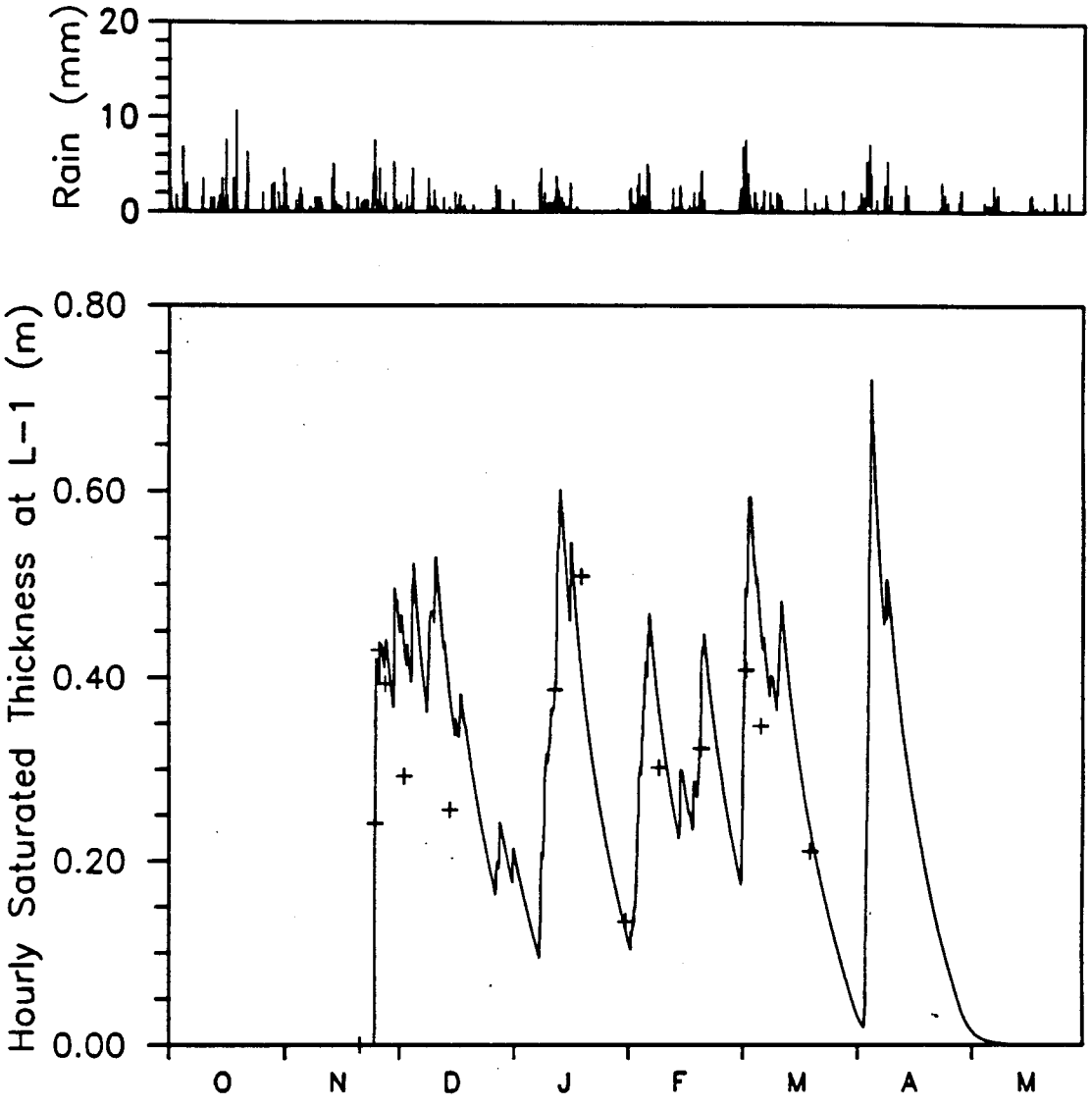

Fig. 5-22. Hourly rainfall, and recorded (crosses) and simulated (solid line) saturated zone thickness at piezometer L-1 for the period October 1, 1990 through May 26, 1991.

evapotranspiration and leakage through the Vashon till.

Field measurements were used to estimate soil hydrologic properties (θ_e, K_s, and f). The estimates of saturated lateral conductivity show good agreement and suggest an increase in hydraulic conductivity with distance above the till layer, perhaps due to the increased availability of macropores in the root zone.

The combination of relatively simple field measurements and hydrologic monitoring, along with the physical representation of model input parameters allowed the hydrology and hydraulics of the central swale to be simulated without calibration. Only four land segment input parameters required calibration, with the same values used in all ten segments. The final calibrated values of soil hydrologic properties were in general agreement with results from other studies in forested watersheds.

The model was verified using data from Water Year 1991. Despite having only three and one-half months of concurrent gage operation during calibration, the agreement between simulated and recorded mean flows and volumes was excellent. Model simulation of storm hydrograph peaks was good, however storm volumes were over-simulated.

Simulated water table fluctuations were compared with recorded at three locations during verification, one near the basin headwater (P-5) and two near the outlet (L-1 and L-4). No data were available at the locations of piezometers L-1 and L-4 during model calibration. Model simulations for all three piezometers were generally good.

The satisfactory model performance during verification demonstrates that at Novelty Hill it is possible to estimate spatially averaged soil hydrologic properties through the combination methodology, and that these values can be used along with topography and measured soil depths to simulate with acceptable accuracy water table fluctuations (and hillslope discharge) at several different locations. This approach allows distributed hydrologic modeling using a minimal number of calibration parameters. The model structure also allows the simulation results to be verified at any location within the catchment.

The combination methodology has proven successful in describing the hydrologic sates and fluxes of a small, relatively homogeneous forested (natural) basin. The methodology was also applied in an urbanized basin (Klahanie) which, prior to development, was similar to Novelty Hill. Application of the methodology in this catchment, and a discussion of the differences in hydrologic responses between Klahanie and Novelty Hill, are described in Chapter 6.

Chapter 6. Illustration of the Methodology at the Klahanie Catchment and a Comparison with the Natural Catchment at Novelty Hill

Application of the combination methodology to the Klahanie catchment is described in this chapter along with a comparison of runoff production in the two study basins. Physical features of the Klahanie basin, field mapping, and a model-independent analysis of field measurements are presented in Sections 6.1, 6.2, and 6.3. Model representation of the basin and model calibration are described in Sections 6.4 and 6.5. Application results are summarized Section 6.6. The chapter closes with a comparison of runoff production in the urbanized Klahanie catchment and the natural Novelty Hill basin.

6.1 Physical Features

A 16.7 ha subbasin within the residential development of Klahanie near Issaquah, Washington was used to test the combination of field mapping, hydrologic monitoring, and hydrologic modeling for describing catchment hydrologic states and fluxes under urbanized conditions. The catchment is located in the North Fork Issaquah Creek drainage basin, 21 km east of Seattle and 14 km south of the Novelty Hill Basin. Land use is entirely residential, with 117 single family homes, a tennis court, and a community center with a pool and parking lot. The site is contained within a broad, till-capped upland plateau with ground surface elevations ranging between 145 m in the southeast portion of the site to about 125 m near the basin outlet (Figure 6-1). Side slopes average between 5 and 17 percent. The site is drained by a 480 m long engineered swale that receives runoff from the road drainage network. The

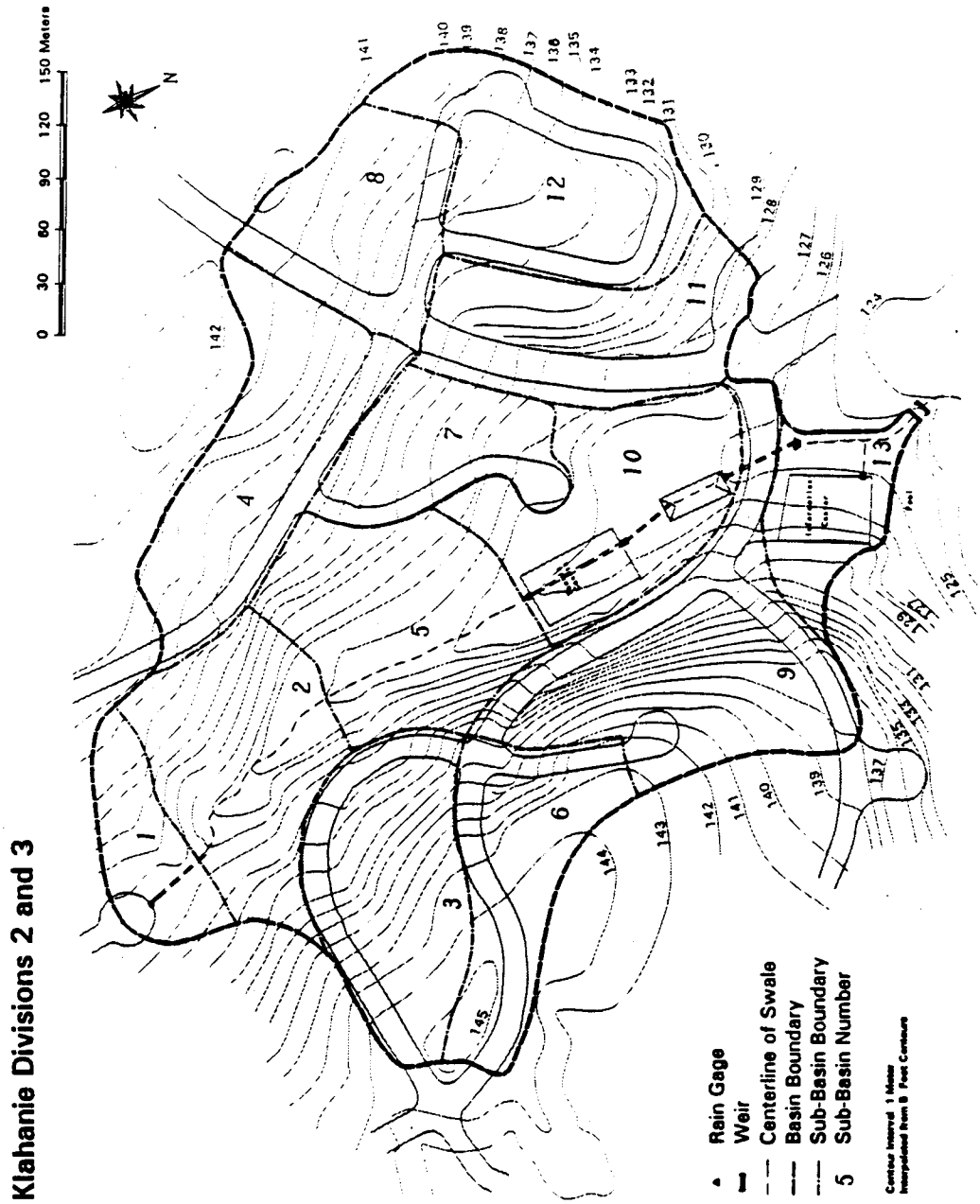

Fig. 6-1. Site map of the Klahanie basin showing the basin boundary and rain gage and weir locations.

catchment outlet is located at the northern border where discharge is measured using separate v-notch and rectangular weirs.

Site soils are formed within the Vashon till layer and are classified as either Alderwood or Everett gravelly sandy loam, both with a permeability of 0.05 to 0.15 m/hr (U.S. Dept. of Agriculture, Soil Conservation Service, 1973). Trees were cut and removed and stumps, roots, and the litter layer and natural top soil were removed immediately prior to construction. Prior to development soil depths were 0.6 to 1 m; present soil thickness is from 0.08 to 0.15 m.

In its natural state, apart from being steeper, the Klahanie catchment was similar to the Novelty Hill basin. Geologic conditions and native soils at the two sites are generally the same and prior to development soil depths were nearly equal. Changes to the natural landscape at Klahanie have altered runoff mechanisms, resulting in a more rapid runoff response to rainfall. Hydrologic differences between the two catchments will be discussed in Section 6.7.

6.2 Field Mapping

As-built engineering plans for the site were not available. However, pre-construction engineering plans with 1.5-m (5-feet) contours of the original topography and the proposed storm drainage system were available prior to field mapping which was conducted on June 18, 1991. All relevant plan information was checked and refined in the field. The storm water conveyance system is almost entirely associated with the road network. Road runoff is routed through gutters to catchbasins. Roof drainage is also transmitted to the catchbasins through closed conduits. Catchbasins are linked with 0.305-m (12-

inch) diameter concrete pipes running below the road grade. The collected runoff discharges to the swale at several locations.

As a result of the field mapping, the site was broken into 13 subcatchments based on existing topography, the road network, and the stormwater conveyance system. Hydrologic process zones were mapped within each subbasin. Horton overland flow is generated on roads, sidewalks, driveways, and roofs. Almost all of this flow is transmitted directly to the stormwater conveyance system. Most residential lawns in the subdivision consist of imported top-soil overlain by sod. Lawns, flower beds, and gardens are well maintained and appear to infiltrate most, if not all rainfall. Low areas are generally drained with French drains and/or perforated pipe. While there is little evidence of overland flow on lawns, saturation overland flow was observed on the western footslopes of land segments 5 and 10, in the common area adjacent to the swale (Figure 6-1).

The distribution of impervious and pervious areas is given by subbasin in Table 6-1. Column 2 gives the plan view area for each subbasin. Total road surfaces areas are given in column 3. Total roof and driveway areas are shown in columns 4 and 5, respectively. The roof area for each style of home was measured and a typical driveway area was determined. Total roof and driveway areas were rapidly determined by counting the number of houses (of a given style) in each subbasin. The total impervious area within each subbasin is shown in column 6. In some parts of Klahanie impervious runoff collected in a portion of one subbasin may be routed against the surface grade to the storm conveyance system of an adjacent subbasin. As a result the effective

TABLE 6-1. Pervious and Impervious Areas by Subbasin at Klahanie

Sub-Basin	Plan View	Area (ha) Road	Roof	Drive	Total Imp.	Eff. Imp.	Perv.	Actual Total
1	0.54	0.04	0.03	0.01	0.08	0.08	0.46	0.54
2	1.68	0.00	0.12	0.05	0.17	0.10	1.51	1.61
3	1.54	0.32	0.17	0.07	0.56	0.56	0.98	1.54
4	2.12	0.26	0.10	0.04	0.40	0.40	1.72	2.12
5	1.41	0.00	0.13	0.05	0.18	0.18	1.23	1.41
6	0.69	0.32	0.09	0.03	0.44	0.52	0.25	0.77
7	0.91	0.17	0.09	0.03	0.29	0.30	0.62	0.92
8	0.80	0.28	0.07	0.02	0.37	0.37	0.43	0.80
9	2.37	0.57	0.13	0.05	0.75	0.79	1.62	2.41
10	1.39	0.19	0.03	0.01	0.23	0.22	1.16	1.38
11	1.00	0.31	0.07	0.03	0.41	0.34	0.59	0.93
12	1.59	0.39	0.20	0.08	0.67	0.75	0.92	1.67
13	0.56	0.15	0.03	0.00	0.18	0.18	0.38	0.56
Total	16.60	3.00	1.26	0.47	4.73	4.79	11.87	16.66

impervious area (EIA) in a subbasin may be larger or smaller than shown in column 6. The EIA associated with each subbasin is given in column 7. The pervious area in a subbasin (column 8) equals the difference between the plan view area (column 2) and the total impervious area in the subbasin (column 6). Column 9 gives the total effective area of each subbasin (sum of columns 7 and 8). The basin totals for columns 2 and 9 (16.60 and 16.66, respectively) should agree. The difference between these totals is less than one percent and results from measurement errors.

6.3 Model-Independent Hydrologic Analysis of Field Measurements

6.3.1 Hydrologic Instrumentation

One tipping bucket rain gage, with a bucket capacity of 0.51 mm (0.02 inch) has been recording at 15-minute intervals continuously since October 16, 1990. The rain gage is located 90 m northwest of the basin outlet (Figure 6-1). Rainfall data for the period from December 24, 1990 through January 1, 1991 were lost during data retrieval. Fortunately, little precipitation of hydrologic consequence occurred during that period. The missing data were replaced with data from a 15-minute gage located 3 km to the east.

Streamflow at the outlet is measured at 15-minute intervals using separate sharp crested v-notch and rectangular weirs. Water levels are measured by Unidata capacitative sensors that record in 3.05 mm (0.01 foot) increments. The sensors have been in place and functioned correctly since November 21, 1990. The weirs are keyed into the till at a depth of about 0.2 m

and are sealed with Portland cement grout. As a result, nearly all surface and subsurface discharge exiting the catchment above the Vashon till layer passes over the weirs.

The stage-discharge relationship for a v-notch weir is more sensitive to stage and less sensitive to stage errors than the relationship for a rectangular weir. As all flows to date have been contained within the v-notch weir, data from this weir will be used in the remainder of the study.

The v-notch weir was calibrated from 8 flow measurements with discharges between 3.5 and 43 l/s (Appendix D). During the study period, this discharge range was only exceeded 3 percent of the time. The calibrated weir should provide good estimates of discharge for the vast majority of flows. Weir estimated discharge for the peaks of several large storms is in excess of 200 l/s; the errors associated with these estimates are unknown because no observer was present to note the weir hydraulics during peak flow levels.

6.3.2 Mass Balance

During the study period (November 21, 1990 through May 15, 1991), 881 mm of precipitation was recorded, resulting in 640 mm of runoff at the weir (73 percent of precipitation). Field mapping shows 4.79 ha of impervious surfaces that are connected directly to the storm conveyance system. These areas generated about 254 mm of Horton overland flow. The discharge volume from pervious areas (primarily lateral subsurface flow) was about 386 mm (60 percent of the total discharge volume).

Flow components were determined for the large storms of November 23-

24, 1990 and April 2-5, 1991. Discharge from pervious areas accounted for the majority of recorded runoff volume, 63 percent in the November storm and 61 percent in the April storm. During the November storm 70 percent of the precipitation falling on pervious areas resulted in measured runoff. This percentage dropped to 64 in the April storm. At Klahanie, runoff from pervious areas is significant and can not be neglected, even at the relatively short duration of large storms.

Information from test-pits dug prior to development at Klahanie indicate the soil thickness under natural conditions was about 0.8 m. During development soil thickness was reduced to 0.15 m. At the same time forest cover was replaced with impervious surfaces and short grass. Increasing the impervious area causes an increase in the contribution of Horton overland flow. Field mapping suggests that there should be an increase in runoff from pervious areas primarily because of the loss of soil water storage capacities and a decrease in soil water removal via evapotranspiration. (This increase in flow production is not caused by a large increase in Horton overland flow due to soil compaction and reduced infiltration.) Even with limited amounts of saturation overland flow, examination of the runoff hydrograph indicates that discharge from pervious areas (total runoff volume minus the contribution from impervious areas) accounts for the majority of storm runoff volumes. This suggests a subsurface runoff mechanism, perhaps rapid flow through lawn thatch layers or the grass root zone near the soil surface.

6.4 Model Representation

All 13 subcatchments contain two types of hydrologic process zones: Impervious surfaces that generate Horton overland flow; and pervious surfaces (residential lawns and grassed common areas) that generate primarily subsurface flow. Zones of return flow and saturation overland flow are also present on the footslopes of subcatchments 5 and 10. These zones were identified during field mapping.

It is not practical nor necessary to model each individual process zone (e.g. each lawn) separately. Instead, within each subcatchment the areas of similar process zones were aggregated into either a single impervious or a single pervious land segment. With the exception of subcatchment 5, each land segment was modeled as a plane with a slope and length equal to the average of the process zones it represents. While averaging dampens the influence of smaller scale topographical variations on simulated flow production, most of the hillslopes are represented using several subcatchments so larger scale topographic affects are preserved. Subcatchment 5 generates saturation overland flow and return flow, therefore its pervious land segment was modeled using a steep upper slope and a flatter footslope (the low gradient in subcatchment 10 allows saturation overland flow to be generated using a single slope). Runoff from the entire basin was simulated using 26 planes of various slopes, lengths, and widths. Subcatchment breakdowns are not automated and rely on judgment by the model user. Information derived from field mapping of hydrologic process zones serves to guide basin dissagregation.

The central swale was modeled as a series of four channel reaches (numbers 1 -4 from top to bottom). Flow conveyance was estimated using

Manning's equation and surveyed channel cross-sections and channel slope. A roughness coefficient of 0.05 was used. The channel consists of cobbles resting on till and was modeled as impervious. Analysis of pipe flow rates in the storm water conveyance system showed that the travel time from land segments to the central swale is less than the 15-minute time interval of the recorded data. Therefore, runoff from land segments collected by the pipe system was input (without routing) directly to the swale. Subcatchments 1 and 2 discharge to reach 1; subcatchments 3, 5, and 6 to reach 2; subcatchments 7 and 10 to reach 3; and subcatchments 4, 8, 9, 11, 12, and 13 to reach 4.

The values of most model input parameters used to represent the basin were estimated from field measurements or taken from the hydrologic literature (Table 6-2). There is no litter zone. Soil depths were measured non-systematically at 20 locations (most homeowners are reluctant to have probes used on their property) and an average value of 0.15 m was used in all pervious land segments. The vertical unsaturated zone lag of precipitation reaching the water table was assumed to be negligible. The majority of canopy storage is provided by short grass. This storage capacity and all overland flow parameters were estimated from the literature and held constant across the catchment. Vertical saturated conductivity, soil moisture content, soil field capacity, and the wilting point moisture content were also taken from the literature and assumed constant throughout the basin. The till saturated vertical hydraulic conductivity of 6×10^{-5} m/hr determined from calibration at Novelty Hill was used in all pervious land segments. Potential evapotranspiration was estimated (without adjustment) from Penman's equation using the City of Redmond

TABLE 6-2. Model Input Parameters for the Klahanie Basin

Input Parameter	Value	Source
Topography		
Ground Surface Elevations (m)	Variable	FE
Hillslope Top Width (m)	Variable	FE
Hillslope Bottom Width (m)	Variable	FE
Hillslope Length (m)	Variable	FE
Canopy and Litter Zone		
Canopy Storage (mm)	2.5	LIT[1]
Soil Characteristics		
Soil Depths (m)	0.152	FM
Vertical Sat. Conductivity (m/hr)	0.026	LIT[2]
Saturated Moist. Cont. (m^3/m^3)	0.45	LIT[2]
Moist. Cont. at Field Capacity (m^3/m^3)	0.21	LIT[2]
Moist. Cont. at Wilting Point (m^3/m^3)	0.10	LIT[2]
Overland Flow Routing		
Impervious Roughness Coefficient	0.015	LIT[3]
Impervious Depression Storage (mm)	2.4	LIT[4]
Pervious Roughness Coefficient	0.030	LIT[3]
Pervious Depression Storage (mm)	5.2	LIT[4]
Glacial Till		
Saturated Conductivity (m/hr)	0.00006	NVH

FM: Field Measurement, LIT: Literature, FE: Field Estimate
NVH: Novelty Hill Calibration
1) Dinicola (1990, p.27); 2) Sandy Loam, Rawls and Brakensiek (1989)
3) Crawford and Linsley (1966, p. 68); 4) Aron (1982)

weather station data.

The coefficient and exponent for lateral saturated conductivity (K_s and f) were the only parameters determined through calibration. Little if any Horton overland flow is generated on the pervious land segments, therefore the two parameters (K_s and f) control the simulated runoff response. The physical mechanism responsible for the relatively rapid discharge from pervious areas at the site is unknown. For modeling purposes I have assumed that it is a near surface response with characteristics between those of rapid subsurface flow and overland flow. The two lateral conductivity parameters were adjusted until simulated flows agreed with recorded and the lateral conductivity at the ground surface was equal to an average overland flow velocity of 90 m/hr (estimated for a plane with a slope and length equal to the average of all pervious areas). Conceptually, this allows saturated flow velocities in the near surface root zone or thatch layer to approach overland flow velocities. The final values for K_s and f of 0.549 m/hr and 33.86 were applied to all pervious land segments.

This modeling approach is consistent with the hypothesis of Henderson and Wooding (1964) who felt that in flow over clipped turf, the fluid near the base of the plants may qualitatively resemble flow in a porous medium of varying intrinsic permeability while the motion above the plants may be better described by either laminar or turbulent overland flow.

6.5 Model Calibration

The model was driven using rainfall and potential evapotranspiration data for the period October 16, 1990 (start of precipitation record) through May

15, 1991. The simulations began October 16 to allow the effects of assumed initial conditions to be removed by the start of the weir record on November 21, 1990. Final calibration results for the study period are presented in Figure 6-2. Daily values are used in this plot which, given the fast response of the basin to rainfall, are more representative of flow volumes than peaks. The model over-simulates flows during storms and under-simulates slightly during inter-storm periods (Figures 6-2 and 6-3). Recorded and simulated mean flows for the study period are within 0.12 l/s and total flow volumes are within 2 percent. This close agreement in mass balance results without any adjustment to the estimated values for the saturated conductivity of the till (calibrated at Novelty Hill) or potential evapotranspiration. The model simulation produces a RMSE of 4.03 l/s, a coefficient of determination equal to 0.98, and a modeling efficiency of 0.92.

The largest model simulation errors occurred for the November and April storms. Individual hydrographs for these two storms and for a sequence of moderate storms in February are plotted at 30-minute intervals in Figures 6-4 through 6-6. Simulation results for the November storm are generally quite good. The timing and shape of the rising limb is excellent and simulated peak discharge is within 4 percent of recorded. The timing of the initial complex falling limb is good but the discharge volume is too high. The recession at moderate and low flows is good.

A sequence of storms moved across the catchment between January 30, 1991 and February 8, 1991 (Figure 6-5). The timing of simulated flows is very good and simulated hydrograph peaks generally show good agreement with

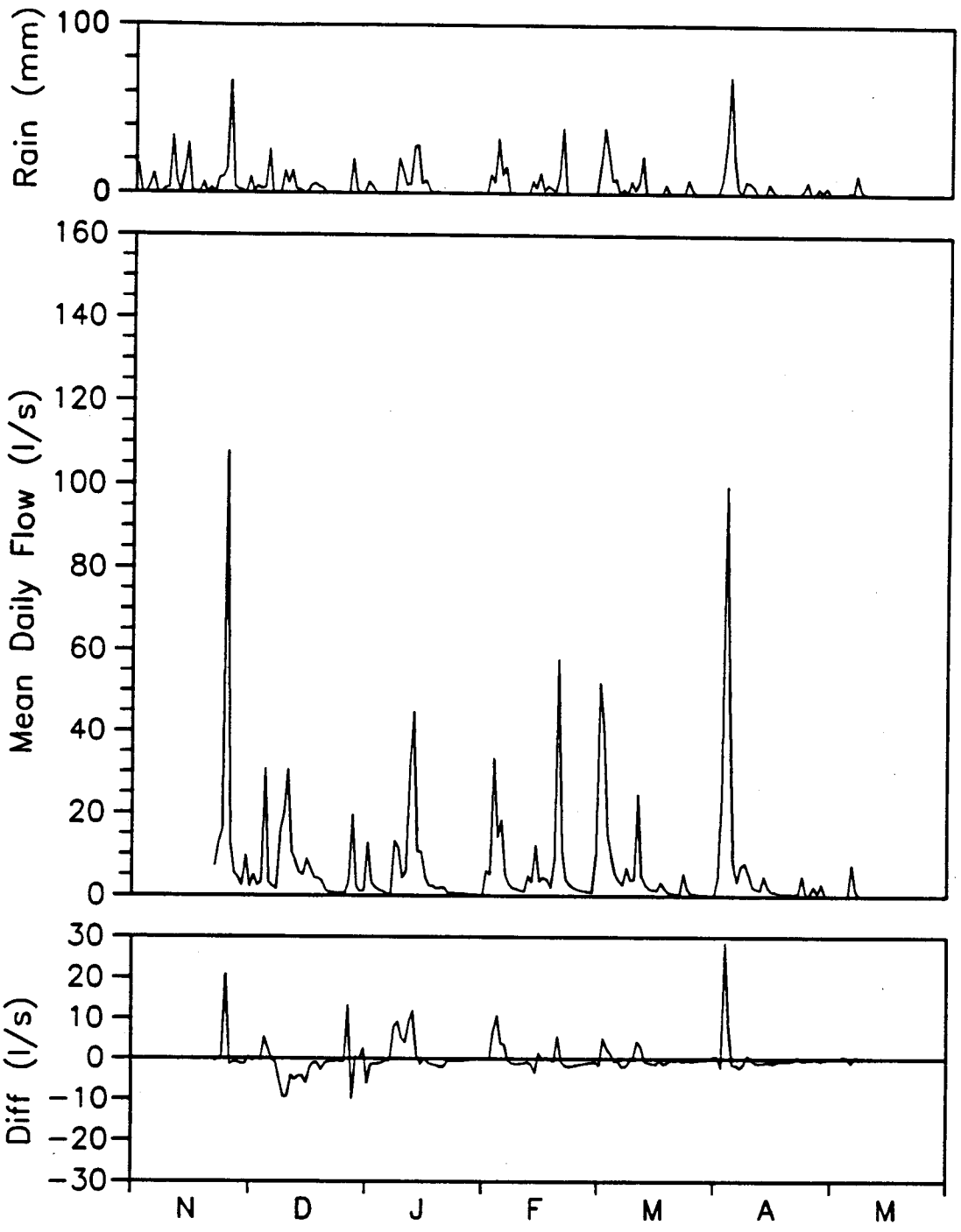

Fig 6-2. Daily time series of rainfall, recorded streamflow, and simulated minus recorded discharge ($Q_s - Q_r$) for the period November 1, 1990 - May 15, 1991.

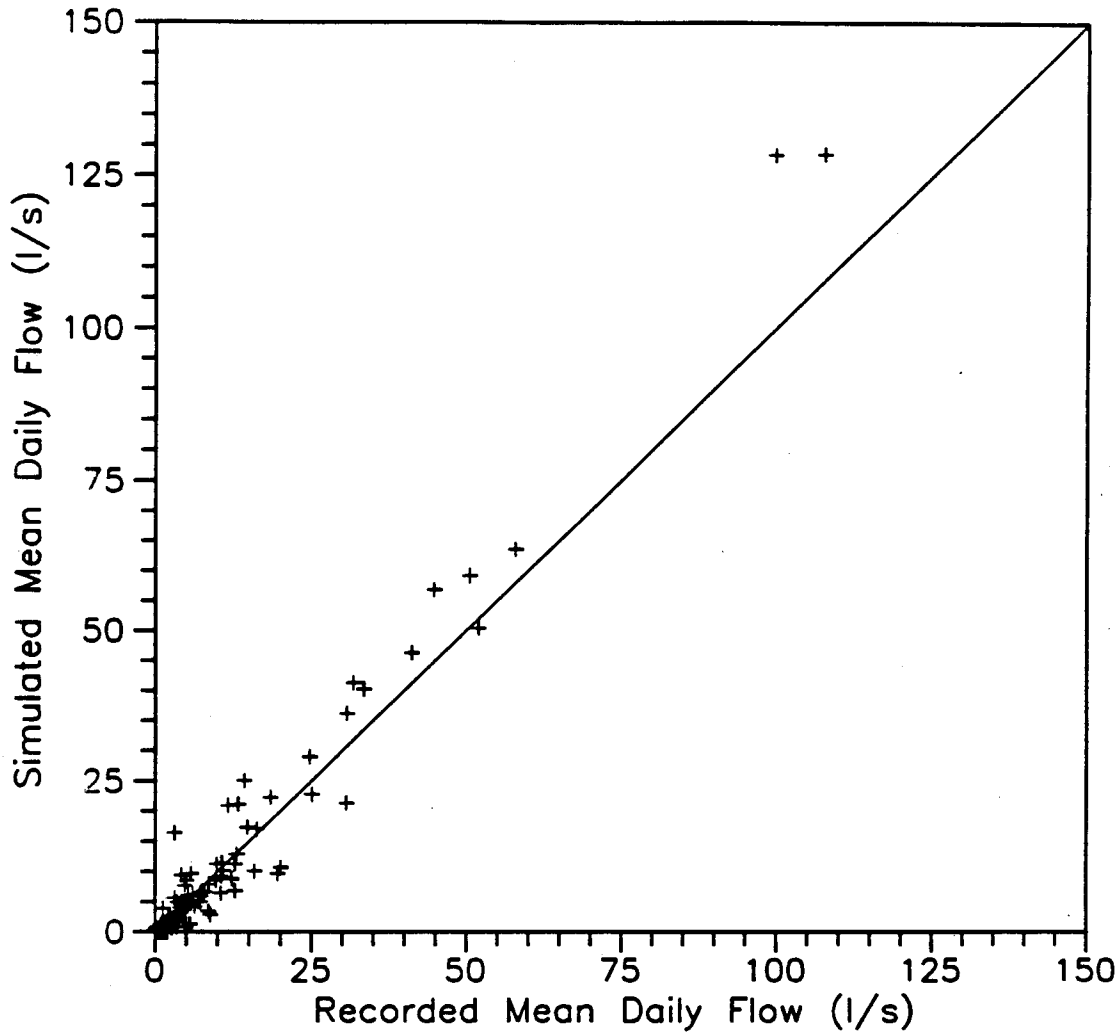

Fig. 6-3. Daily values of simulated versus recorded streamflow for the period November 21, 1990 - May 15, 1991.

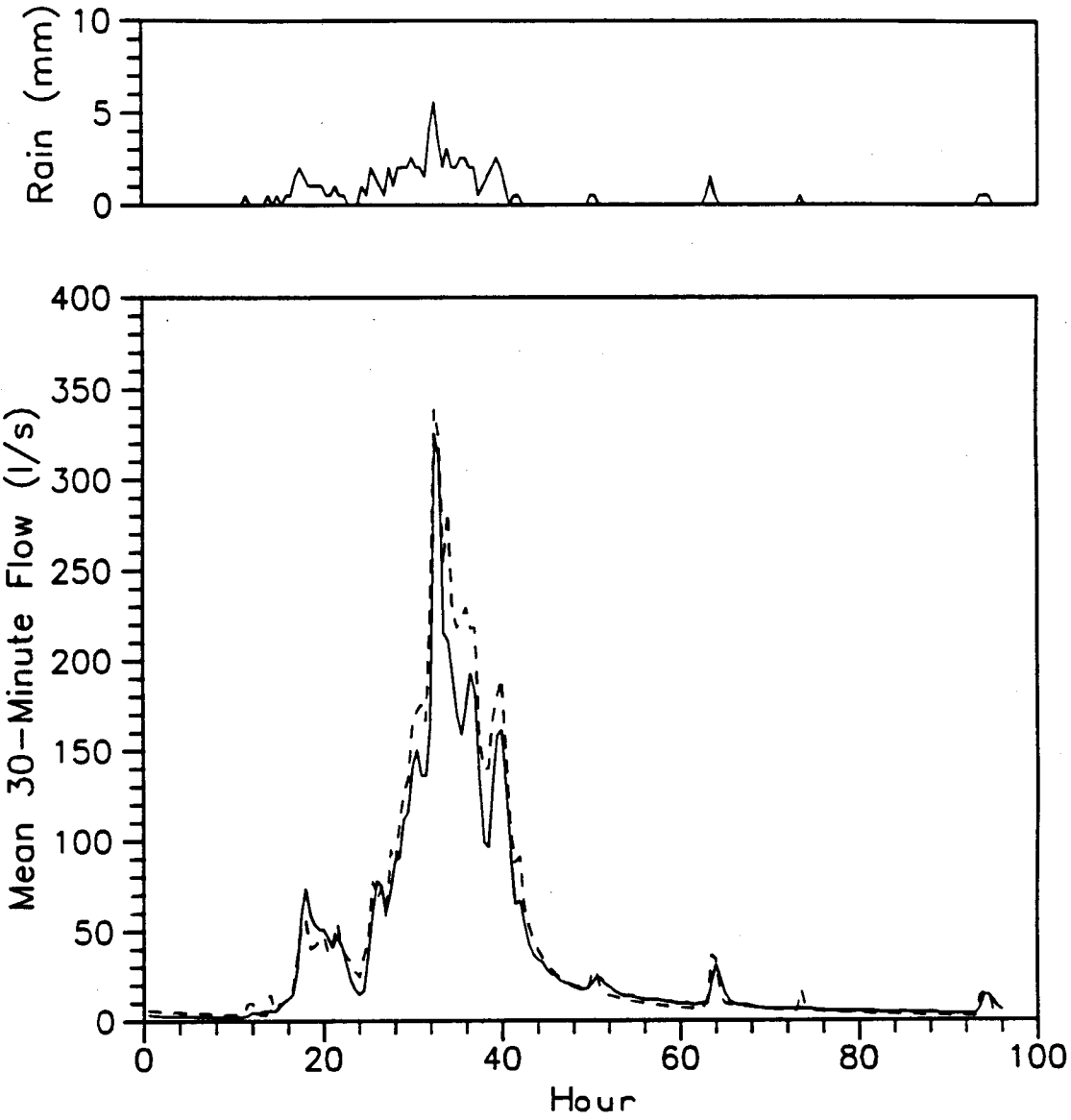

Fig. 6-4. Time series of rainfall, and recorded (solid line) and simulated (dashed line) streamflow at 30-minute intervals for the period November 23 - 26, 1990.

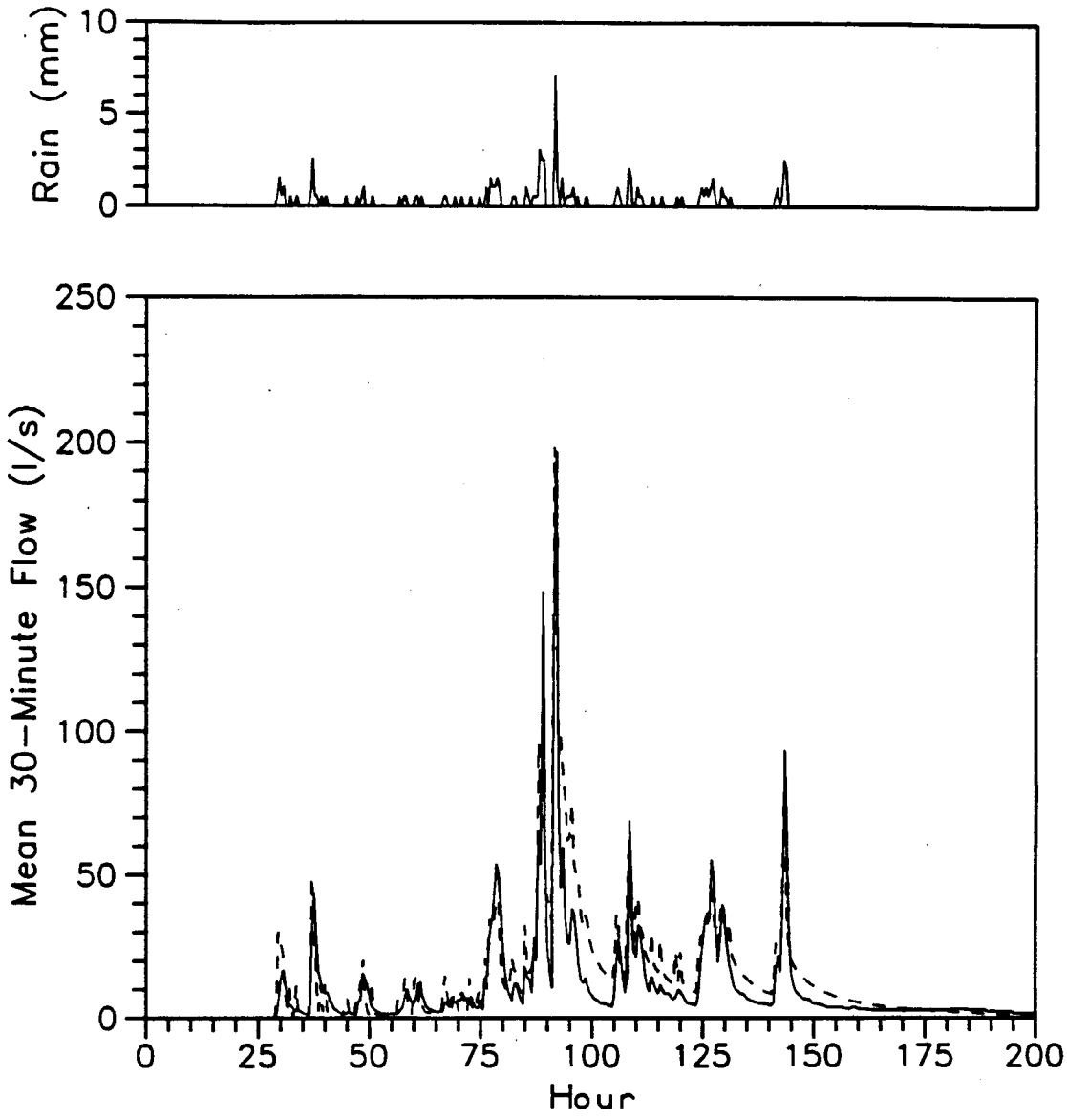

Fig. 6-5. Time series of rainfall, and recorded (solid line) and simulated (dashed line) streamflow at 30-minute intervals for the period January 30, 1991 - February 8, 1991.

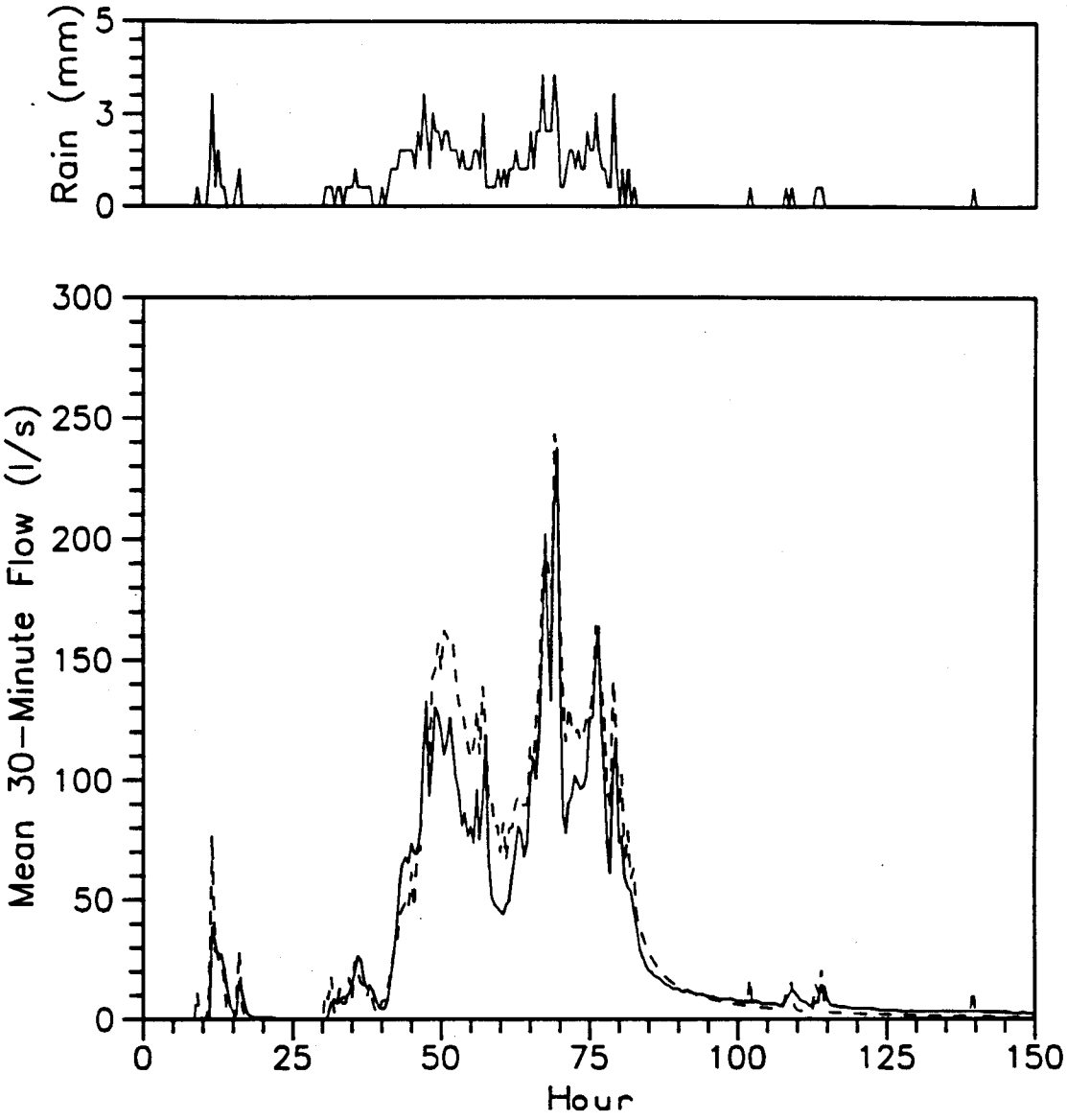

Fig. 6-6. Time series of rainfall, and recorded (solid line) and simulated (dashed line) streamflow at 30-minute intervals for the period April 2 - 9, 1991.

recorded. Simulated and recorded flows for the largest peak are within 1 percent. Simulated hydrograph recessions are too long, resulting in a 25 percent over-simulation of flow volumes.

Recorded and simulated flows for the large April storm are shown in Figure 6-6. The timing and shape of the simulated hydrograph rise is good, but the first peak is over-simulated. Simulation of the second combination peak (hours 60-65) is good, although the quick rise and fall between peaks is missed. Simulated discharge for the largest storm peak is within 2 percent of recorded. The total flow volume is over-simulated by about 14 percent.

6.6 Summary: Klahanie

During the study period 73 percent of the recorded precipitation volume became flow over the weir. Pervious areas contributed 60 percent of this total runoff volume. Discharge from pervious areas accounts for 63 percent of recorded runoff during the large November 1990 storm and 61 percent of the April 1991 storm volume. At Klahanie, runoff from pervious areas is significant and can not be neglected, even at the relatively short duration of large storms.

The mechanism(s) generating this rapid pervious area response are not known in detail. The quick basin response to rainfall makes direct observation of runoff generation during typical short duration rainfall bursts associated with storms difficult. The runoff response seems to be intermediate between overland flow and rapid subsurface flow. Most yards in the subdivision consist of imported top-soil overlain by sod. Subsurface drainage systems are present in many parts of the basin. There is little indication of Horton overland flow on

pervious areas and saturated overland flow generally appears to be restricted to the footslopes of subcatchments 5 and 10. This would suggest a predominately subsurface (largely near surface) response to rainfall, perhaps rapid lateral flow through the thatch and roots of the landscaped grass sod layer.

Runoff from pervious areas was modeled as a near surface response with characteristics between those of rapid subsurface flow and overland flow. The coefficient and exponent for lateral saturated conductivity were the only parameters determined through calibration. The calibration results are generally good. The total simulated runoff volume is within 2 percent of recorded. This was obtained using the till saturated conductivity determined through calibration at Novelty. The close agreement in total runoff volumes suggests the value of till conductivity may be applied regionally. Simulated storm peaks show excellent agreement with recorded, although the model tends to over-simulate storm volumes.

6.7 Comparison of Runoff Production in the Klahanie and Novelty Hill Catchments

Geologic conditions at the Klahanie and Novelty Hill basins are similar, both are contained within broad, till-capped plateaus. The two sites also received similar amounts of rainfall between November 21, 1990 and May 15, 1991; 881mm at Klahanie and 843 mm at Novelty Hill (Table 6-3). Although the Klahanie site is generally steeper, differences in runoff production between the two sites are dictated to a large extent by land use. At the Klahanie site 73

TABLE 6-3. Klahanie and Novelty Hill Flow Components
November 21, 1990 through May 15, 1991

	Klahanie		Novelty Hill	
	(mm)	(percent)	(mm)	(percent)
Precipitation	881	100	843	100
Weir Discharge	640	73	402	48
Surface Flow*	254	29	33	4
Pervious Land	386	44	369	44

* Based on an average saturated area of 1.44 ha at Novelty Hill and and 4.79 ha of effective impervious area at Klahanie

percent of the precipitation discharges through the weir as stream flow compared to 48 percent during the same period of time at Novelty Hill. Overland flow accounts for 29 percent of the precipitation at Klahanie versus 4 percent at Novelty Hill. Flow from pervious areas equals 44 percent of the rainfall at both sites. However, this flow is generated by a smaller percentage of the basin at Klahanie, where 62 percent of the precipitation falling on pervious areas becomes flow at the catchment outlet, compared to 46 percent at Novelty Hill.

Simulated actual evapotranspiration over the study period was 64 percent of potential evapotranspiration at Klahanie. For the same period of time simulated evapotranspiration at Novelty Hill was nearly 100 percent of potential. Much of this difference results from the reduction in soil water storage capacity at Klahanie. At Novelty Hill precipitation was stored in the soil for longer periods of time. As a result, water was rarely limiting during the generally wet simulation period and evapotranspiration could proceed at close to the potential rate. The thin soils and rapid flow response of pervious areas at Klahanie meant less water was stored in the soil and evapotranspiration opportunity was lower than for what would have been in the natural catchment state. The comparison period does not include the part of the year when artificial irrigation is supplied at Klahanie. Water loss through the till was 130 mm at Klahanie compared to 178 mm at Novelty Hill. Most of this difference can be attributed to the large impervious area at Klahanie and reduced saturated soil zone contact time with the till.

The reduction in soil depths during development at Klahanie and the

resulting decrease in soil water removal via evapotranspiration means the soil water storage capacity is exhausted earlier in storms than would have occurred under natural conditions. These physical changes, along with the introduction of impervious surfaces, increase the basin's sensitivity to rainfall patterns. During the study period there were 12 distinct storm hydrographs (Figure 6-2). For the same period of time there were only 6 independent storm hydrographs at Novelty Hill (Figure 5-2). The larger soil water storage capacities at Novelty Hill serve to dampen the affects of rainfall patterns on runoff production.

Chapter 7. Summary and Conclusions

7.1 Summary of Methodology

The need to develop suitable quantitative hydrologic tools for describing flow paths and fluxes that are important when considering alternative land use measures is the primary focus of this work. Because change takes place incrementally, small catchments are the hydrologic units considered here. I have applied a combination of field mapping, simple hydrologic monitoring, and hydrologic modeling (combination methodology), to describe and predict the internal catchment states and fluxes, as well as integrated basin outflow in two small catchments. One catchment is undeveloped forest and the other has been urbanized.

In this approach a catchment is first field mapped using techniques described by Dunne (1975) and Burges et al. (1989) to delineate wet-season areal extents of hydrologic process zones. This information provides guidance for the location of monitoring stations and preliminary basin dissagregation for hydrologic modeling. The hydrologic process zones identified during field mapping indicate lower bounds on spatial scales for further hydrologic analysis.

I have used relatively simple hydrologic monitoring which includes streamflow, precipitation, and limited piezometer information. Measurements used in this study were intentionally restricted to those methods which are simple, low cost, and manual or semi-automated (e.g., piezometers with crest gages), so that data collection time and expense are minimized, and observers are not required to be in the catchment during all storms. Such measurements

are of great value in model validation because they provide essential information about actual flow paths not contained in measured channel flow hydrographs.

A relatively simple continuous simulation model was developed to represent the broad spatial and temporal features of field observable flow processes. The model uses commonly measured hydrologic fluxes (e.g., precipitation and channel flow) as well as easily obtainable supplemental spatial and point measures of hydrologic states (e.g., shallow water table elevations and the plan extent of saturation zones). It was designed specifically for application in catchments that will experience land-use change and simulates Horton overland flow, subsurface stormflow, return flow, and saturation overland flow. The model preserves the effects of topography and the spatial variation of hydrologic properties, and is computationally efficient.

The model requires three input parameters to represent canopy and litter zone storage, eight parameters to describe soil characteristics, four parameters for overland flow routing, and one parameter for leakage through a lower less permeable boundary. The model user specifies top and bottom widths of land segments and supplies ground surface elevations, soil depths, and soil saturated hydraulic conductivity as a function of downslope distance. Storage discharge relationships for channel reaches are also supplied by the model user. All model parameters have a physical basis. Most of the parameters are determined by field measurements or estimated from the hydrologic literature.

7.2 Summary of Method Application

The combination methodology was applied in two zero-order drainage basins in King County, Washington. A 37 ha forested catchment east of Lake Washington (designated Novelty Hill) was selected to represent natural conditions and a 17 ha subbasin east of Lake Sammamish (Klahanie) was chosen as representative of urbanized conditions. The two basins were selected so that differences in runoff production and evapotranspiration were dictated primarily by land use.

Initial application of the combination methodology began at Novelty Hill in October 1989 and continued through the remainder of Water Year 1990 (October 1, 1989 - September 30, 1990). Application began at the urban site in early October 1990. Basin boundaries were defined and soil depths were measured using a hand auger. Infiltration areas and locations that generate Horton overland flow were mapped. The seasonal extent of saturated areas were determined in the field from topography, soil morphology, and, to a lesser extent, vegetation. The maximum extents of saturated zones were defined from field observations during large storms.

7.2.1 Novelty Hill Basin

Field mapping and the first year of data at Novelty Hill were used to separate total basin outflow into flow components (surface, subsurface, etc.) at the annual scale. It was found that surface runoff generation is confined to a central swale containing a seasonal wetland that occupies about 4 percent of the basin area. During the study period catchment discharge accounted for 29

percent of annual precipitation and 42 to 47 percent of wet season precipitation. Saturation overland flow represents 9 to 12 percent of this discharge. Seventy-one percent of the precipitation falling on the catchment was lost to evapotranspiration and vertical leakage through the underlying Vashon till.

The physical basis of model input parameters allowed the hydrology and hydraulics of the central swale to be simulated without calibration. Only four land segment input parameters required calibration (using recorded rainfall, streamflow, and piezometer information), with the same values used in all ten segments. The final calibrated values of soil hydrologic properties were in general agreement with results from other studies in forested watersheds.

Model simulations provided an estimate of water loss through the glacial till, and provided addition information on soil hydrologic properties (saturated moisture content and field capacity). The simulations of flow components and spatial locations of hydrologic process zones provided guidance in determining where additional monitoring stations would be useful.

Limited verification of the model was done using the next eight months of data from Water Year 1991. The agreement between simulated and recorded mean flows and volumes was excellent. Model simulation of storm hydrograph peaks was good, however storm volumes were over-simulated. Simulated water table fluctuations were compared with recorded at three locations during verification, one near the basin headwater (P-5) (Figure 5-1) and two near the outlet (L-1 and L-4). No data were available at the locations of piezometers L-1 and L-4 during model calibration. Model simulations for all three piezometers (P-5, L-1, and L-4) were generally good.

7.2.2 Klahanie Basin

Field mapping at Klahanie provided the locations of impervious surfaces that are connected directly to the surface flow conveyance system. This information was used along with recorded rainfall and streamflow to separate the volumes of Horton overland flow generated on impervious surfaces from discharge originating in pervious areas of the catchment. This allowed runoff from pervious and impervious surfaces to be analyzed independently.

During the study period 73 percent of the recorded precipitation volume at Klahanie became flow over the weir. Pervious areas contributed 60 percent of this total runoff volume. Discharge from pervious areas accounts for 63 percent of recorded runoff during the large November 1990 storm and 61 percent of the April 1991 storm volume.

Runoff from pervious areas was modeled as a near surface response with characteristics between those of rapid subsurface flow and overland flow. Only two model parameters were determined through calibration. The calibration results are generally good. The total simulated runoff volume is within 2 percent of recorded. Simulated storm peaks show excellent agreement with recorded, although the model over-simulates storm volumes. Data are to be collected through June 1993 and will be used at a later date to verify the calibrated model.

7.3 Conclusions

The primary contribution of this dissertation is the development of a methodology that provides detailed information on internal catchment states and fluxes which can not be obtained using traditional methods of analysis such as the application of a rainfall-runoff model using recorded rainfall and the basin integrated stream flow measured at the outlet. The methodology provides a physical basis for separating flow into its several components and allows field estimates of soil hydrologic properties to be made at scales consistent with the dominant runoff mechanisms in the basin.

Satisfactory model performance during the albeit limited verification at Novelty Hill demonstrates that field estimated, spatially-averaged soil properties can be used along with measurements of topography and soil depths to predict spatial and temporal distributions of internal catchment states and fluxes (i.e., accurate simulation of water table fluctuations at several different locations). The model structure allows simulation results to be verified directly at any desired location within the catchment.

Subsurface flows were found to dominate storm runoff in the Novelty Hill basin. This results from high saturated lateral conductivities that increase with distance above the till layer. During the winter, soil moisture remains near field capacity and storm rainfall infiltrates rapidly to the water table. The rapid recharge rates, high lateral saturated soil conductivities, and a well confined zone of surface soil saturation permit subsurface generated flow to dominate both hydrograph peaks and volumes.

Discharge from pervious areas in the Klahanie basin is significant even at the relatively short duration of large storms. While the mechanism(s)

generating this rapid pervious area response are not known in detail, qualitatively the runoff response seems to be intermediate between overland flow and rapid subsurface flow. Field mapping and model simulations suggest a predominately subsurface (largely near surface) response to rainfall, perhaps rapid lateral flow through the thatch and roots of grassed areas.

It was not possible to determine a priori what runoff mechanism would dominate storm runoff in the study basins. Prior to application of the combination methodology, it was suspected that saturation overland flow would drive peak discharge in the Novelty Hill catchment and Horton overland flow from impervious surfaces would dominate storm runoff at Klahanie. Use of the combination methodology developed here proved both of these assumptions false.

7.4 Future Investigations

Additional work remains at both study sites. The model has yet to be verified under the urbanized conditions at Klahanie. Proper verification will require additional field measurements and observations during large storms to quantify the mechanism(s) responsible for the rapid pervious area response to rainfall. It will be necessary to map zones of pervious area surface runoff generation that only occur during large storms. These areas may have been missed in the original field mapping. This additional information will allow a more accurate separation between surface and subsurface flow volumes from pervious areas. A rainfall simulator could be used to characterize the soil conditions and rainfall intensities required to generate Horton overland flow in

grassed areas typical of this environment. The physical mechanism producing the rapid, apparently subsurface pervious area response needs to be identified. The hypothesis of lateral flow through the roots and thatch of grassed areas should be tested. If the hypothesis is valid, the physics of such a flow needs to be quantified.

Soil samples should be collected at a limited number of locations in each basin and analyzed to determine their moisture retention characteristics. These point measurement values will provide more information on hydrologic conditions in the catchments and can be compared to the spatially-averaged field estimates and calibrated model parameters.

Catchment water flow production varies by climatic and geologic region and by the specific basin characteristics. The adaptive approach has been developed using two small basins in the Pacific Northwest. It remains to be tested in different hydro-climatic environments. The model has been evaluated in basins with relatively thin, coarse grained soils. Model application in basins with deeper or finer grained soils would provide a further test of subsurface components. More arid conditions may provide a suitable test of the model's representation of evapotranspiration. It is expected that both the model and the methodology will evolve as they are applied in different hydro-climatic environments.

REFERENCES

Abbott, M. B., J. E. Bathurst, J. A. Cunge, P. E. O'Connel, and J. Rasmussen, "An introduction to the European hydrological system-Systeme Hydrologique Europeen, SHE, 1: history and philosophy of a physically-based, distributed modeling system", *J. of Hydrology*, 87, 45-59, 1986.

Aron, G., "Rainfall abstractions", in *Urban stormwater hydrology*, edited by D. F. Kibler, Water Resources Monograph 7, AGU, p. 72, 1982.

Balci, A. N., "Physical, chemical, and hydrological properties of certain Western Washington forest floor types", Ph.D. dissertation, University of Washington, Seattle Wash., 1964.

Betson, R. P., "What is watershed runoff?", *J. Geophys. Res.*, 69, 1541-1551, 1964

Beven, K. J., "Kinematic subsurface stormflow", *Water Resour. Res.*, 17(5), 1419-1429, 1981.

Beven, K. J., "On subsurface stormflow: Predictions with simple kinematic theory for saturated and unsaturated flows", *Water Resour. Res.*, 18(6), 1627-1633, 1982a.

Beven, K. J., "On subsurface stormflow: An analysis of response times", *Hydrological Sciences J.*, (4), 505-521, 1982b.

Beven, K. J., "Distributed models", in *Hydrological Forecasting*, edited by M. G. Anderson and T. P. Burt, p. 405, John Wiley & Sons Ltd., 1985.

Beven, K. J., "Lecture 2: Spatially distributed modeling: conceptual approach to runoff prediction", *Current Modeling Issues and Technological Trends*, NATO Advanced Study Institute, Sintra, Portugal, 1988a.

Beven, K. J., "Lecture 1: Infiltration and soil moisture, interception and surface detention, unsaturated flow" *Current Modeling Issues and Technological Trends*, NATO Advanced Study Institute, Sintra, Portugal, 1988b.

Beven, K. J., "Changing ideas in hydrology--the case of physically-based models", *J. of Hydrology*, 105, 157-172, 1989a.

Beven, K. J., "Interflow", in *Unsaturated flow in hydrologic modeling -- theory and practice*, edited by H.J. Morel-Seytoux, NATO ASI Series C: Mathematical and Physical Sciences, Vol. 275, Kluwer Academic Publishers, 191-219, 1989b.

Beven, K. J., and P. Germann, "Macropores and water flow in soils", *Water Resour. Res.*, 18(5), 1311-1325, 1982

Beven, K. J., and M. J. Kirkby, "A physically based, variable contributing area model of basin hydrology", *Hydrological Sciences Bulletin*, 24(1), 43-69, 1979.

Binley, A., J. Elgy, and K. J. Beven, "A physically-based model of heterogeneous hillslopes. I. Runoff production", *Water Resour. Res.*, 25(6), 1989a.

Binley, A., K. J. Beven, and J. Elgy, "A physically-based model of heterogeneous hillslopes. II. Effective hydraulic conductivities", *Water Resour. Res.*, 25(6), 1989b.

Bresler, E., and G. Dagan, "Unsaturated flow in spatially variable fields 2. Application of water flow models to various fields", *Water Resour. Res.*, 19(2), 421-428, 1983.

Buchanan, P., K. W. Savigny, and J. De Vries, "A method for modeling water tables at debris avalanche headscarpes", *J. of Hydrology*, 113, 61-88, 1990.

Burges, S. J., B. A. Stoker, M. W. Wigmosta, and R. A. Moller, "Hydrologic information and analysis required for mitigating hydrologic effects of urbanization", *Water Resource Series Technical Report No. 117*, University of Washington, pp. 131, June 1989.

Childs, E. C., "Drainage of groundwater resting on a sloping bed", *Water Resour. Res.*, 7(5), 1256-1263, 1971.

Chow, V. T., D. R. Maidment, and L. W. Mays, "Applied Hydrology", McGraw-Hill Book Company, New York, 1988.

Crawford, N. H., and R. K. Linsley, "Digital simulation in hydrology: Stanford watershed model IV", *Stanford Univ., Dept. Civ. Eng. Tech. Rep. 39*, 1966.

Dawdy, D. R., J. C. Schaake, Jr., and W. M. Alley, "User's guide for distributed routing rainfall-runoff model", *Water Resources Investigations Report 78-90*, U.S. Geological Survey, pp. 146, 1978.

Dietrich, W. E., and T. Dunne, "The channel head", manuscript in preparation, 1990.

Dinicola, R. S., "Characterization and simulation of rainfall-runoff relations for headwater basins in western King and Snohomish Counties, Washington", *Water Resource Investigations Report 89-4052*, U.S. Geological Survey, Tacoma, Wash., 1990.

Ducken, S., "A water budget for a small forested catchment -- evaporation estimation and hydrologic modeling with limited data", unpublished manuscript, 1990.

Dunne, T., "Models of runoff processes and their significance", in *Scientific Basis of Water-Resource Management*, Nat. Academy Press, Washington, D.C., 17-30, 1982.

Dunne, T., "Relation of field studies and modeling in the prediction of storm runoff", *J. of Hydrology*, 65, 25-48, 1983.

Dunne, T., "Hydrology, mechanics and geomorphic implications of erosion by subsurface flow", in *Groundwater geomorphology; The role of subsurface water in earth-surface processes and landforms*, U.S. Geological Society of America, Special Paper 252, 1990.

Dunne, T., and R. D. Black, "An experimental investigation of runoff production in permeable soils", *Water Resour. Res.*, 6(2), 478-490, 1970a.

Dunne, T., and R. D. Black, "Partial area contributions to storm runoff in a small New England watershed", *Water Resour. Res.*, 6(5), 1296-1311, 1970b.

Dunne, T., and L. B. Leopold, "Water in environmental planning", W.H. Freeman and Company, San Francisco, 1978.

Dunne, T., T. R. Moore, and C. H. Taylor, "Recognition and prediction of runoff production zones in humid regions", *Hydrological Sciences Bulletin*, 20(3), 305-327, 1975.

Engman, E. T., and A. S. Rogowski, "A partial area model for storm flow synthesis", *Water Resour. Res.*, 10(3), 464-472, 1974.

Freeze, R. A., "Three-dimensional, transient, saturated-unsaturated flow in a groundwater basin", *Water Resour. Res.*, 7(2), 347-366, 1971

Freeze, R. A., "Role of subsurface flow in generating surface runoff 1: Baseflow contributions to channel flow", *Water Resour. Res.*, 8(3), 609-623, 1972a.

Freeze, R. A., "Role of subsurface flow in generating surface runoff 2: Upstream source areas", *Water Resour. Res.*, 8(5), 1272-1283, 1972b.

Gan, T. Y., "Applications of scientific modeling of hydrologic responses from hypothetical small catchments to assess a complex conceptual rainfall-runoff model.", *Water Resource Series Technical Report No. 111*, University of Washington, 1988.

Gan, T. Y, and S. J Burges, "An assessment of a conceptual rainfall-runoff models ability to represent the dynamics of small hypothetical catchments 1. Models, model properties, and experimental design", *Water Resour. Res.*, 26(7), 1595-1604, 1990.

Harr, R. D., "Water flux in soil and subsoil on a steep, forested slope", *J. of Hydrology*, 33, 37-58, 1977.

Henderson, F. M., and R. A. Wooding, "Overland flow and groundwater flow from a steady rainfall of finite duration", *J. Geophys. Res.*, 69(8), 1964.

Hewlitt, J. D., and A. R. Hibbert, "Moisture and energy conditions within a sloping soil mass during drainage", *J. Geophys. Res.*, 68(4), 1081-1087, 1963.

Hewlitt, J. D., and A. R. Hibbert, "Factors affecting the response of small watersheds to precipitation in humid areas", in *Forest Hydrology*, edited by W.E. Sopper and H.W. Lull, Pergamon Press, Oxford, 275-290, 1967.

Horton, R. E., "The role of infiltration in the hydrologic cycle", *EOS: Trans. American Geophysical Union,* 14, 446-460, 1933.

Horton, R. E., "An approach towards a physical interpretation of infiltration capacity", *Soil Sci. Soc. Proc.*, 5, 399-417, 1940.

Huber, W. C., J. P. Heaney, S. J. Nix, R. E. Dickinson, and D. J. Polmann, "Stormwater management model user's manual -- Version III", *Project No. CR-805664*, U.S. Environmental Protection Agency, Cincinatti, Ohio, Nov., 1981.

Humphrey, N. F., "Pore pressures in debris failure initiation", *Washington State Water Resources Center, Report 45*, Pullman Washington, 1982.

Hurley, D. G., and G. Pantelis, "Unsaturated and saturated flow through a thin porous layer on a hillslope", *Water Resour. Res.*, 21(6), 821-824, 1985.

Ibbitt, R. P., "Derivation of a continuous version of the Sloan and Moore hillslope model", *Internal Report No. WS 1311*, Hydrology Centre, Christchurch, New Zealand, pp. 9, 1989a.

Ibbitt, R. P., "Modelling the unsaturated zone using a Green-Ampt approach", *Internal Report No. WS 1316*, Hydrology Centre, Christchurch, New Zealand, pp. 14, 1989b.

Izzard, C. F., "The surface profile of overland flow", *Trans., American Geophysical Union, Part VI*, 959-986, 1944.

Izzard, C. F., "The hydraulics of runoff from developed surfaces", *Proceedings, Highway Research Board*, Twenty-Sixth Annual Meeting, 1946.

Johanson, R. C., J. C. Imhoff, J. L. Kittle, and A. S. Donigan, "Hydrologic simulation program -- FORTRAN (HSPF): Users manual for release 8.0", *U.S. Environmental Protection Agency Report EPA-600/3-84-066*, 1984.

Kibler, D. F., and D. A. Woolhiser, "The kinematic cascade as a hydrologic model", *Hydrology Paper No. 39, Colorado State Univ.*, Fort Collins, pp. 27, 1970.

Linsley, R. K., M. A. Kohler, and J. L. H. Paulhus, "Hydrology for engineers", McGraw-Hill Book Company, pp. 508, 1982.

McDonell, J. J., "A rationale for old water discharge through macropores in a steep, humid catchment", *Water Resour. Res., 26(11)*, 2821-2832, 1990.

Megahan, W. F., and J. L. Clayton, "Tracing subsurface flow on roadcuts on steep, forested slopes", *J. Soil Sci. Soc. Am.*, 47(6), 1063-1067, 1983.

Mosely, M. P., "Streamflow generation in a forested watershed, New Zealand", *Water Resour. Res.*, 15(4), 795-806, 1979.

Musgrave, G. W., and H. N. Holtan, "Infiltration", in *Handbook of Applied Hydrology*, edited by V.T. Chow, McGraw-Hill Book Co., New York, 12-1 to 12-30, 1964.

Nash, J. E., and J. V. Sutcliffe, "River flow forecasting through conceptual models, 1, A discussion of principles, *J. of Hydrology*, 10, 282-290, 1970.

Neumann, S. P., "Saturated-unsaturated seepage by finite elements", *J. Hydraulics Div.*, ASCE, 99(HY12), 2233-2250, 1973.

Nieber, J. L., "Hillslope soil moisture flow, approximation by a one dimensional formulation", *Paper No. 82-2026*, ASAE, 1-28, 1982.

Nieber, J. L., and M. F. Walter, "Two-dimensional soil moisture flow in a sloping rectangular region: Experimental and numerical studies", *Water Resour. Res.*, 17(6), 1722-1730, 1981.

Olmsted, T. L., "Geological aspects and engineering properties of glacial till in the Puget Lowland, Washington", in *Proc. 7th Annual Eng. Geol. and Soils Eng. Symp.*, Moscow, Idaho, 223-233, 1969.

O'Loughlin, C. L., "Stability of steepland forest soils", Ph.D. dissertation, University of British Columbia, Vancouver, B.C., 1972.

Ormsbee, L. E., and A. Q. Khan, "A parametric model for steeply sloping forested watersheds", *Water Resour. Res.*, 25(9), 2053-2065, 1989

Park, N. S., "Subsurface flow modeling by the kinematic cascade", M.S. Thesis, Penn. State Univ., College Park, Penn., 1985.

Penman, H. L., "Natural evaporation from open water, soil and grass", *Proceedings of the Royal Society of London, Series A*, 193, 120-145, 1948.

Philip, J. R., "The theory of infiltration: 1. the infiltration equation and its solution", *Soil Sci.*, 83(5), 345-357, 1957.

Philip, J. R., "Theory of infiltration", in *Advances in Hydroscience*, Academic Press, New York, 215-296, 1969.

Pilgrim, D. H., D. D. Huff, and T. D. Steele, "A field evaluation of subsurface and surface runoff. II. Runoff processes", *J. of Hydrology*, 38, 319-341, 1978.

Ragan, R. M., "An experimental investigation of partial area contributions", *Proc. of the Berne Symposium*, Int. Assoc. Sci. Hydro., Publ. No. 76, 241-249, 1968.

Rawls, W. J., and D. L. Brakensiek, "Estimation of soil water retention and hydraulic properties", in *Unsaturated flow in hydrologic modeling -- theory and practice*, edited by H.J. Morel-Seytoux, NATO ASI Series C: Mathematical and Physical Sciences, Vol. 275, Kluwer Academic Publishers, 275-300, 1989.

Reddi, L. N., I. M. Lee, and T. H. Wu, "A comparison of models predicting ground water levels on hillside slopes", *Water Resour. Bull.*, AWRA, 26(4), 1990.

Reeves, M., and J. O. Duguid, "Water movement through saturated unsaturated porous media: a finite-element Galierkin model", Oak Ridge National Lab., *ORNL-4927*, Oak Ridge, Tennessee, pp. 236, 1975.

Richards, L. A., "Capillary conduction of liquids through porous mediums", *Physics*, 1, 318-333, 1931.

Running, S. W., R. N. Ramakrishna, and R. D. Hungerford, "Extrapolation of synoptic meteorological data in mountainous terrain and its use for simulating forest evapotranspiration and photosynthesis", *Can. J. For. Res.*, 17, 472-483, 1987.

Sklash, M. G., and R. N. Farvolden, "The role of groundwater in storm runoff", *J. of Hydrology*, 43, 45-65, 1979.

Sloan, P. G., I. D. Moore, G. B. Coltharp, and J. D. Eigel, "Modeling surface and subsurface stormflow on steeply-sloping forested watersheds", *Univ. of Kentucky, Water Resour. Res. Inst.*, Lexington, KY, 1983.

Sloan, P. G., and I. D. Moore, "Modeling subsurface stormflow on steeply sloping forested watersheds", *Water Resour. Res.*, 20(12), 1815-1822, 1984.

Smith, R. E., and R. H. B. Hebbert, "Mathematical simulation of interdependent surface and subsurface hydrologic processes", *Water Resour. Res.*, 19(4), 987-1001, 1983.

Smith, R. E., and R. H. B. Hebbert, "Hillslope model users manual", Fort Collins, Colorado (unpublished manuscript), 1984.

Smith, R. E., and D. A. Woolhiser, "Overland flow on an infiltrating surface", *Water Resour. Res.*, 7, 899-913, 1971.

Thornthwaite, C. W., and J. R. Mather, "The Water Balance", *Laboratory of Climatology, Publ. No. 8*, Centerton, N. J., 1955.

U.S. Army Corps of Engineers, "Storage, treatment, overflow runoff model STORM", *Computer Program No. 723-28-17520*, Hydrologic Engineering Center, Davis, CA, 1976.

U.S. Army Corps of Engineers, "HEC-1 users manual", U.S. Army Corps of Engineers, Davis, CA, 1985.

U.S. Dept. of Agriculture, Soil Conservation Service, "Soil Survey of King County Area, Washington", pp 102, and 21 maps, 1973.

Veihmeyer, F. J., "Evapotranspiration", in *Handbook of Applied Hydrology*, edited by V. T. Chow, McGraw Hill, New York, 1964.

Weyman, D. R. "Throughflow on hillslopes and its relation to the stream hydrograph", *Int. Assoc. Sci. Hydrol. Bull.*, 15(3), 25-33, 1970.

Weyman, D. R., "Measurement of the downslope flow of water in a soil", *J. of Hydrology*, 20, 267-288, 1973.

Whipkey, R. Z., "Subsurface stormflow from forested slopes", *Int. Assoc. Sci. Hydro. Bull.*, 10(2), 74-85, 1965.

Wigmosta, M. S., and S. J. Burges, "Proposed model for evaluating urban change", *Journal of Water Resource Planning and Management*, ASCE, 116(6), 742-762, 1990.

Woods, R. A., and R. P. Ibbitt, "Analytical solution for kinematic flow over an infiltrating plane", *Internal Report No. WS 1281*, Hydrology Centre, Christchurch, New Zealand, pp. 11, 1988.

Woolhiser, D. A., and J. A. Liggett, "Unsteady one-dimensional flow over a plane -the rising hydrograph", *Water Resour. Res.*, 3(3), 753-771, 1967.

Appendix A. Novelty Hill Weir Specifications and Discharge Error Analysis

A.1 Weir Specifications

Streamflow at the outlet of the forested Novelty Hill catchment is measured at 15-minute intervals using a combination v-notch and sharp-crested rectangular weir. The combination weir is located 4.3 m downstream of the closest base of an abandoned railroad grade (Figure 5-1). Flow from the swale passes under the railroad grade through a 8.8-m long, 0.305-m (12-inch) corrugated metal culvert before entering a pool upstream of the weir. Both the railroad fill and the weir act as barriers to lateral subsurface flow above the till layer. The weir is keyed into Vashon till at a depth of about 0.6 m and has been sealed using Portland cement grout. As a result, nearly all surface and subsurface discharge exiting the catchment *above* the till layer passes over the weir.

Weir dimensions are given in Figure A-1. Discharge for the 98.7 degree v-notch weir is calculated as:

$$Q = 1.607H^{2.5} \qquad \text{(A-1)}$$

where H is the head on the weir in meters and Q is in liters per second. (The coefficient of 1.607 becomes 2.91 when H is measured in feet and Q is in cfs.) Only during the uncommonly large January 1990 rain storm did flow exceed the capacity of the v-notch weir. Flow through the sharp-crested rectangular weir was calculated as

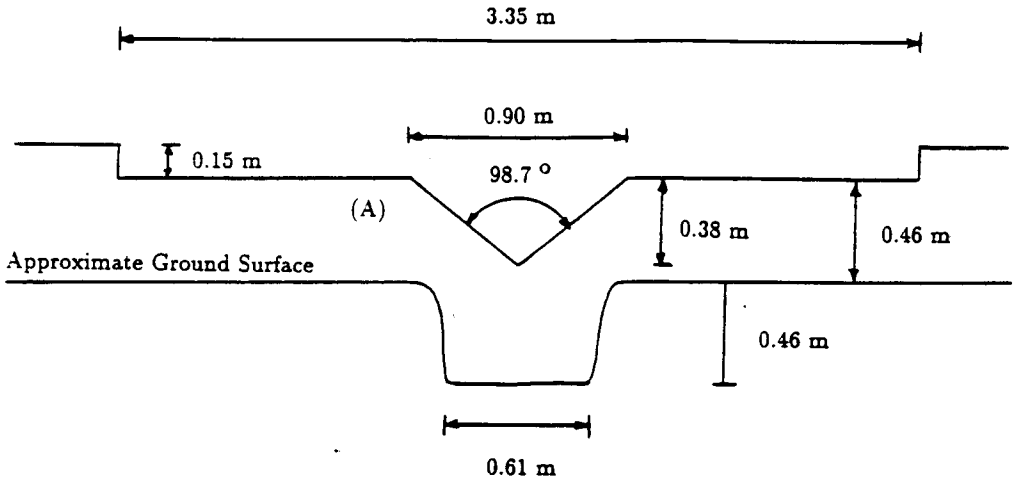

Fig. A-1. Novelty Hill compound weir composed of a 3.35 m wide by 0.15 m high sharp-crested rectangular weir centered over a 98.7 degree sharp-crested v-notch weir with a top width of 0.9 m. Manual measurements of weir pool stage are made at location **A**.

$$Q = 1.838 L_w \left[L_w - 0.2H \right] H^{\frac{3}{2}} \qquad \text{(A-2)}$$

where L_w equals 2.44 m (8 ft) (total length of the rectangular weir minus the top width of the v-notch weir) and H is the head on the rectangular weir in meters. (The coefficient of 1.838 becomes 3.33 when H is measured in feet and Q is in cfs.) The two weirs were treated independently, and the total discharge taken as the sum from equations (A-1) and (A-2).

Water levels in the upstream weir pool are recorded in 3.05 mm (0.01 foot) increments at 15-minute intervals using an Instrumentation Northwest PS-7000 pressure transducer. The transducer is contained within a 152 mm (6-inch) in diameter steel pipe located in quiescent water approximately 4 m from the weir. A crest gage is also attached to the weir.

A.2 Discharge Error Analysis

During each site visit a manual weir stage measurement was made near the crest gage at location A in Figure A-1. The estimated error in water surface height from these manual measurements could be no larger than $+/-$ 3 mm ($\frac{1}{8}$ - inch). There may be some drawdown of the water surface at location A caused by converging flow in this region close to the weir. This will result in underestimation of head on the weir and therefore underestimation of discharge. The pressure transducer is located in quiescent water and does not suffer from this problem. Discharge calculated from manual stage measurements is plotted against discharge estimated from the pressure transducer in Figure A-2. The

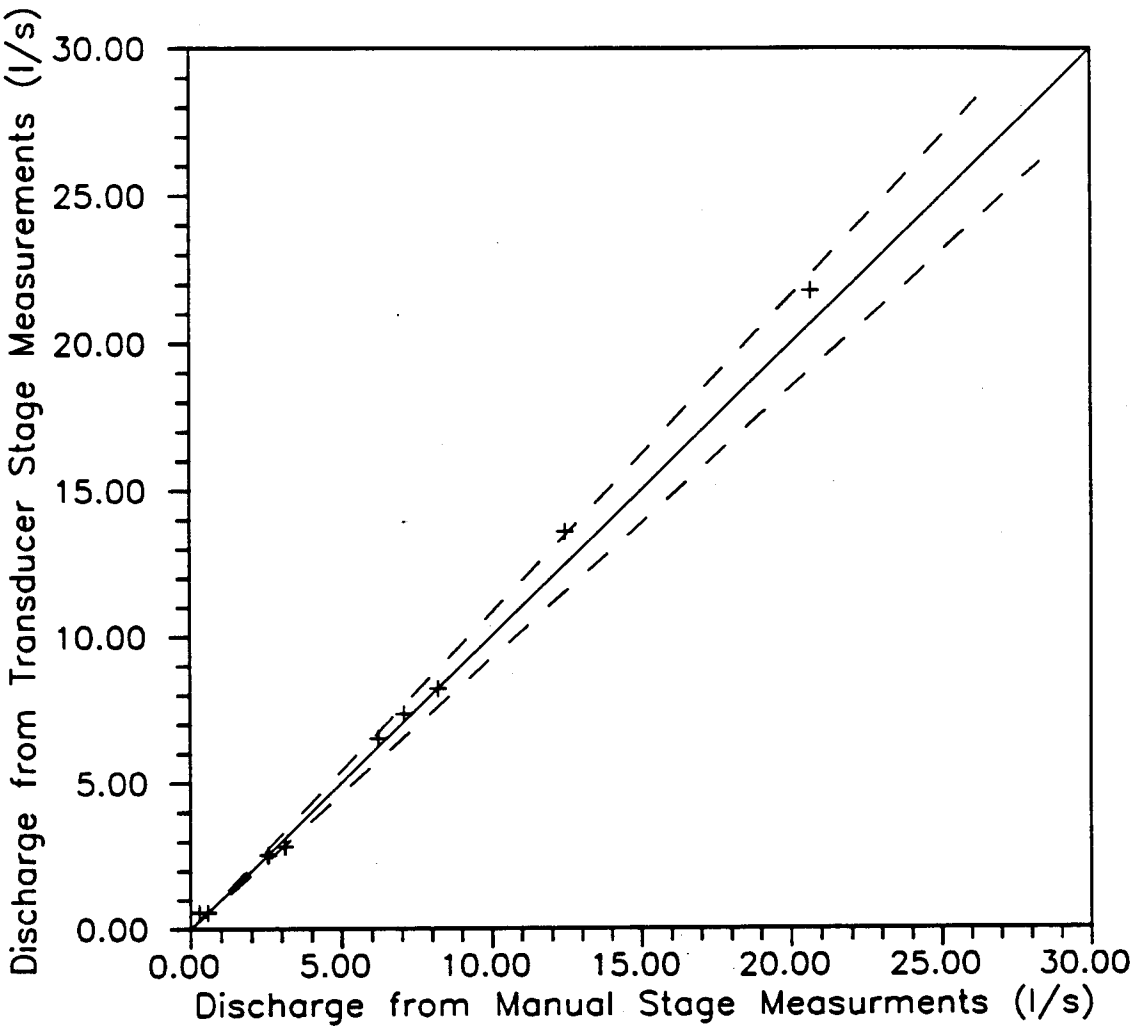

Fig. A-2. Discharge at the Novelty Hill site calculated from manual measurement of weir pool stage versus discharge computed from pressure transducer measurements of stage. Dashed lines correspond to an estimated stage measurement error of +/ − 6 mm.

resolution of the pressure transducer is 3.05 mm. For each manual measurement there is a potential transducer measurement error of $+/-$ 3 mm and an estimated manual measurement error of $+/-$ 3 mm. The dashed error lines in Figure A-2 were generated by propagating a combined transducer and manual measurement error in weir stage of $+/-$ 6 mm through (A-1). For discharge above 1 l/s all but one data point is within the estimated measurement error. The transducer estimated discharge is generally larger than discharge from manual measurements. The mean error is +0.28 l/s with a standard deviation of 0.57 l/s. There are no large or systematic errors. Most of the apparent error is most likely associated under estimation of discharge caused by water surface draw down at manual measurement point A.

Appendix B. Novelty Hill Piezometer Specifications and Water Level Measurement Error Analysis

B.1 Piezometer Specifications

Six piezometers were installed in the northeast corner of the basin (Figure 5-1, Piezometer Group P) on December 6 and 7, 1989. The piezometers are spaced along a 176 m transect extending from the ridge crest to the swale. The transect runs perpendicular to the ground surface contours, presumably coincident with a local flow line. A second set of four piezometers was installed in the southeastern portion of the catchment (Figure 5-1, Piezometer Group L) on November 13, 1990.

Each piezometer is made of 64 mm ($2\frac{1}{2}$-inch) diameter PVC pipe with the lower 0.3 m slotted. Borings 0.15 m in diameter were excavated to Vashon till using a post-hole digger. The top of the till layer was easily identified by morphology and a noticeable increase in resistance felt while digging. Pea gravel was placed around each PVC pipe to a height 0.15 m above the slots. A filter fabric collar was placed on top of the gravel pack and the hole was back-filled. About 90-percent of the excavated soil was used for back-fill, assuring greater compaction than the surrounding soil. Piezometer locations and elevations were determined by stadia surveying. This information along with soil characteristics are presented in Tables B-1 and B-2.

Piezometer No. 5 (P-5, Group P), located 155 m downslope from the ridge crest contains a Unidata capacitative sensor which records the local water table height in 3.05 mm increments at 15-minute intervals. The remaining

Table B-1 Characteristics of Novelty Hill Piezometer Group P

Parameter	Piezometer Number 1	2	3	4	5	6
Downslope Dist.* (m)	68	105	119	137	155	176
Elev. of Till (m)	180.23	178.37	177.46	176.15	175.53	175.02
Litter Thickness (mm)	50	60	60	75	150	100
Soil Thickness (m)	0.86	0.90	0.88	1.04	0.81	0.71

* Straight line distance from eastern catchment boundary (Figure 5-1)

TABLE B-2 Characteristics of Novelty Hill Piezometer Group L

Parameter	Piezometer Number 1	2	3	4
Downslope Dist.* (m)	165	178	73	61
Elev. of Till (m)	168.16	168.07	167.58	168.07
Litter Thickness (mm)	90	240	140	150
Soil Thickness (m)	0.74	0.61	0.76	0.84

* For piezometers L-1 and L-2 straight line distance from eastern catchment boundary; for piezometers L-3 and L-4 straight line distance from western boundary (Figure 5-1).

piezometers each contain a 12.5 mm diameter PVC crest gage to record peak water table heights between site inspections. The sensor has been operated continuously between December 7, 1989 and May 18, 1990.

B.2. Water Level Error Analysis

Saturated thickness at piezometer P-5 for 19 manual measurements is plotted against corresponding sensor recorded values in Figure B-1. The sensor values are generally lower than manual measurements, with a mean difference of -6 mm and a standard deviation of 12 mm. The estimated error of the hand measurements is 3 to 6 mm.

At each site visit the distance from the top of the piezometer to the water surface in the piezometer was measured. Saturated thickness was taken equal to the total piezometer length minus the distance to the water surface. The sensor rests at the bottom of the piezometer and measures saturated thickness directly (without reference to the piezometer length). The manual measurement values plotted in Figure B-1 were calculated using the original measured piezometer length of 1343 mm obtained December 19, 1989. A remeasure on January 21, 1990 showed a piezometer length of 1334 mm. It was assumed that the smaller measurement value in January resulted from sediment accumulation at the bottom of the piezometer. However, if the length of 1343 mm used in Figure B-1 were too large, manual estimates of saturated thickness are also too large. The difference in piezometer length measurements is similar to the mean difference of 6 mm between manual and sensor measurements of saturated thickness.

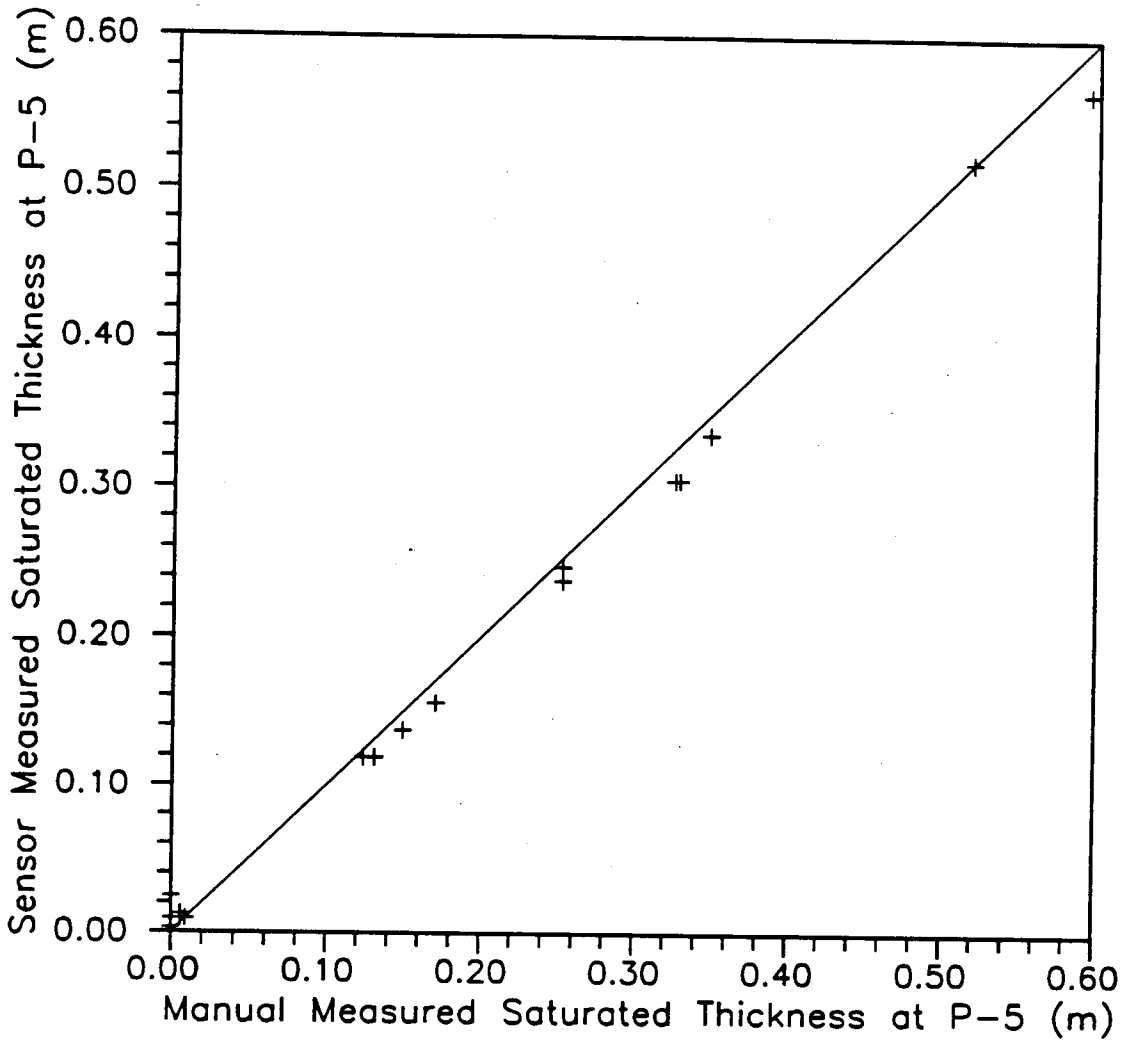

Fig. B-1. Manual measurements of saturated zone thickness at piezometer P-5 versus sensor recorded values. The estimated error in manual measurements is 3 - 6 mm.

Appendix C. Estimation of Potential Evapotranspiration

Potential evapotranspiration as it is represented in the model is assumed equal to the potential evaporation from a thin free water surface. Daily values of potential evapotranspiration were estimated using data from a "Rain Bird WS-100 weather station" operated by the City of Redmond, Washington. The station is operated by the City Parks Department to determine park artificial irrigation requirements. Daily values of total incoming solar radiation, percent relative humidity, average wind speed, rain fall, and maximum and minimum temperate were available from October 1, 1989 to the present.

Potential evapotranspiration was calculated using Penman's equation (1948)

$$E = \frac{\Delta}{\Delta + \gamma} Q_n + \frac{\gamma}{\Delta + \gamma} E_a \qquad \text{(C-1)}$$

where E is the potential evaporation from a thin free water surface, Δ is the slope of the curve relating saturation vapor pressure to temperature, γ is the psychometric constant, Q_n is the net radiation exchange, and E_a describes the contribution of mass-transfer to evaporation. The last term was calculated through the empirical relation (Dunne and Leopold, 1978)

$$E_a = (0.013 + 0.00016u_2)(e_{sa} - e_a) \qquad \text{(C-2)}$$

where E_a is in cm/day, u_2 is the wind speed (km/day) measured at a height of two meters from the ground, e_{sa} (mb) is the saturation vapor pressure of a

water surface at the air temperature, and e_a (mb) is the atmospheric vapor pressure. The City of Redmond anemometer is positioned three meters above the ground. Wind speed was corrected to an elevation of two meters (z_2) assuming a log profile

$$\frac{u_2}{u_3} = \frac{ln\left(z_2/z_o\right)}{ln\left(z_3/z_o\right)} \tag{C-3}$$

where u_3 is the wind speed at three meters (z_3) and z_o is the roughness length taken equal to 0.7cm (corresponding to the grass height below the weather station of about 3 cm).

Linsely et al. (1982) present an equation for the saturation vapor pressure

$$e_{sa} = 33.8639\left[(0.00738T_a + 0.8072)^8 - 0.000019|1.8T_a + 48| + 0.001316\right] \tag{C-4}$$

which is valid between -50 and $+55$ degrees Celsius, allowing atmospheric vapor pressure to be determined from relative humidity (H_r)

$$e_s = e_{sa}H_r \tag{C-5}$$

Average daily air temperature was calculated from daily maximum (T_{max}) and minimum (T_{min}) temperatures using the method of Running et al (1987) which assumes the diurnal temperature trace to be sinusoidal, i.e.

$$T_a = 0.606T_{max} + 0.394T_{min} \tag{C-6}$$

Linsley et al. (1982) present equations that allow $\frac{\Delta}{\Delta+\gamma}$ and $\frac{\gamma}{\Delta+\gamma}$ in (C-1) to be calculated from air temperature (T_a), and Q_n to be estimated from air temperature and daily solar radiation (Q_s):

$$\frac{\Delta}{\Delta+\gamma} = \left[1 + \frac{0.66}{(0.00815T_a + 0.8912)^7}\right]^{-1} \tag{C-7}$$

$$\frac{\gamma}{\Delta+\gamma} = 1 - \frac{\Delta}{\Delta+\gamma} \tag{C-8}$$

$$Q_n = 7.14 \text{ X } 10^{-3}Q_s + 5.26 \text{ X } 10^{-6}Q_s(T_a + 17.8)^{1.87} + 3.94 \text{ X } 10^{-6}Q_s^2 - 2.39 \text{ X } 10^{-9}Q_s^2(T_a - 7.2)^2 - 1.02 \tag{C-9}$$

Appendix D. Klahanie Weir Specifications

Streamflow at the outlet of the Klahanie catchment is measured at 15-minute intervals using a 151 degree sharp crested v-notch weir. The weir is keyed into Vashon till at a depth of about 0.2 m and has been sealed using Portland cement grout. As a result, nearly all surface and subsurface discharge exiting the catchment *above* the till layer pass through the weir.

The weir was calibrated using 8 flow measurements with discharges between 3.5 and 43 l/s (Figure D-1). Weir discharge in liters per second is calculated as:

$$Q = 7189H^{2.5} \qquad \text{(D-1)}$$

where H is the head on the weir in meters. (The coefficient of 7189 becomes 13.02 when H is measured in feet and Q is in cfs.) Water levels in the upstream weir pool are recorded in 3.05 mm (0.01 foot) increments at 15-minute intervals using an Unidata capacitative sensor. A water level crest gage is also attached to the weir.

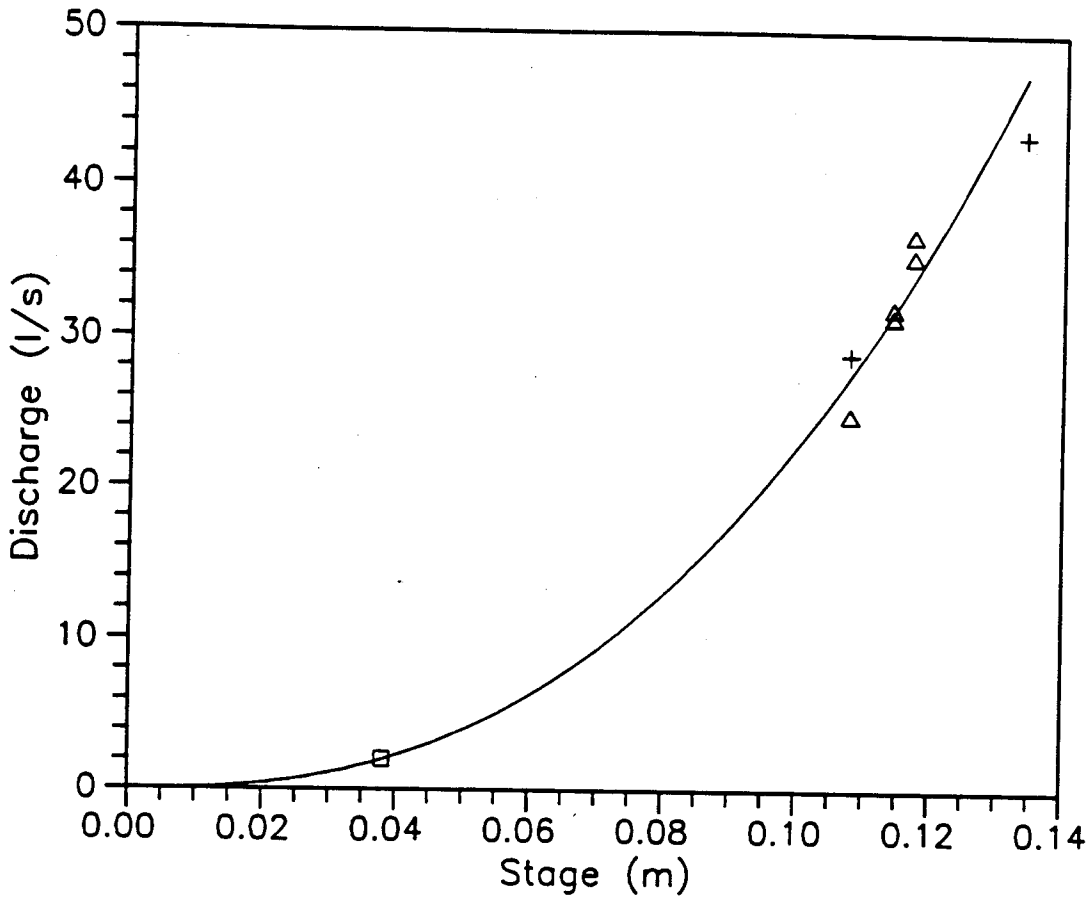

Fig. D-1. Weir pool stage versus discharge for the Klahanie v-notch weir. The square represents a volumetric discharge measurement, the triangles correspond to discharge estimated using a 90 degree v-notch insert in the lower rectangular weir, and crosses are from current meter measurements. The calibrated stage-discharge relationship is shown as the solid line.

Modeling and Monitoring to Predict Spatial and Temporal Hydrologic Characteristics in Small Catchments -- Part B: Extended Record Testing For Two Small Catchments

by

Stephen J. Burges

and

Jack M. Meena

TABLE OF CONTENTS

LIST OF FIGURES

LIST OF FIGURES (Continued)

Chapter 8. Consideration of Additional Catchments, Extended Testing -- Novelty Hill and Klahanie Sites, and Development of a Catchment Mapping Aid

8.1 Consideration of Additional Catchments

A second planned objective of the work was to apply the methodology developed in Part A to catchments in different hydro-climatic settings and to extended time series measurements taken in the Novelty Hill and Klahanie test catchments described in Chapters 5 and 6. We anticipated applying the approach to the 10.1 ha R-5 catchment near Chickasha, Oklahoma where precipitation and catchment flow data had been measured during the International Hydrological Decade. The climatological and hydrologic instruments at the catchment are no longer in operation, so we planned to use Professor Keith Loague, University of California, Berkeley (Loague, 1991) as an expert who would indicate the likely hydrological process zone activity that would have corresponded to the measured record that is available to the research community. Professor Loague has modeled this catchment (Loague and Freeze, 1985, Loague, 1990), and has taken extensive measurements of infiltration (Loague and Gander, 1990). He has observed catchment processes during a range of storm and antecedent catchment wetness states (Loague, 1992). No measurements of catchment outflow were made during his extensive field measurements of infiltration; the instrument station had been closed prior to his field work. In addition to this site we planned to use the data collected by Professor Tom Dunne, University of Washington, at the Sleepers River Site described in Dunne and Black (1970 a, b). Both Professors Loague and Dunne had agreed generously to provide us with their data sets. The former were in digital form, the latter were in field research books. While we were investigating these two data sets, we became aware of what had the

promise to be an exceptional data set for the small experimental catchment "Hydrohill" in China (Jakeman and Hornberger, 1993). Other data sets known to us or mentioned by colleagues to us for consideration were of the "event type" and proved unsuitable for the broad range of eco-hydrologic representation that is needed by our methodology (or any continuous simulation approach) to characterize pre- and post-development land form hydrology.

8.2 R-5 Catchment Chickasha, Oklahoma

The data for this catchment have been used by many investigators, and we based our original plans for using them on the many reports of their use in the literature. Given that we would be using data series that had been collected without the ancillary measurements and field observations of hydrologic processes that are integral parts of the methodology we have developed, we made extensive inquiries to obtain all possible information about the catchment and the data sets to be sure that we could extract the maximum possible information for this small pasture land catchment. It was while we were making these inquiries that we determined that several crucial pieces of information were unobtainable. Comments made about cattle grazing practices in the catchment by various observers indicate that the "grass was shoulder high before cattle were put there for grazing." After grazing, the grasses were short and typical of grazed land. (A photograph of part of the catchment during storm conditions which shows the short grass grazed state and flow production on land compacted by vehicles is given in Loague (1992, Figure 1).) There are no consistent and reliable records that indicate the state of vegetation as a function of time. This would pose a significant problem for any continuous simulation modeling. An additional problem came to light when we investigated the quality of the data

taken at the outlet weir from the catchment. We consulted Dr. David Goodrich, Agricultural Research Service, Tucson, Arizona (Goodrich, 1992) after we learned that he and colleagues had been checking on the quality of the measured records at the R-5 Catchment. He informed us that the careful review of the outlet weir measurement that he and colleagues had undertaken showed that the previously reported values were in error, and the values were not correctable because a second stage recorder would have been needed to characterize properly the weir flow regime. The errors would be largest for storms falling on a relatively dry catchment and of less importance for the largest flow events. Given all that is known now about this catchment, the data series that have been used appropriately in previous investigations are unsuitable for use with our methodology or any continuous simulation modeling approach. While all early inquiries supported inclusion of this catchment in our investigation, detailed examination of the records showed that the site was unusable, and we had to abandon any hope of including it in our work.

8.3 Sleepers River Catchment, Vermont (Dunne and Black, 1970 a, b)

The excellent measurements taken by Dunne and Black (1970 a, b) provided the basis for elucidation of dominant mechanisms of flow production at the hillslope scale and provided clear proof of both return flow and what is now know as the "Dunne Mechanism" of saturated overland flow. The data supporting these findings were obvious candidates for use with the methodology we have developed, and Professor Dunne would act as the supplier of descriptions of hydrologic process zones for the catchment. When we explored the data set more fully, it was clear that we would have to use the measured flow rates to back calculate the relevant hydraulic conductivities. This would rob us of the opportunity to test the approach because we

would have to use the same information twice and there could be no verification checks. This otherwise excellent data set proved unsuitable for either continuous simulation or verification of our modeling and measurement methodology.

8.4 Hydrohill Experimental Catchment, China

In early 1993 we became aware of the Hydrohill engineered experimental hydrology facility in China (Jakeman and Hornberger, 1993) and made inquiries of colleagues to determine if the data measured at this extremely small hillslope test facility would be suitable for testing our approach. Dr. Carol Kendall, U.S. Geological Survey, Menlo Park, California supplied us with the hydrologic data that she had been using with colleagues Dr. Jakeman and Hornberger to elucidate flow paths at the hillslope scale. While these data are extensive they were available for only a few events, and we had no basis for initializing model soil moisture states adequately preparatory to modeling event rainfall. This facility may prove to be of considerable value in future for the approach we have developed when continuous hydrologic time series and spatial flow production zone information are recorded for a sufficient period of time. At present, production zone information would have to be inferred from the tensiometer data that have been gathered. The instrumentation was developed for scientific hydro-geo-chemistry purposes; data gathering would need to be modified to make the information of wider utility.

8.5 Pasture Site near Kent, Washington State

We instrumented what appeared to be a gaugable pasture site near Kent Washington for a little over one year. Our intention was to obtain information about hydrologic process zones for pasture land that consisted of a relatively thin soil (about

1 m deep) that overlay dense till. We also sought to obtain time series of precipitation and inflow to and outflow from the small catchment. Because pasture land in the region is being converted to suburbs, it is desirable to obtain information about the typical pre-urbanization pasture land hydrology. We emphasized in Chapter 5 the need for and importance of catchment flux measurements for at least one year to be sure that the measurements provided sufficient information to effect the water balance for the catchment. This is particularly important in small catchments (on the order of ten to a few tens of hectares) because of the possibility that flow from the catchment might bypass the downslope measuring station. Despite our best efforts and those of experienced gauge installers, it was clear that after one year of measurements the site we had selected for measurement could not be monitored with the installed weirs without building an extremely expensive flow barrier at the downslope location to force all downslope catchment water movement through an engineered gauging station. Such work would have been unacceptable to the land owners who had agreed graciously to let us conduct our measurements on their property.

8.6 Novelty Hill and Klahanie Catchments, Washington State

In the remainder of this report we provide measurement and modeling results for the Novelty Hill and Klahanie Catchments. Models that use measured climatic data need to be operated for a wide range of climatic conditions to demonstrate their versatility. Even though a model may describe a wet season accurately, its performance under dry conditions becomes essential to the overall ability to simulate basin runoff. For this reason, the moisture accounting models for the developed and non-developed catchments presented in Chapters 5 and 6, respectively, are tested in Chapters 9 and 10, respectively, using more recent data which included two dry years.

This activity required the reconstruction of the potential evapotranspiration, precipitation, and runoff data files to include July 1, 1991, through June 30, 1993.

We were fortunate that for the entire measurement period the precipitation gauges were not damaged. Both weir sites were accessible to the public. The weir at Novelty Hill was next to a pathway used by recreationalists and could have been vandalized easily as it was not close to any residences. The two weirs at Klahanie were attractive to small children who appreciated the small ponds formed behind them. Fortunately, on the few occasions where the hydraulic properties were modified by the children at one of the weirs, the other could be used to estimate the outflow hydrograph. We were much less fortunate with the piezometers at Novelty Hill. For the work reported in Chapter 5, we had one continuous depth record augmented with field observations in the other piezometers. The upstream piezometers were fitted with automatic water depth recorders in early 1992. These were vandalized and we had to abandon them, so we have no data (apart from information that the damaged piezometer holes were dry on the occasions when we visited the site) for ancillary spatial catchment measurements. The piezometer data had been of greatest utility when determining the model hydraulic conductivity properties (Chapter 5). While they would have been of considerable benefit for checking model saturated depth predictions for the extended period, the lack of them is not critical to the work we report in Chapter 9.

8.7 Development of a Catchment Mapping Aid

Figures 5-1 and 6-1 show the major plan view features of the Novelty Hill and Klahanie Catchments, respectively. We needed to extract slope and area information from maps of this kind for use in the model applications. For both catchments, we

used base maps that had been prepared previously from relatively coarse-scale surveying information and added to them hydrologic process zones identified in the field. It would have been more convenient to have had the information in a Digital Elevation Model (DEM) form to facilitate determination of sub-areas and the average downslope for each of them. The catchment map information was not in digital form, and we determined from field inspections that the contours were approximately correct The contours were not sufficiently accurate to justify digitizing them to create a DEM. The Novelty Hill Catchment had been re-surveyed to provide accurate data for planning a suburban development during the period we had been taking hydrological measurements. We hoped to obtain the surveying data for possible use with an appropriate DEM algorithm to explore the possibility of extracting the key physical features (boundaries, slopes and the location of the main swale). (We obtained the surveying data too late in our project to be able to convert them to a rectangular DEM form for inclusion in this report.) While we were waiting for the raw data we examined all known DEM algorithms and determined that improvements were needed in them for application to the hydrology of catchments of the size of Novelty Hill and Klahanie. Consequently we developed an alternative DEM algorithm, DEMON (Costa-Cabral and Burges, 1994) which has the capability of extracting relevant landscape features for both small and large catchments. Its application at small scale requires use of fine scale surveying information with coordinate spacing much closer than the 30 m grids that have been reported in hydrological DEM applications in the relatively recent literature. A full description of the algorithm is given in Costa-Cabral and Burges (1994) and is not repeated here.

8.8 Summary Observations

Our experience in trying to use measurements that have been taken by observers at other sites emphasizes the importance for coupling measurement schemes to the objectives of the work. The measurements we have for the Novelty Hill and Klahanie Catchments represent the only sets of data at the scale of a few tens of hectares in Western Washington State that provide relevant hydrologic information essential for improved decision making in the context of evaluating alternative hydrologic schemes for mitigating hydrologic effects of urbanization and land use change in general. The measurements reported in Chapter 6 indicate that considerable insight into catchment dynamics in a small urbanized catchment can be obtained by careful examination of the measured catchment outflow in conjunction with measured precipitation and separating the outflow continuous hydrograph into the approximate components produced from the impervious surfaces and the inferred contribution from the pervious area. Many measurements have been made for larger catchments but it is not possible from those measurements to infer unambiguously the production sources of the integrated measured outflow hydrographs. Our work reported in Chapters 9 and 10 shows the utility of continuous measurement of hydrologic fluxes rather than attempting to use information from several storms to infer catchment behavior.

The support of homeowners in the Klahanie development and the landowner of the undeveloped Novelty Hill site as well as the excellent work by the stream gauging staff members from the Surface Water Management Division of King County made it possible to gather these useful data sets.

Chapter 9. Extended Testing -- Novelty Hill Catchment

9.1 Summary of Catchment Physical and Hydrological Features

The 37 ha Novelty Hill Catchment is located 6 km northeast of Redmond, Washington. The vegetation consists of a mature, thick, second growth forest with a well-established undergrowth. The main drainage feature is a central swale that runs approximately 800 m upstream from the outlet (Figure 5-1). The elongated catchment is approximately 1000 m long and has a maximum width of 366 m. The longitudinal slope is approximately 2.5%; lateral slopes to the swale are 3 to 5% in the upper catchment and 1 to 2% in the lower catchment. A bumpy forest litter and organic soil layer approximately 0.15 m thick overlay a sandy soil 0.6 to 1.0 m deep. The sandy soil is underlain by a dense glacial till (Vashon Till) which has a saturated areal averaged vertical hydraulic conductivity of between 0.15 and 0.3 m/year. Plant and tree roots extend to the till. A more detailed description of the site is given in Chapter 5. The catchment behaves hydrologically as if it is a sponge which soaks up rainfall and feeds evapotranspiration, swale flow, and till recharge.

9.2 Model Performance for Extended Data Series

The data used in Chapter 5 for developing and testing the model developed in Chapter 4 start on October 1, 1989 and end on June 30, 1991. We use extended recorded precipitation, runoff, and climate data time series to test the model and to examine aspects of catchment behavior for drier conditions than examined in Chapter 5. The extended series include water years 1991, 1992, and 1993 (through the end of June 1993). (The piezometers, used to determine the saturated depth of the soil column, were

vandalized in Autumn 1992, so those time series could not be extended for the present work.) The extended time series include several successive seasons of below average rainfall depth. The model output from these extended data series shows the model's performance for conditions that were not experienced in its development and calibration. The data used to calibrate the model were for water year 1990 and included measurements from piezometer P5 and the recorded weir outflow time series.

Figure 9-1 shows recorded daily precipitation depth, modeled ten-day average evapotranspiration, the recorded daily average streamflow rate, and the residual (recorded minus simulated) average daily flow rate. The horizontal scale is in days from October 1, 1989. It is evident in Figure 9-1 that the model does not simulate well the measured short duration, higher flow rates that follow dry periods. The most obvious examples of this process are the storms in February 1992 (days 845-858) and January 1993 (days 1176-1183). The differences between the simulated and recorded flow time series (the residuals) in these cases equal more than 75 percent of the recorded values. After a period of rainfall whose cumulative volume exceeds cumulative evapotranspiration, the soil moisture level increases and the model again provides an accurate simulation We have no independent check to know if the limitations in "dry soil" model response result from inaccurate estimates of potential evapotranspiration or if the soil water dynamics are not well represented for dryer soil conditions.

There were substantial storms in November 1989, January 1990, November 1990 (Thanksgiving storm), and April 1991. The automatic weir recording equipment was not operational up to and including the January 1990 storm. During that storm, weir pool depths were measured manually but are not shown in Figure 9-1. (Those measurements are shown in Chapter 5). The hydrograph of outflow in water year 1991 shows the

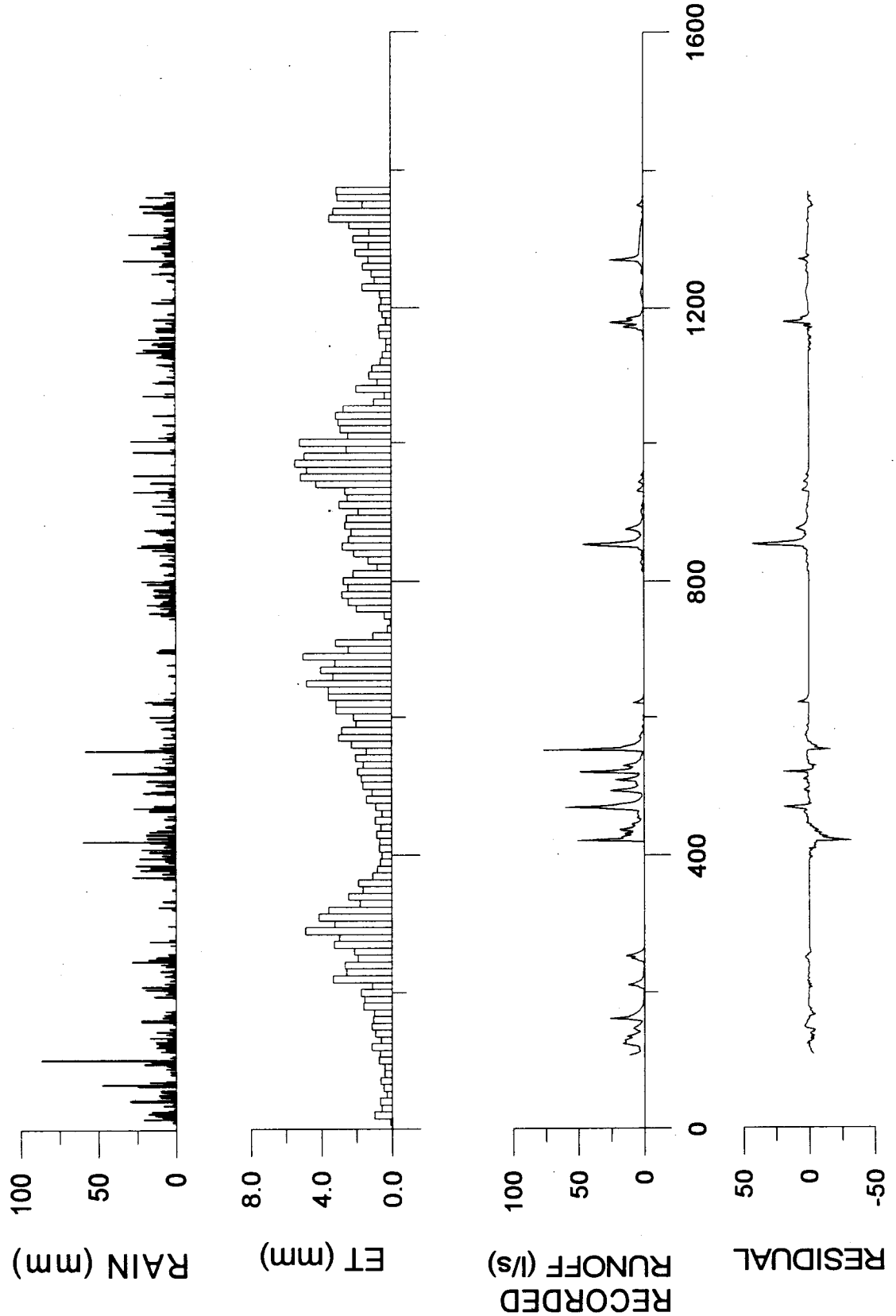

Figure 9-1 Novelty Hill Recorded Average Daily Flow Rate and Daily Precipitation Depth, Modeled Ten-Day Average Evapotranspiration Depth, and Recorded Minus Modeled Average Daily Flow Rate (Residual) from October 1, 1989.

catchment at its most responsive state for the four years of observation. Here the patterns of storm depth, duration, and time between storms show that the response is relatively rapid and relatively short lived. There are distinct recessions following storm induced peak hydrograph responses. The influence of antecedent catchment wetness is clear when the second largest response for this water year is considered. Relatively benign rain depth caused this response. Comparable rain depth falling in water year 1992 (between about days 825 and 850) with a noticeable time between storms produced almost no response. These observations which are based entirely on measured fluxes emphasize the need for continuous hydrological representation of a catchment of this type if the pre-urbanization hydrologic state is to be characterized adequately. To put the rainfall depths into perspective, the largest twenty-four hour depths for the January and November 1990 storms were in excess of the estimated 50-yr storm for the region. The April 1991 storm was of approximately the same magnitude. The measured responses emphasize the inappropriateness of an event type of model for attempting to characterize the hydrology of the catchment.

9.3 Approximate Seasonal Mass Balances

Wet and dry season measured precipitation and catchment outflow (runoff), and modeled evapotranspiration and recharge to the till (till leakage) are given in Figures 9-2 to 9-5 to show the major hydrologic fluxes. All quantities are expressed as average depth over the catchment. The wet season was chosen arbitrarily as November 1 to April 30; 65 to 70 percent of annual precipitation falls during this period. The dry season was from May 1 to October 31. If initial and ending season modeled soil and interception water storages were included in Figures 9-2 to 9-5, they would contain all information

for complete mass balance to be effected at annual time increments. The four quantities presented show the relative distributions by wet and dry seasons of the inputs to and outputs from the catchment. Some of the water stored in the soil and swale during the wet season evaporates and recharges the till while some of the water added to the soil column during the wet season also recharges the till during the dry season. The net addition to soil water storage during the wet season results in modeled evapotranspiration greater than precipitation during the following dry season. The catchment is approximately at the same (relatively dry) moisture state at the start and end of each year. The differences in moisture state (the change in modeled moisture zone storage) are small (less than 2 percent of the annual precipitation in all years) and are not shown in Figures 9-2 to 9-5.

Flow production from the catchment occurs after some soil water threshold volume is reached. All rainfall apart from that which falls directly on the saturated swale area and that which is intercepted by the vegetation enters the forest litter. When the soil column is relatively dry, flow to the swale occurs only after a series of storms deliver sufficient rain to feed the soil column to some level beyond field capacity. Soon thereafter flow is observable at the catchment outlet where it is measured. Rainfall depth and time between storms are important to flow response. The pattern of rain delivery is more important here than for a shallower soil as is the case in the Klahanie Catchment.

With reduced precipitation in dry years, the fraction of rainfall that becomes catchment outflow is small. During the water years of relatively normal precipitation, 1990 and 1991, approximately 40 percent of the precipitation delivered during the wet season became runoff. In contrast, during the dry water year of 1992, most of the precipitation that reached the litter layer was stored in the soil column. This water left

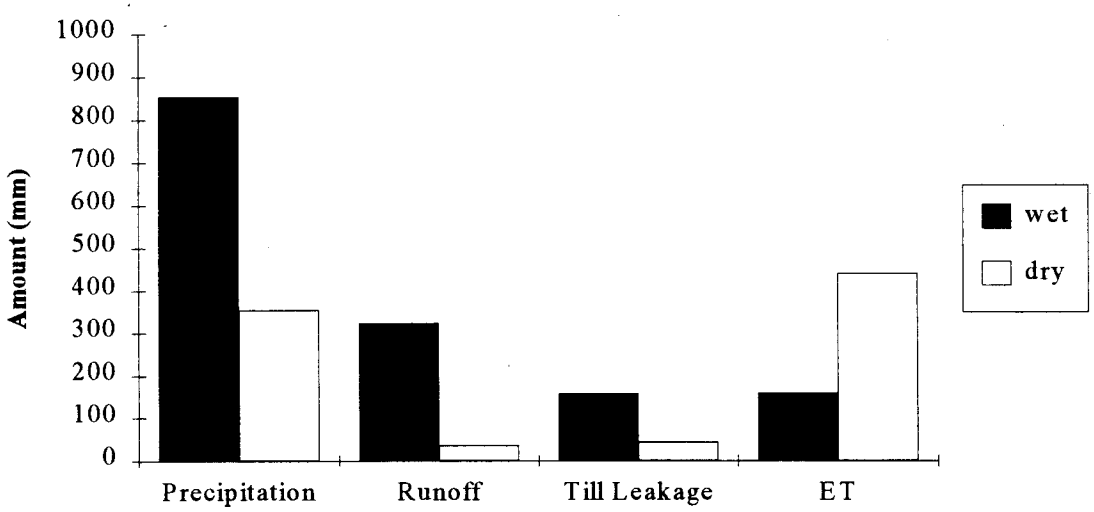

Figure 9-2 Wet and Dry Season Novelty Hill Measured Precipitation and Runoff, and Calculated Till Leakage and Evapotranspiration for Water Year 1990.

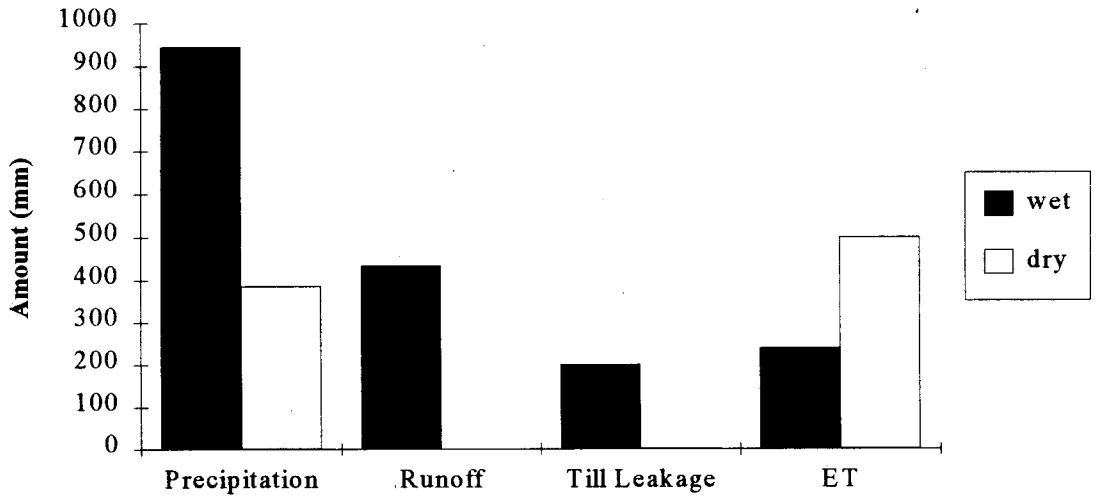

Figure 9-3 Wet and Dry Season Novelty Hill Measured Precipitation and Runoff, and Calculated Till Leakage and Evapotranspiration for Water Year 1991.

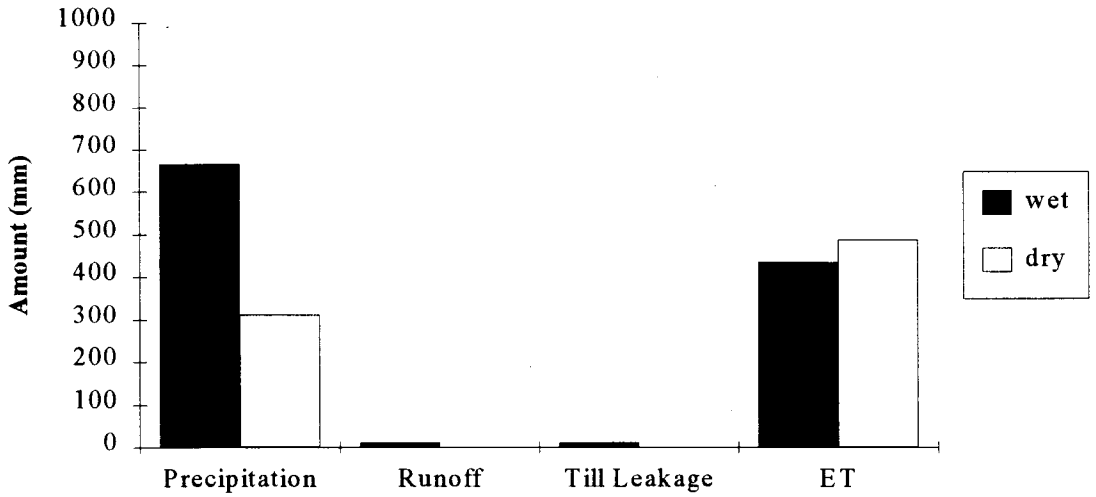

Figure 9-4 Wet and Dry Season Novelty Hill Measured Precipitation and Runoff, and Calculated Till Leakage and Evapotranspiration for Water Year 1992.

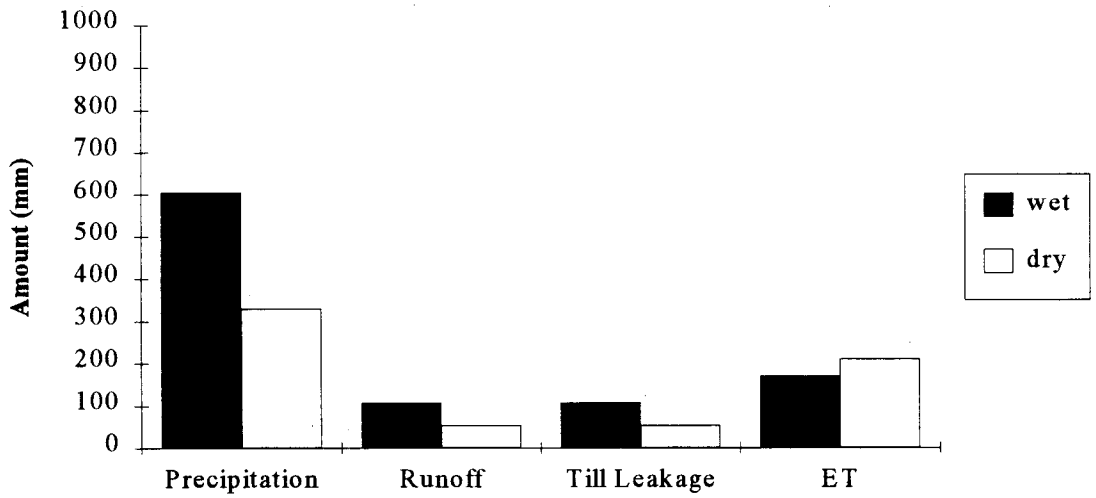

Figure 9-5 Wet and Dry Season Novelty Hill Measured Precipitation and Runoff, and Calculated Till Leakage and Evapotranspiration for Water Year 1993 through June 30, 1993.

the basin primarily in the form of evapotranspiration; estimated till leakage and measured runoff were negligible. The timing of the rainfall in water year 1993 differed from 1992 although the annual totals were similar. In water year 1993, the measured runoff and modeled till leakage were approximately equal in both the wet and dry seasons. The summation of the runoff and till leakage was slightly less than the modeled evapotranspiration depth.

The modeled amount of water lost to till leakage decreases when periods of below average precipitation occur. For these conditions, the water stored in the soil column is less than the field capacity of the soil for much of the year and is not available to infiltrate into the till. Whenever the soil water content is above field capacity, vertical gravity drainage delivers water to the soil-till interface and provides till recharge supply.

9.4 Summary

The Novelty Hill drainage basin acts in two distinctive fashions depending on the timing of storms and the amount of rain the basin receives. In a wet year where there are distinct periods when a significant depth of the soil column becomes saturated, more than a third of the precipitation leaves the area as runoff. During a dry year when the timing of storms is such that only a small depth of the soil column saturates and does so infrequently, the majority of the water leaves as evapotranspiration. In either type of year, however, there is a cumulative threshold amount of precipitation, minus evapotranspiration and additions to soil moisture storage, that must occur before flow to the swale is produced.

Chapter 10. Extended testing -- Klahanie Catchment

10.1 Summary of Catchment Physical and Hydrological Features

The 16.7 ha Klahanie sub-basin is located near Issaquah, Washington and is approximately 21 km east of Seattle. The catchment contains both impermeable (roofs, roadways, and walkways) and permeable surfaces. There are 4.8 ha of impervious surfaces and 11.9 ha of pervious surfaces. The post-developed soil thickness for the pervious areas averages 0.12 m on top of a layer of Vashon till. A 480 m long engineered swale provides drainage for the basin. A detailed description of the site and hydrological instrumentation is given in Chapter 6.

10.2 Model Performance for Extended Data Series

The data used in Chapter 6 to calibrate the model and make preliminary assessments of the hydrological characteristics of the Klahanie sub-basin included the period November 21, 1990 to May 15, 1991. This was a wetter year than normal. The following two years were noticeably drier. The expanded data series examined here extends the recorded precipitation, runoff, and climate data series to include water years 1991, 1992, and 1993 (through the end of June 1993). Seven of the ten largest 1-day storm depths for this extended record occurred during the period November 1990 to May 1991. The expanded data set permits testing the model for dry years as well as the calibration year of above average rainfall. The range of storm patterns included in the extended data set makes it possible to explore the effectiveness of the calibrated model for a wider range of hydrologic conditions than modeled during calibration.

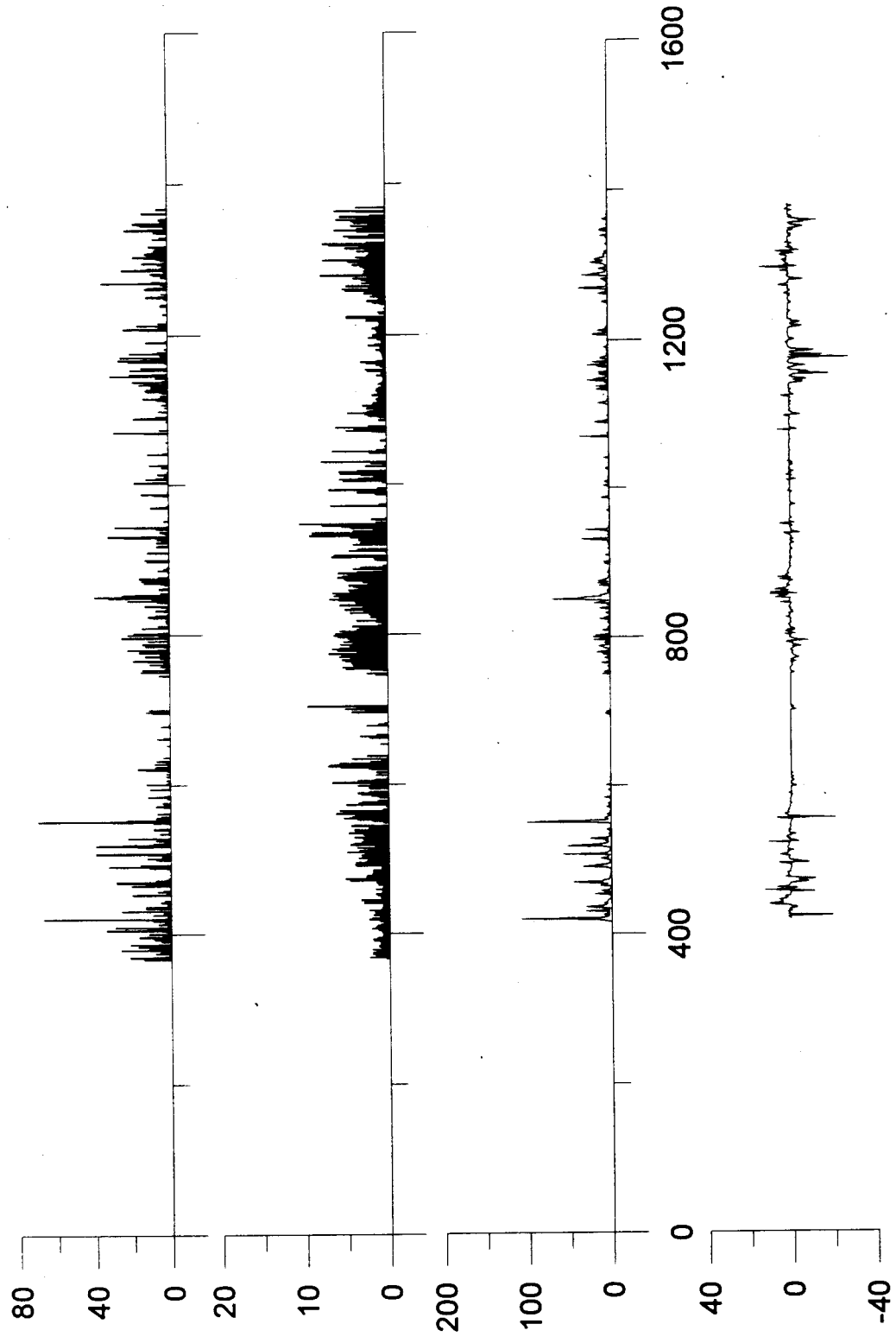

Figure 10-1 Klahanie Recorded Average Daily Flow Rate, and Daily Precipitation Depth, Modeled Two-Day Average Evapotranspiration Depth, and Recorded Minus Modeled Average Daily Flow Rate (Residual) from October 1, 1989.

Figure 10-1 contains information for Klahanie similar to that shown in Figure 9-1 for Novelty Hill. The modeled evapotranspiration is shown as the average value for a two-day period. Figure 10-1 shows that the model simulates catchment flow production equally well for both wet and dry years. The model over simulates flow response to rain falling on the pervious portion of the catchment when the catchment is relatively dry. We comment further about this in Section 10.4. The small soil water storage capacity of the permeable parts of the basin requires much less precipitation to saturate the soil than is the case at Novelty Hill with its deeper soil. Errors in estimating the amount and vertical distribution of soil moisture and evapotranspiration fluxes at Klahanie have much less influence on modeled outflow than for the deeper Novelty Hill soil.

10.3 Approximate Seasonal Mass Balances

The extension of the data to include the additional two years of information allows the Klahanie runoff model to be evaluated in times of drought. This model does not account for any artificial irrigation. Supplemental lawn and garden irrigation water is supplied typically between late April and early October which corresponds to our arbitrarily chosen "dry season". Lawn watering restrictions were in force from May to September 1992 during a regional drought; little if any supplemental irrigation was applied during this period. We do not have any records or ways to estimate the amount of artificial supplemental irrigation, but believe that the hydrologic effects of any supplied irrigation would have been small in the other two years. Wet and dry season measured precipitation and catchment outflow (runoff), and modeled evapotranspiration and till leakage are shown in Figures 10-2 to 10-4. The wet season was defined

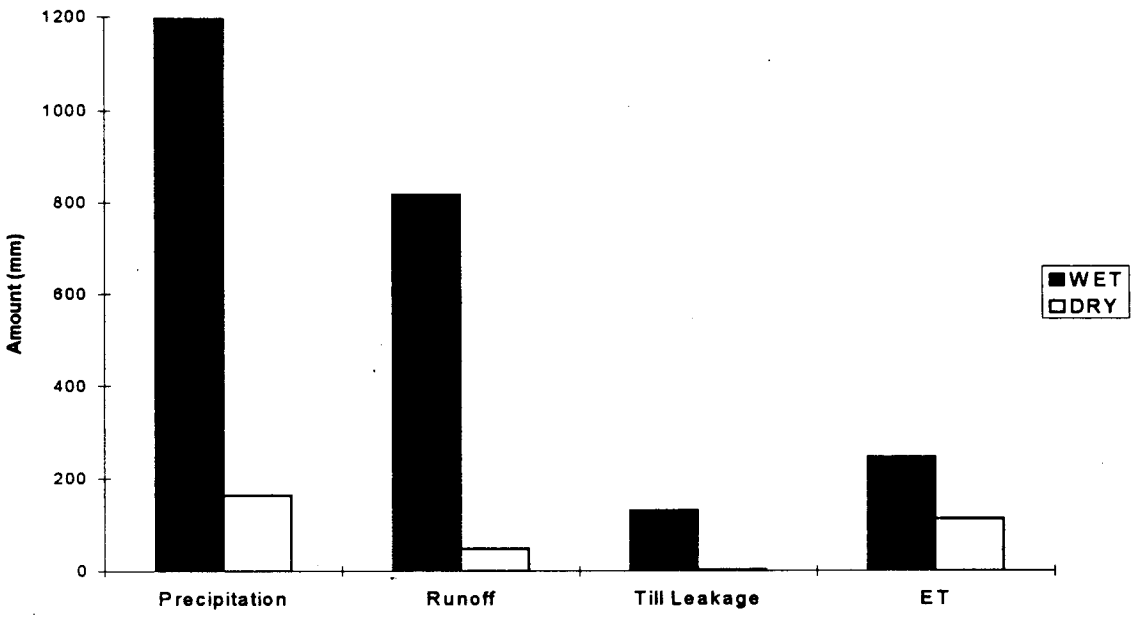

Figure 10-2 Wet and Dry Season Klahanie Measured Precipitation and Runoff, and Calculated Till Leakage and Evapotranspiration for Water Year 1991.

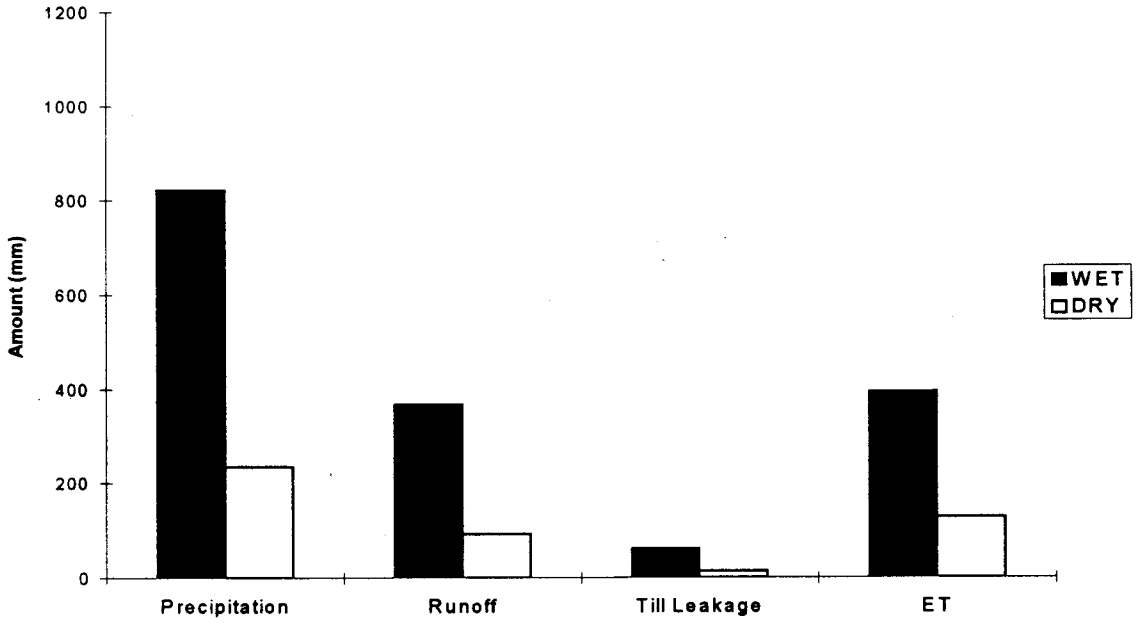

Figure 10-3 Wet and Dry Season Klahanie Measured Precipitation and Runoff, and Calculated Till Leakage and Evapotranspiration for Water Year 1992.

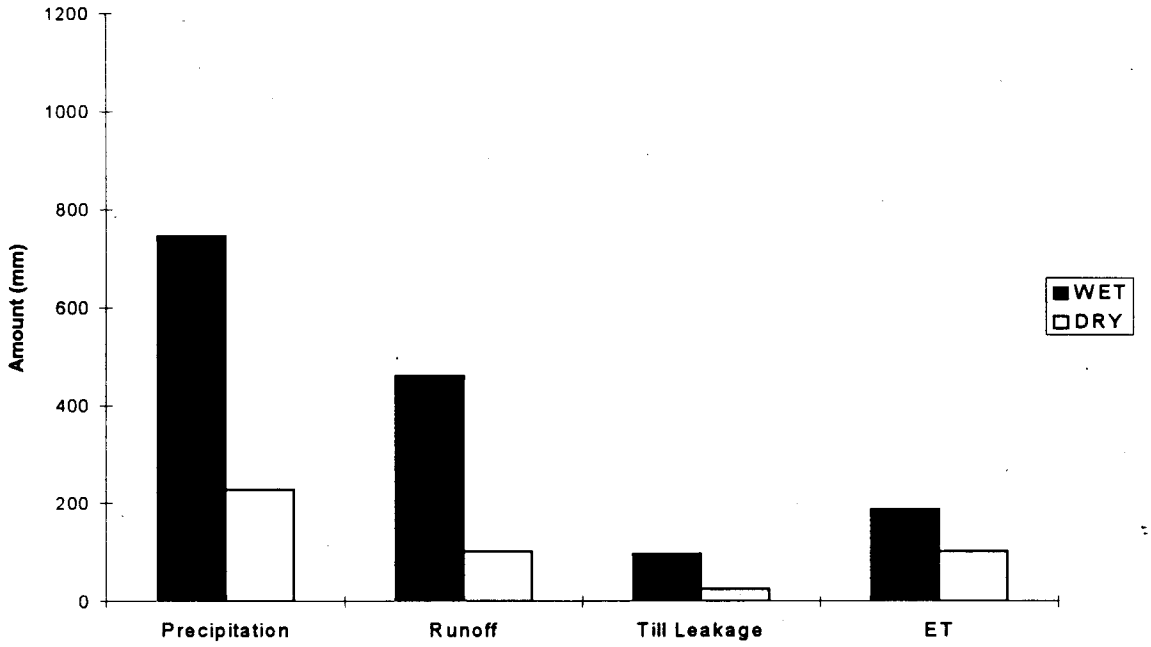

Figure 10-4 Wet and Dry Season Klahanie Measured Precipitation and Runoff, and Calculated Till Leakage and Evapotranspiration for Water Year 1993 through June 30, 1993.

arbitrarily, as it was in Chapter 9, from November 1 to April 30 and accounts for the bulk of rain fall. The dry season is from May 1 to October 31. All quantities are expressed as average depth over the catchment and include runoff and evapotranspiration for both pervious and impervious areas.

There was no modeled till recharge under the impervious surfaces. All modeled till recharge occurred beneath pervious areas, and the catchment till recharge is the amount for the pervious areas expressed as a depth over the 16.7 ha basin. (The reported till leakage depth is the actual leakage from the pervious area multiplied by 11.9/16.7.)

The pervious area moisture storage zones are small relative to the rainfall depth. Figures 10-2 to 10-4 show the dominant components of the catchment mass balance. With the low soil water storage capacity of the relatively thin soils the difference between

the starting and ending soil water storage for each year is nearly zero and is not shown in these figures.

There is appreciable runoff in all three water years in contrast to the reduced runoff production at Novelty Hill in the two dry water years 1992 and 1993. The runoff shown in Figures 10-2 to 10-4 consists of both pervious and impervious area flow. A breakdown of the two components is shown in Figure 10-5 where it is clear that runoff produced from the pervious areas comprises at least 39 percent (1993) and as much as 60 percent (1991) of total runoff.

The small water storage capacity of the thin soil explains this response at Klahanie. The small storage drains relatively quickly and residual soil moisture is depleted faster by evapotranspiration than is the case with a deeper soil. The small soil moisture storage also affects till leakage. Since the shorter soil column dries more frequently than at Novelty, the semi-permeable boundary of the till is saturated less frequently and experiences reduced inflow.

10.4 Flow Production From Impervious and Pervious Areas

Figure 10-5 gives the division by water year of the areally averaged depth of runoff produced on impervious and pervious areas, total catchment runoff, and catchment precipitation. The simple method used to partition runoff into pervious and impervious components was based on the assumption that when flow is recorded at the gauge the impervious areas produce a runoff depth less than or equal to the measured runoff. When the measured daily runoff volume exceeds the daily precipitation depth multiplied by the impervious surface area, the difference is assumed to be the flow volume generated from the pervious area.

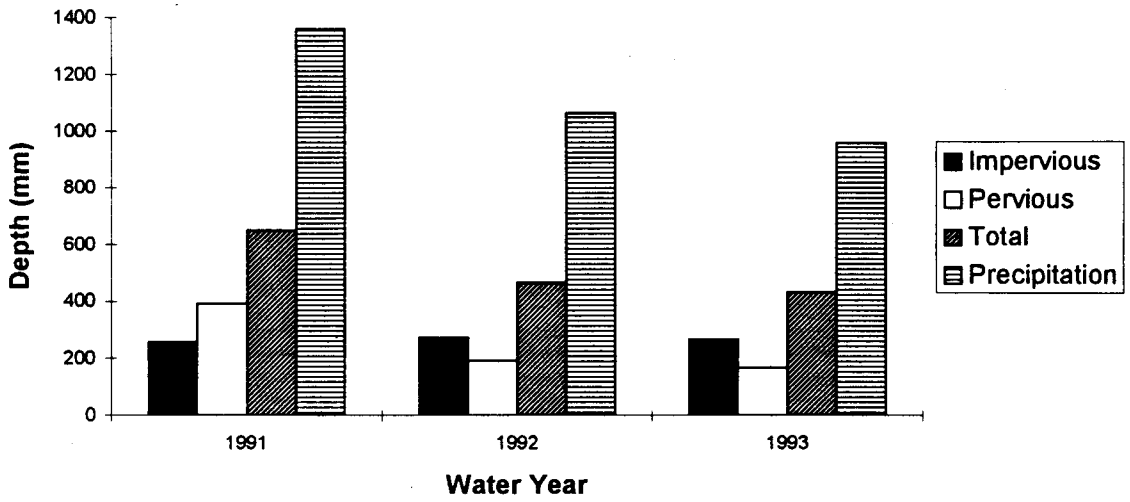

Figure 10-5 Klahanie Calculated Impervious, Pervious, and Measured Total Surface Runoff Depths, and Measured Precipitation Depths for Water Years 1991, 1992, and 1993 through June 30, 1993.

Figure 10-6 shows daily average precipitation depth and daily average estimated impervious and pervious area runoff production rates. The runoff rates were estimated using the measured rainfall depth and channel flow rate and indicate how much can be gained in understanding hydrologic response of small urban catchments by simple analysis of measured fluxes. The estimated impervious area runoff response is slightly larger than actual because no explicit account was taken in this simple analysis of the effects of depression storage and evaporation from impervious surfaces on the resulting runoff. Whenever there was no measured basin outflow and rain was recorded we set impervious surface runoff to zero. It is unlikely that we have overestimated impervious surface runoff contributions for light rainfall falling on a dry surface. For heavier rain falling on an initially wet surface, the estimation scheme is close to the actual response.

Figure 10-7 shows modeled impervious and pervious area average daily runoff production rates. The calibrated model (Chapter 6) takes into account depression storage

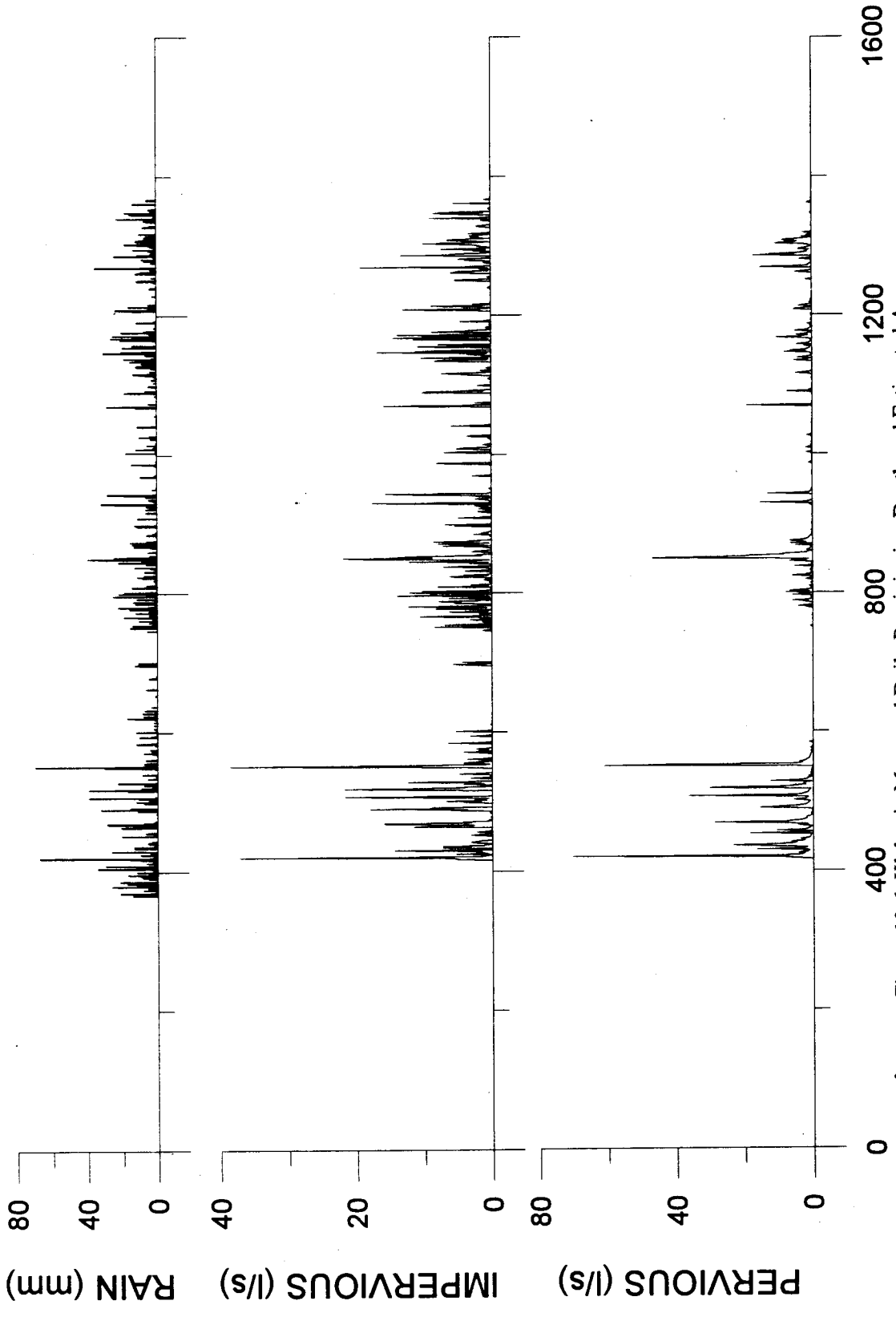

Figure 10-6 Klahanie Measured Daily Precipitation Depth and Estimated Average Daily Flow Rate Produced from Impervious and Pervious Land.

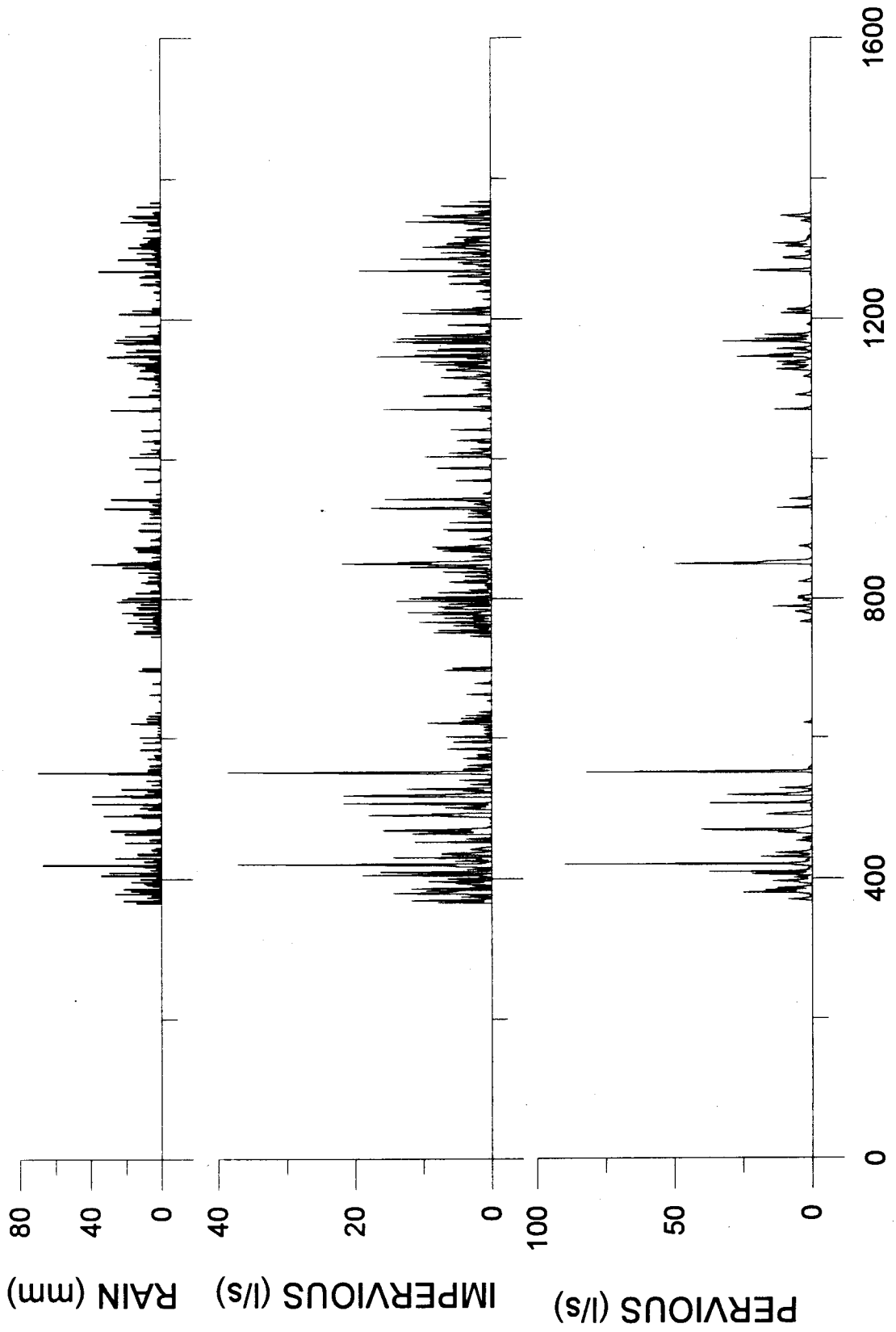

Figure 10-7 Klahanie Measured Daily Precipitation Depth and Simulated Average Daily Flow Rate Produced from Impervious and Pervious Land.

and evaporation from all surfaces. Comparison of impervious area flow production time series in Figures 10-6 and 10-7 shows that the simple flow component separation scheme in Figure 10-6 captures the impervious area response well in all but a few cases. Figures 10-6 and 10-7 show that the model appears to underestimate flow response from pervious areas when rain falls after a relatively dry period. However, after some initial precipitation, the model simulations are good.

Figure 10-6 was created using time series of measured precipitation and measured streamflow. The latter was determined by converting measured water depth to flow rate through a 151 degree "V" notch weir that had been calibrated for a flow rate of approximately 30 l/sec. During the first year (days 366 to 730) the catchment was visited on most occasions when substantial precipitation was anticipated. On those occasions the two weirs (shown at the catchment outlet in Figure 6-1) were free flowing. During several visits in the early autumn and in late spring and summer (when flow rates were low), we noticed that children from the neighborhood had placed rocks a short distance upstream from the "V" notch weir to cause a small shallow pool to form. We removed these obstructions and expect that the recorded flow rates represent reality for almost all of the first year.

Our only opportunities for calibrating the "V" notch weir were for flow rates close to 30 l/sec. For this flow rate the weir equation that was used agreed to within 3.7% of the flow rate determined with a pigmy current meter at a section approximately 15 m upstream of the gauge. Since the maximum average daily flow rate did not exceed 100 l/sec on more than two occasions during the three years of measurement, we believe that the volumetric flow analyses are reliable.

We checked the three highest recorded flow rates for physical plausibility. This was done at the daily average scale by assuming the entire catchment to be saturated and that 100% of measured precipitation could become streamflow. If the recorded average daily streamflow rate exceeded this magnitude, there would be cause to question the measured quantity. Small differences could be accounted for by release of stored water from the shallow soil column. The three hydrograph peaks are apparent in Figure 10-1 and occurred on days 420 (November 24, 1990; 107.7 l/sec), 551 (April 4, 1991; 99.7 l/sec), and 850 (January 28, 1992; 68.6 l/sec). The first two were plausible and consistent with regional rainfall patterns and regional hydrologic responses. We know that the weir equipment functioned properly and that there were no obstructions in the channel upstream of the weirs that would affect the flow rates for those time periods. The January 28, 1992 hydrograph is also plausible. The daily precipitation depths at Seattle Tacoma International airport for the period January 23 to January 31 were consistent with those recorded at Klahanie. The recorded average daily flow rate was less than the maximum estimated rate, assuming that 100% of the measured precipitation became channel flow. Close examination of the pervious flow components in Figure 10-6 ("measured") and in Figure 10-7 (modeled) further supports our observations that the recorded flow pattern is likely to be correct. One possible anomalous pattern in Figures 10-6 and 10-7 occurs on September 4, 1992. This was the Friday before Labor Day weekend, and we think but do not know for sure that the local children impounded water behind the weir. Our modeled hydrographs for the pervious area for September 1992 are consistent with the measured total flow rate. While the measured September 4, 1992 flow rate is greater than the modeled rate, it does not suggest an artificially enhanced water level upstream of the weir. When the gauge was visited afterwards, there was no evidence that water had been

impounded upstream. We did not visit the site regularly during the summer months after the first year because we noted in the first year that there was little to no flow for most of the summer and early autumn.

We have included this discussion to emphasize the difficulty of obtaining reliable hydrograph time series in urban catchments, even in communities where there is strong support for environmental measurements. We also emphasize the value of simple checking schemes and the use of a calibrated model to help check the fidelity of hydrographs estimated from continuous water stage records.

10.5 Summary

The value of concurrent precipitation and catchment outflow measurements for describing the hydrological response of a small urbanized catchment where channel influences have negligible effects on the outflow hydrograph is clear from the analysis presented in Figures 10-5 and Figure 10-6. Much can be learned about the apportionment of volumetric and peak flow production rates from pervious and impervious surfaces by relatively simple analysis of the measured time series of precipitation and basin outflow. Such analyses depend on the quality of the measured time series. We have indicated that some of the apparently large recorded flow rates in years two and three are likely to be artifacts of gauging errors. Despite these limitations, considerable insights into catchment hydrologic behavior can be gained by direct analysis of the time series and from use of a calibrated model which uses measured precipitation and estimated potential evaporation as inputs.

The relatively thin soil column of the pervious zone was modeled well for storm patterns that differed substantially from those that occurred in the record that was used to

calibrate the model. Any inability of the model to represent soil moisture profiles and evapotranspiration precisely had only slight effects on model predictions of basin runoff production.

Chapter 11. Summary and Conclusions

11.1 Summary

This work is an outgrowth of work started at the University of Washington two decades ago. It builds on the early work of Hardt and Burges (1976) and Kemp and Burges (1978) and on the work from almost a decade ago where we started to incorporate field mappable spatial hydrologic zones directly into schemes for quantitative hydrologic descriptions of catchments before and after land-use change. That work, reported by Burges, et al. (1989) and Wigmosta and Burges (1990), was supported by the US Geological Survey and the Surface Water Management Division of King County, Washington, Department of Public Works. The present work includes both process zone descriptions and mapping as well as measurements and model representations of relevant hydrologic fluxes for two small, first-order, Pacific Northwest catchments. The larger of the two (37 ha), "Novelty Hill" catchment, is representative of many forested catchments in the region. The smaller (16.7 ha), "Klahanie" catchment, is representative of a modern urban housing development in the region.

We make comparisons between these two catchments to show the types of changes to hydrologic regimes that may result from urbanization. Our findings should provide guidance to those concerned with mitigating the possible deleterious hydrological consequences of land-use change as land is converted from a relatively natural state to an urban environment. Before making comparisons we summarize the physical differences between the catchments that influence their respective hydrologies.

11.1.1 Catchment Physical Differences - Novelty Hill and Klahanie

The most noticeable differences between the Novelty Hill and Klahanie catchments are the land surface slopes, the impermeable surfaces that cover approximately 30 percent of the Klahanie basin, and the forms of the permeable surfaces. The Novelty Hill catchment has a steady longitudinal slope of about 2.5% and lateral slopes from 3 to 5% in the upper catchment and 2% in the lower catchment. The lateral land slopes at Klahanie ranged from 5 to 17%. The permeable surfaces at Klahanie consist mostly of lawns, unlike Novelty Hill, which consists of second growth forest throughout all of the basin except the drainage swale. The other major difference between the basins is the soil column depth and form. The soil column at Novelty Hill consists of approximately 0.8 to 1.0 meter of organic and mineral soil. The soil column at Klahanie consists of about one-tenth of a meter of mineral soil. The ground surface at Novelty Hill is extremely uneven, while the shallow-rooted lawn areas of Klahanie are much smoother. The surface soils in both catchments are underlain by glacial till that restricts water movement vertically.

11.1.2 Flow Characteristics

The precipitation patterns for both catchments are almost the same in timing and amount of rain. With the approximately 30% of area covered with impermeable surfaces and the shallow soil column, the Klahanie catchment produces higher flow rates per unit area than the Novelty Hill catchment. Novelty Hill, however, provides a sustained base flow that lasts much longer than the recession flows at Klahanie. One measure of the dramatic difference in flow response for the two catchments was observed for the large storm of November 23-26, 1990. This storm gave rise to a recorded peak runoff of nearly 19.8 l/sec/ha at Klahanie and only 1.6 l/sec/ha at Novelty Hill. The hourly (Novelty) and

thirty minute (Klahanie) recorded (and simulated) hydrographs and precipitation patterns for this storm are given in Figure 5-17 and Figure 6-4, for Novelty Hill and Klahanie, respectively. The peak high flow rate at Klahanie is consistent with the high intensity rainfall and the antecedent catchment state of soil moisture. Figure 6-4 shows a rapid return to near zero flow at Klahanie within a day after the cessation of rain. Figure 5-17 shows a much more sustained flow rate at Novelty Hill for many days after the rain stopped. These different responses are due in large part to the respective soil depths. Novelty Hill stores a large portion of all precipitation in the soil column and drains only as fast as the soil allows the water to flow laterally to the receiving swale. Since the soil column is shallow, it requires only a few moderate storms to saturate it. Once the soil is saturated, the surface flow response to the next increment of precipitation is relatively fast. After rain stops there is little stored water in the soil to sustain dry weather flow.

The dramatic difference in response at the two catchments to what was an approximately "fifty-year 24-hr" rainfall volume has significant implications for those concerned with mitigating the hydrologic effects of urbanization. To our knowledge, these are the only gauged catchments at this small scale that provide regional information about the magnitudes of flood response to the smallest receiving channels. We have no way of assigning recurrence frequency to these flood hydrographs: a "fifty-year" rainfall does not give rise to a "fifty-year" flood hydrograph except under restricted circumstances that are not satisfied in natural or engineered catchments. What is important is the magnitude and duration of the flow rates that the channels that are fed by these two land areas experience. The urbanized catchment delivered a flow rate almost twelve times larger than that delivered by the natural catchment to its receiving channel. The potential deleterious effects of an order of magnitude increase in channel flow rate from the pre-

development to the post-development land use state on stream habit and stream ecology are significant. It is imperative that when urban landscapes are created, full attention is given to the complete hydrologic response of the catchment in its pre- and post-development states. The only way that this can be done is by considering the mechanisms by which flow is produced in the catchment as we have described in this report. Indicators of deleterious consequences that may result from land-use change are provided by Burges, et al. (1989) and elsewhere.

11.1.3 Evapotranspiration

The shallow soil column at Klahanie affects more than the outflow from the catchment. The modeled evapotranspiration at Klahanie is less than for the natural condition at Novelty Hill. There is more water stored in the soil column for longer periods at Novelty Hill than at Klahanie and consequently greater evapotranspiration opportunity at Novelty Hill. These differences are illustrated in Figures 9-2 to 9-5 for Novelty Hill and Figures 10-2 to 10-4 for Klahanie. These figures show that for the four-year period, the amount of annual precipitation that becomes (modeled) evapotranspiration at Novelty Hill ranges between 50 and almost 100 percent. The latter condition occurred for the relatively dry 1992 water year. At Klahanie the amount of precipitation that becomes (modeled) evapotranspiration ranges from 26.5 to 50%.

The relative distributions of evapotranspiration also differ between the two catchments. For Klahanie, Figures 10-2 to 10-4 show that the dry season evapotranspiration depth is less than the dry season rainfall depth in each year. This is another consequence of the change from natural to shallower soil urban conditions. For Novelty Hill, the same analysis is given in Figures 9-2 to 9-5. In three of the four years

the modeled dry season evapotranspiration depth exceeded the dry season precipitation depth. These differences in catchment scale evapotranspiration contribute to different meso-scale climatologies for the two different vegetation regimes.

11.1.4 Regional Ground Water Recharge

The water flows to the strata beneath the catchments after passing through a relatively impermeable (but fractured) dense layer of Vashon till. The till can transmit water, as long as the upper surface of the till is supplied with water constantly, at a rate equivalent to approximately a depth of water ranging from 150 mm to 300 mm per year. This water supplies the ground water recharge for plateau regions in King County. Any reduction in the supply to the till layer will reduce the recharge to the regional ground water. This is an issue that must not be overlooked. The recharge to the till layer at Klahanie (Figures 10-2 to 10-4) is less than for the Novelty Hill site (Figures 9-2 to 9-5) except in water year 1992 when modeled till leakage was negligible at Novelty Hill and modeled evapotranspiration dominated the vertical movement of water.

11.1.5 Flow Production From Pervious and Impervious Areas -- Klahanie

Figure 10-5 provides a summary by water years of the contributions of the impervious and pervious land segments to annual flow volume production. The volume is expressed as an equivalent depth of water distributed uniformly over the plan area of the entire catchment. Impervious surfaces that are connected hydraulically to the receiving channel account for almost 30% of the catchment area. There is no simple way to determine what fraction of total flow per year is contributed from which land form; the time patterns and depths of rainfall determine the respective distributions. Figure 10-5

was produced by analysis of the measured precipitation record and measured catchment outflow hydrograph. For the three water years, the pervious areas contributed between 39% (1993) and 60% (1991) of total basin runoff. During the November 1990 storm (Figure 6-4), the 70% of pervious area contributed 60% of the peak flow rate and 63% of the total flow volume. These findings emphasize the need to consider contributions to surface flow from all sources in the catchment when considering alternative urban designs and associated mitigative measures. Consideration of the impervious area alone or assuming that a "pervious area" is relatively benign will lead to designs that will have deleterious ecological effects on receiving streams and their aquatic habitats.

11.1.6 Adaptive Modeling and Monitoring

A major thrust of this work was to develop combined hydrological monitoring and modeling to describe relevant flow paths and fluxes to improve our understanding of catchment hydrology and to provide information that would lead to designs that would mitigate hydrologic effects of urbanization. The model that was developed was essential for providing information that has been used to determine the components of the catchment balance that are not readily measurable. Our observations are based on measured precipitation and streamflow time series, but we had to use the model developed and calibrated in Part A of the report to estimate catchment evapotranspiration and recharge to the till layer beneath each catchment. We have no direct measurements of evaporation fluxes and had to revert to estimating potential evapotranspiration from measurements taken some distance from each site. This is a far from satisfactory state of affairs, but we believe that the combination of using a conceptual model for which key parameters are estimated directly from field integrated measurements (soil lateral hydraulic

conductivity) with measurements of precipitation and estimates of potential evapotranspiration offers an effective blend of modeling and measurements that will lead to improved hydrological and environmental design.

We emphasize the value of using continuous time series of measured precipitation and basin outflow, and modeled evapotranspiration and basin recharge (vertical leakage) over a period of several years to obtain quantitative measures or estimates of all relevant catchment hydrologic fluxes and volumes. These fluxes and volumes, on time scales on the order of the duration of a storm to seasonal and annual, are likely to change when the land-use is altered, and the magnitude of change is needed to assess the adequacy of different hydrologic designs. This makes a strong argument for additional monitoring in small catchments of the scale examined here; without measurements of hydrologic fluxes and states, model predictions have little plausibility. Wigmosta and Burges (1990) suggested that the costs of monitoring both for several years prior to development and after development, while not inconsequential, were a relatively small price to pay to learn more about the effectiveness of various measures taken to mitigate the hydrologic effects of land-use change and urbanization in particular. That suggestion, which has been made by others, was made before measurements were available for the type of model they proposed. The present work reports on development and testing of such a model and measurement scheme. The vastly different hydrologic time series from the two catchments for the common three years of measurement and modeling support the earlier qualitative argument

11.2 Conclusions

The conclusions of Chapter 7 were based on almost two years of measurements at Novelty Hill and less than one year of measured time series of precipitation and streamflow at Klahanie and the associated modeling at both small catchments. Apriori reasoning for the likely flow production mechanisms at both sites proved erroneous; it was the combination of modeling and measurements -- continuous precipitation and streamflow (and piezometer water depths at Novelty) -- that was essential to elucidate the likely mechanisms and flow paths. The model that we developed was designed to be compatible with field observable spatial hydrologic process zones (infiltration, Horton overland flow, saturated overland flow, etc.) and to use block average soil vertical and lateral hydraulic conductivities. While it is compatible with static geographic information system (GIS) mapping and spatial display schemes, the hydraulic continuity features of the model require more features of a GIS system than exist at present if such a GIS is to be used dynamically.

Ten land segments were used to represent the 37 ha Novelty Hill catchment, and thirteen segments (based on topography, the road network, and the storm water conveyance system) were used for the 16.7 ha Klahanie catchment. Land shapes and areas were determined manually but could be taken directly from a digital elevation model (DEM). Our sub-areas were assigned after field mapping. Relevant features identified in the field would not be contained in even the most detailed DEM. If a DEM is used, it would need to have, at a minimum, the capabilities of DEMON (Costa-Cabral and Burges, 1994) to provide similar sub-area information to that which we determined from the field.

The model was calibrated separately for each catchment for relatively wet conditions. The limited tests of the model that we were able to perform subsequently

were for two relatively dry years of continuous data. The modeled outflow hydrographs for each catchment for these conditions, shown in Chapters 9 and 10, indicate that the wet catchment states experienced during calibration had undue influence. Too little relatively dry soil information was contained in the calibration signal time series to assure that the calibrated model could represent prolonged dry catchment state hydrology well for either the deeper Novelty Hill soil column or the shallower Klahanie soil column.

Our demonstration of the use of a calibrated model to check the fidelity of the recorded hydrograph time series in Chapter 10 emphasizes the need for concurrent modeling and measuring, particularly in urban catchments where there may be interference with the recording equipment. For both catchments, the combination of measurements and modeling, even for relatively short (one water year or slightly longer), was critical to help elucidate the principal hydrologic mechanisms, their magnitudes at short and seasonal time horizons, and the resulting flow paths. Such information is essential when the hydrology of post-change land-use needs to be estimated. It will be necessary to continue combined continuous simulation modeling and monitoring, no matter what model or suite of models are used, until we gain greater hydrologic predictive capability for land elements on the order of a few tens of hectares and can produce hydrologic designs that will minimize potential environmentally harmful consequences of land-use change.

REFERENCES

Costa-Cabral, M. C., and S. J. Burges, "DEMON (digital elevation model networks): a model of flow over hillslopes for computation of contributing and dispersal areas", *Water Resour. Res.*, 30(6), 1681-1692, 1994.

Burges, S. J., B.A. Stoker, M.S. Wigmosta, and R.A. Moeller, "Hydrologic Information and Analyses Required for Mitigating Hydrologic Effects of Urbanization", Water Resources Series, Technical Report #117, Department of Civil Engineering, University of Washington, p131, June 1989. (NTIS PB90 109448)

Dunne, T. Personal Communication, March, 1993.

Dunne, T., and R. D. Black, "An Experimental investigation of runoff production in permeable soils", *Water Resour. Res.*, 6(2), 478-490, 1970a.

Dunne, T., and R. D. Black, "Partial area contributions to storm runoff in a small New England watershed", *Water Resour. Res.*, 6(5), 1296-1311, 1970b.

Goodrich, D. Personal Communication November, 1992.

Hardt, R. A. and S.J. Burges, "Some Consequences of Area Wide Runoff Control Strategies in Urban Watersheds," Technical Report 48, Harris Hydraulics Laboratory, Department of Civil Engineering, University of Washington, Seattle, Washington, p81, 1976.

Jakeman, A. J., and G. M. Hornberger, "How much complexity is warranted in a rainfall-runoff model", *Water Resour. Res.*, 29(8), 2637-2649, 1993.

James L.D. and S.J. Burges, "Selection, Calibration, and Testing of Hydrologic Models," Chapter 14 in C.T. Haan, H.P. Johnson and D.L. Brakensiek, (Eds) Hydrologic Modeling of Small Watersheds, American Society of Agricultural Engineers, Hydrologic Modeling Monograph, Chapter 14, 1982.

Johanson, R. C., J. C. Imhoff, J. L. Kittle Jr., and A. S. Donigian Jr., "Hydrological Simulation Program--Fortran (HSPF): Users Manual for Release 8.0", Environmental Research Laboratory, U.S. E.P.A., Athens, Georgia, 1984.

Kemp, G. J. and S.J. Burges, "Hydrologic Modeling and Data Requirements for Analysis of Urban Streamflow Management Alternatives," Technical Report 49, Harris Hydraulics Laboratory, Department of Civil Engineering, University of Washington, 1978.

Loague, K. Comment on "Terrain-based catchment partitioning and runoff prediction using vector elevation data" by I. D. Moore and R. B. Grayson, *Water Resour. Res.*, 28(6), 1741-1744, 1992.

Loague, K. M. Personal Communication August, 1991.

Loague, K. "R-5 revisited, 2. Reevaluation of a quasi-physically based rainfall runoff model with supplemental information", *Water Resour. Res.*, 26(5), 973-987, 1990.

Loague, K. M. and R. A. Freeze, "A comparison of rainfall-runoff modeling techniques on small upland catchments", *Water Resour. Res.*, 21(2), 229-248, 1985.

Loague, K. and G. A. Gander, "R-5 revisited, 1. Spatial variability on a small rangeland catchment", *Water Resour. Res.*, 26(5), 957-971, 1990.

Wigmosta, M. S. and S.J. Burges, "Proposed Model for Evaluating Urban Hydrologic Change", *Journal of Water Resources Planning and Management*, ASCE, Vol 116, No. 6, 742-763, 1990.